DTU Library

European wind turbine testing procedure developments. Task 2: Power quality

Sørensen, Poul Ejnar; Friis Pedersen, Troels; Gerdes, G.; Klosse, R.; Santier, F.; Robertson, N.; Davy, W.; Koulouvari, M.; Morfiadakis, E.; Larsson, Å.

[Link back to DTU Orbit](#)

European Wind Turbine Testing Procedure Developments

Task 2: Power Quality

Poul Sørensen	RISØ	Task coordinator
Troels Friis Pedersen	RISØ	Project coordinator
Gerhart Gerdes	DEWI	
Rainer Klosse	DEWI	
Fritz Santier	DEWI	
Niel Robertson	NEL	
Wily Davy	NEL	
Maria Koulouvari	CRES	
Evangelis Morfiadakis	CRES	
Åke Larsson	Chalmers	
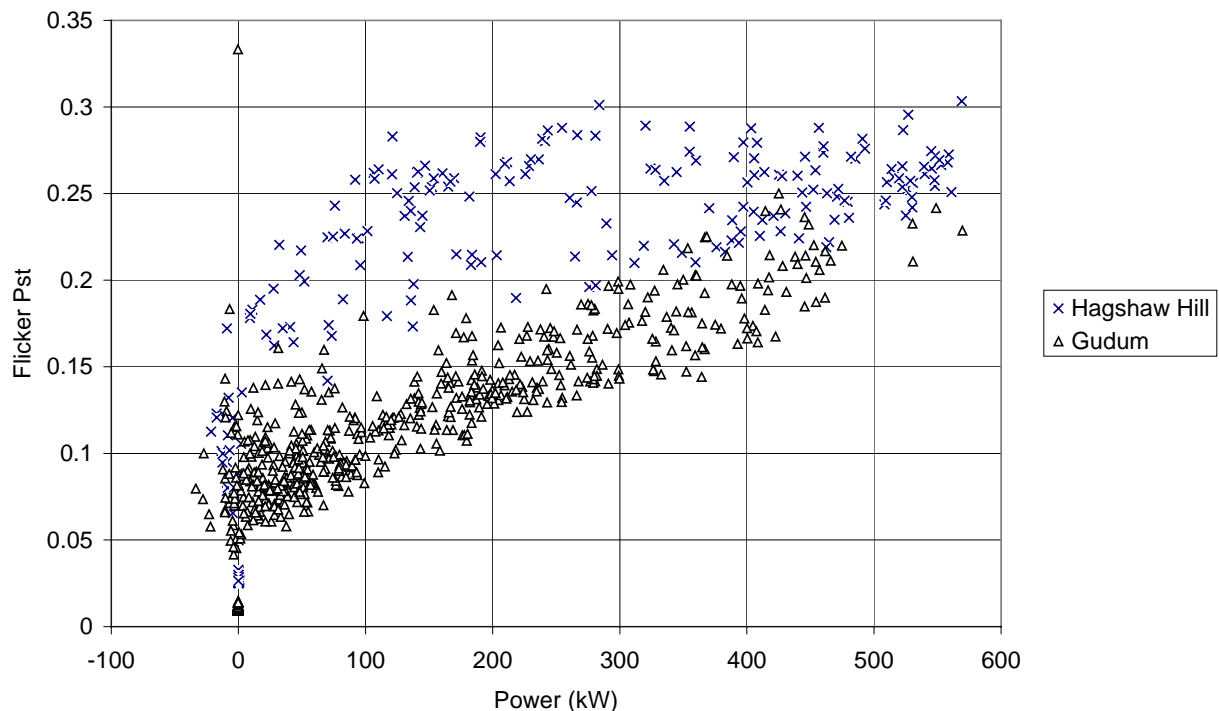
Abstract

The present report describes the work done in the power quality subtask of the European Wind Turbine Testing Procedure Developments project funded by the EU SMT program. The objective of the power quality subtask has been to make recommendations and provide background for new standards for measurement and testing of wind turbine power quality. The focus in the work has been to support the ongoing standardisation work in IEC with a new standard IEC61400-21 for measurement and assessment of power quality characteristics of grid connected wind turbines. The work has also been based on the power quality measuremnet procedure in the Measnet cooperation of European test stations for wind turbines. The first working item of the project has been to verify the state of the art of the measurement procedures by analyses and comparisons of the measurements and data processing software of the participating partners. The next item has been to investigate the influence of terrain, grid properties and wind farm summation on the power quality of wind turbines, considering both wind turbines with fixed rotor speed(s) and wind turbines with variable speed drives.

Contents

Preface

This report describes research work carried out by a research consortium with researchers from seven different research institutes from five different European countries. The European Commission supported the work partly through the Standards, Measurements and Testing (SMT) research program under the Fourth Framework program. This research project, "European Wind Turbine Testing Procedures" SMT4-CT96-2116, was divided in four different tasks. This report describes results from one of the tasks. The four tasks are:

Part 1   "Measurement Method to Verify Wind Turbine Power Performance Characteristics"
Part 2   "Power Quality"
Part 3   "Blade Testing Methods"
Part 4   "Wind Turbine Load Measurement Instrumentation"

Project coordinator: Troels Friis Pedersen, RISØ, Denmark.
Task coordinators:
Part 1   Raymond Hunter, RES, UK
Part 2   Poul Sørensen, RISØ, Denmark
Part 3   Bernard Bulder, ECN, Netherlands
Part 4   E. Morfiadakis, CRES, Greece

Part 2 "Power Quality"

This published report is based on the final task report to the European Commission.
The work was carried out by the following researchers:
Poul Sørensen, RISØ, Denmark
Gerhart Gerdes, Rainer Klosse and Fritz Santier, DEWI, Germany
Niel Robertson and Wily Davy, NEL, UK
Maria Koulouvari and Evangelis Morfiadakis, CRES, Greece.
Åke Larsson, Chalmers, Sweden

RISØ, DEWI, NEL and CRESs work was partly funded by the of the above mentioned contract, whereas Chalmers participation was a part of Åke Larssons PhD. Åke Larssons contribution is on variable speed wind turbines, and it was made on a three months sojourn in RISØ with Poul Sørensen as co-supervisor.

1   Introduction

The standardisation on power quality for wind turbines was initiated in IEC in 1995 as a part of the wind turbine standardisation in TC88. IEC technical committee TC88 initiated a working group WG10 in January 1996, and 15 November 2000 IEC issued a committee draft for vote (CDV) of IEC-61400-21 "Measurement and assessment of power quality characteristics for grid connected wind turbines" [1]. The members of TC88 have voted pro this CDV as a final draft international standard (FDIS), which will be issued in the near future.

   The work presented in this report has served as technical background for WG10. It has been based on existing procedures on national and international level. On the national level, a German guideline for power quality tests of wind turbines has been developed through the last decade. Based mainly on the German standard, the EU project "European Wind Turbine Standards" (EWTS) funded by the Joule II Programme defined an "Electrical Power Quality Measurement Procedure" in February 1996. This procedure again formed the basis for the Measnet measurement procedure on "Power Quality of Wind Turbines" (Measnet-1) [2]. In this procedure, it was stated that Measnet should modify the procedures in order to meet the coming IEC standard. As a consequence, a new Measnet procedure (Measnet-2) [3] based on IEC61400-21 has now been issued in November 2000.

   The European standardisation institute CENELEC has taken a waiting position so far. CENELEC has in other occasions adopted IEC standards, and this will probably also be considered with the IEC 61400-21 standard.

2   Standards and measurement procedures

The research work in this report is based on a review of IEC/TC88/WG10 Working Draft #5 (IEC/WD5), and the Measnet draft Power Quality Procedure 27.11.96 (Measnet-1). This review took place in June 1997. The main conclusions of the reviews were:

- IEC/WD5 states some general requirements to the grid characteristics and to the meteorological parameters where the measurements are performed. Measnet-1 does not have similar requirements.
- Concerning reactive power, the same measurements can be used for both documents.
- The power variability characteristics specified in IEC/WD5 and Measnet-1 are unlike each other, but a data logger can log sufficient data for the statistical analyses required for both documents.
- Concerning flicker, IEC/WD5 proposed power based flicker evaluation whereas Measnet-1 proposes current and voltage based evaluation. Analyses of measurements should be used to compare these methods. IEC/WD5 uses 10 minutes flicker Pst values whereas Measnet-1 uses 1 minute Pst values. There are also different methods to the estimate the 99% percentiles, which should be clarified.

- Concerning voltage changes, IEC/WD5 used a worst case assessment based on current measurements whereas Measnet-1 uses a simulated voltage change based on current and voltage measurements.
- Concerning harmonics, a method is described in Measnet-1 but IEC/WD5 did not finish this subject.

This review has pointed out the need for further analyses, which has been done in the SMT project. The analyses in the SMT project have been implicated in the discussions in IEC/TC88/WG10, and have influenced the development of IEC61400-21 to the present version. The main changes since the review has been:

- IEC61400-21 now propose a voltage and current based flicker evaluation like in Measnet-1 did. But IEC61400-21 describes how to simulate the voltage, which would be generated by the wind turbine if it was connected to a fictitious grid. Such a description was not given in the Measnet-1 procedure.
- Concerning voltage changes, the difference between IEC/WD5 and Measnet-1 has been analysed in this project, using the same measurements for both methods, and the results have been presented as a note for IEC/TC88/WG10. This note showed that the original worst case proposal for IEC/WD5 is often too simple, so as a consequence, IEC61400-21 uses a simulated voltage like Measnet-1. The method for simulation of the voltage is similar to the method used for flicker evaluation.
- Concerning harmonics, a method has now been proposed by IEC61400-21, whereas interharmonics are still under consideration. The reason is that IEC TC77A is working with an update of IEC 61000-4-7 [4], which defines a methods to measure interharmonics. The Measnet-2 procedure is, as mentioned in the introduction, based on IEC61400-21, but on top of that, the Measnet-2 procedure includes a specification of a measurement procedure for interharmonics, which is based on the

3 Wind turbines

Measurements on Bonus 600 kW MK I wind turbine has been selected as basis for most of the verification of measurement procedures and for most of the analysis of power quality for constant speed wind turbines. For the analysis of summation of flicker, measurements on Bonus 450 kW wind turbines have been used. For the analysis of variable speed wind turbines, measurements on Enercon 500 kW wind turbines have been used.

3.1 Bonus 600 kW

The main data of the turbine is:

Type	600 kW MK I
Power regulation	Stall regulation
Number of blades	3
Rotor diameter	41 m
Hub height	35 m
Synchronised rotor speed	29 rpm
Synchronised generator	1500 rpm

speed

Generator type	Induction generator
Generator rated voltage	690 V
Generator rated frequency	50 Hz
Generator rated power	600 kW
Reference power	605 kW
Reactive power compensation	Idle level compensation

3.2   Bonus 450 kW

The main data of this turbine is:

Type	450 kW Mk III
Power regulation	Stall regulation
Number of blades	3
Rotor diameter	35 m
Hub height	35 m
Synchronised rotor speed	35 rpm
Synchronised generator speed	1500 rpm
Generator type	Induction generator
Generator rated voltage	690 V
Generator rated frequency	50 Hz
Generator rated power	450 kW
Reference power	443 kW
Reactive power compensation	Idle level compensation

3.3   Enercon 500 kW

The main data of this turbine is:

Type	E-40
Power regulation	Variable speed and pitch regulation
Number of blades	3
Rotor diameter	40 m
Generator type	Multipole, directly connected to rotor (no gear)
Power converter type	12 pulse IGBT based inverters

4   Measurement sites

The verification of measurement procedures is mainly based on measurements on a Bonus 600 kW wind turbine in Hagshaw Hill wind farm in Scotland. The analysis of power quality of constant speed wind turbines is based on comparison of measurements in complex terrain in Hagshaw Hill in Scotland and on flat terrain in Gudum in Denmark on the same type of wind turbine. The measurements in Hagshaw Hill and Gudum were performed within the present SMT project. The summation of flicker has been analysed using measurements on the offshore wind farm Vindeby in Den-

mark. The measurements in Vindeby were performed by Risø as part of the EU Joule project JOU-CT93-0350.

The analysis of variable speed wind turbines is based on measurements on Enercon 500 kW wind turbines. Measurements from three sites with this wind turbine have been used. The first site is Wind Farm Emden in Germany, where the wind turbines are connected to a strong grid. The measurements in Emden were performed by DEWI. The other two sites are in Sweden: one on a strong grid in Öster Län and one on a weak grid on the island Gotland. The measurements in Sweden were performed by Chalmers Technical University in Göteborg.

4.1   Hagshaw Hill

The Hagshaw Hill wind farm in Scotland is owned by Scottish Power and maintained by Wind Farm Management Services Limited. Figure 1 shows the layout of the wind farm. It consists of twentysix 600 kW Bonus MK I wind turbines H1 – H26. The wind farm is also permanently equipped with two meteorological masts M1 – M2 with similar height as the wind turbine hubs. The terrain is complex, and the wind turbines and meteorological masts are sited on the tops of hills.

The measurements on a single wind turbine were performed on wind turbine H15 because it is free of wakes from other wind turbines when the wind direction is in the interval from south (180 deg) to north-west (315 deg). The dominating wind direction on the site is west.

To fulfil the requirements for power quality measurements, the wind speed should also be measured, as a minimum on the nacelle anemometer. The meteorological masts M1 and M2 are in a position where they can not be used to measure the wind speed at wind turbine H15. Thus, measurements from the nacelle anemometer would have been preferable. To avoid problems with interconnection of the wind turbine control system signals and our measurement equipment, we agreed with the Wind Farm Management Services Limited not to measure directly on the nacelle anemometer. Instead, we planned to use the time stamped data which is logged from the wind turbine control systems by the wind farm monitoring system. Unfortunately, this system was out of work during our stay. As an improvised solution, NEL erected an 11 m mast with a cup anemometer from CRES, so we could get an indication of the wind speed that way. The mast was erected 2 rotor diameters (70 m) to the south of the wind turbine, indicated in Figure 1 as MN.
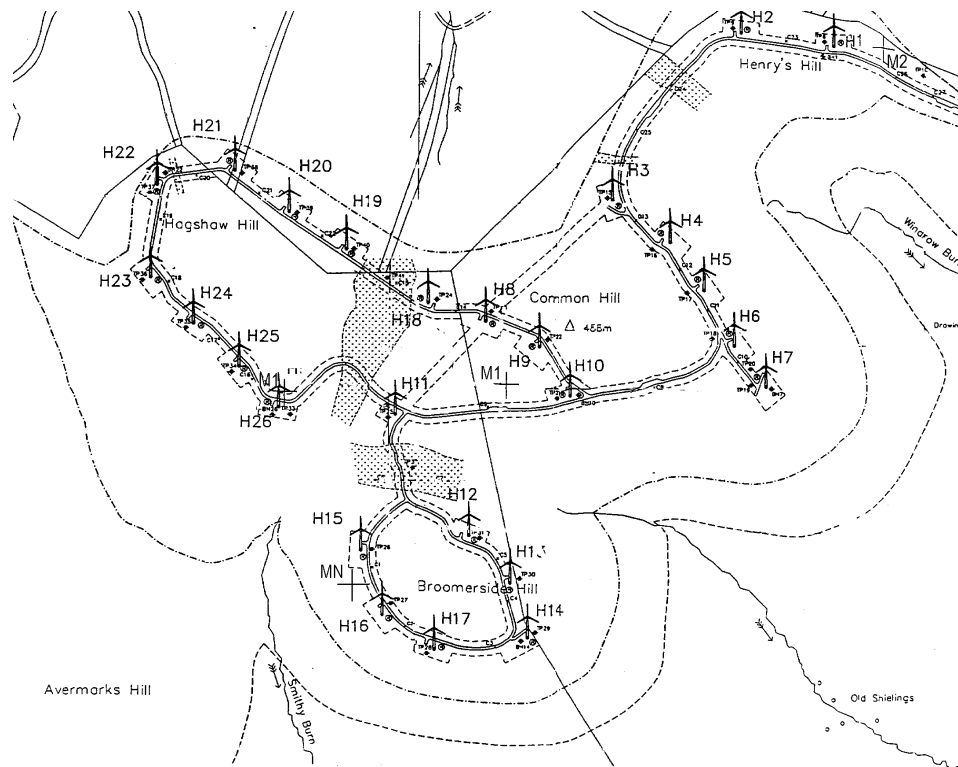
Figure 1. Hagshaw Hill wind farm in Scotland. The wind farm consists of twentysix 600 kW Bonus wind turbines H1-H26 and of two meteorological masts M1-M2. The terrain is complex, and the wind turbines and meteorological masts are sited on the tops of hills.

4.2   Gudum

The other site with Bonus 600 kW MK I wind turbines is Gudum wind turbine cluster in Denmark. Figure 2 shows the site. The cluster consists of 3 wind turbines. The wind turbines are owned and maintained by the Danish utility NVE. There are no meteorology masts on the site.

The terrain is rather flat, and the landscape is relatively open, except for village Gudum 400-600 m to the west of the wind turbine cluster. NVE's consultant SK Energy has evaluated the roughness at the wind turbines to 0.8 and roughness 2.2 in a distance 550 in the West sector.
The measurements were performed on wind turbine G3 which is more free of wake effects from the village than the other wind turbines when the wind comes from the dominating South West direction.
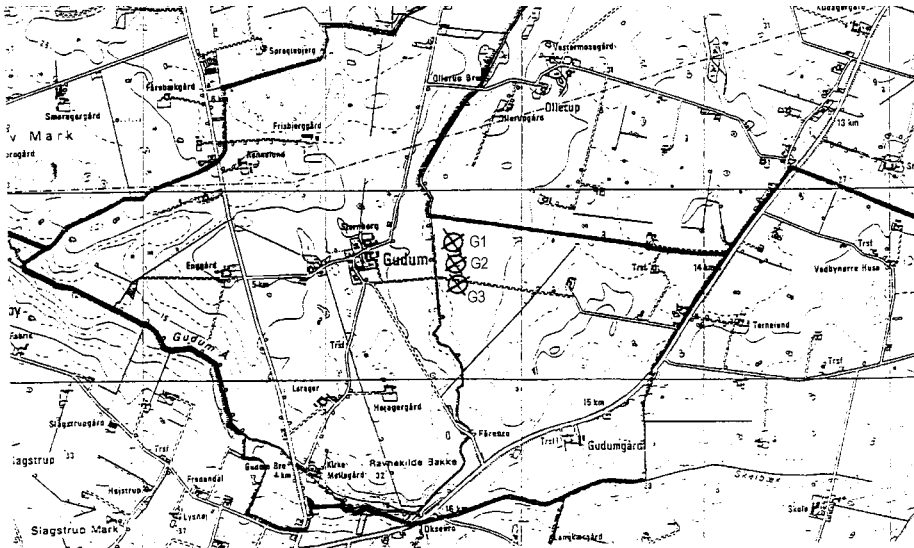
Figure 2. Gudum wind turbine cluster.

4.3 Vindeby

Measurements on Vindeby offshore wind farm in Denmark have been applied to analyse the summation of flicker from more wind turbines. Figure 3 shows the wind farm. It is owned and maintained by the Danish utility SEAS. The wind farm consists of 11 Bonus 450 kW wind turbines (1W – 5W and 1E – 6E). Risø has installed one meteorological mast on land (LM) and two masts in the sea (SMW and SMS) and power transducers and other measurement instruments in the two wind turbines 4W and 5E.

Figure 3. Vindeby offshore wind farm

4.4   Emden

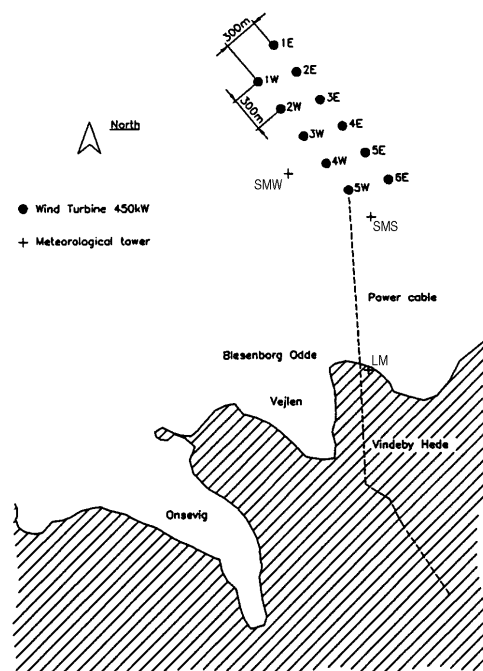Measurements have been performed by DEWI at the Emden wind farm in Germany. There are ten wind turbines in the Emden wind farm, five 500 kW Enercon E-40 and five 500 kW Tacke. Measurements were taken simultaneously at the low voltage side of two Enercon and one Tacke and on the high voltage side of one Enercon wind turbine. A schematic diagram of the electrical configuration of the wind farm is shown in Figure 4.
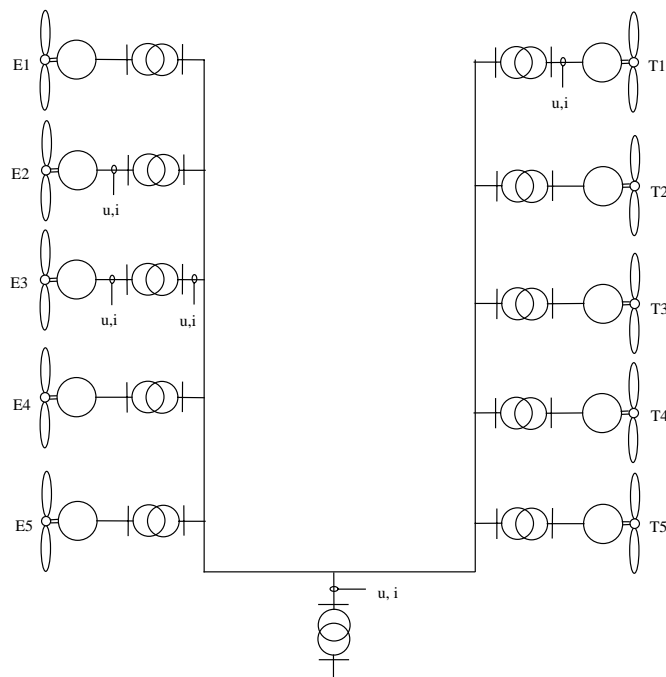
Figure 4. A schematic diagram of the electrical configuration of the Emden wind farm. The location of the voltage and current measurement equipment is also indicated.

4.5   Gotland

Measurements on an Enercon E-40 located at the island of Gotland in Sweden has been performed by Chalmers University of Technology. At Gotland the site consists of two Enercon wind turbines. Since the distance between the wind turbines is approximately 500 meters, measurements were taken only at one Enercon. A schematic diagram of the electrical configuration of the wind turbines at Gotland is shown in Figure 5.

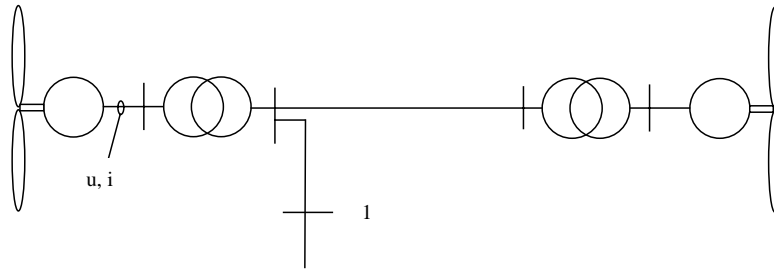*Figure 5. A schematic diagram of the electrical configuration of the wind turbines at Gotland*

5 Measurement equipment

All partners have measured the power quality characteristics with their individual power quality measurement equipment described below.

5.1 CRES

CRES Power Quality measurement system features the parallel operation of two measuring devices, which are the PM3000A analyser and the AT-MIO-16E-10, NI-DAQ card. The parallel operation is controlled by a software developed using Visual Basic, which requires a Pentium PC for execution.

The **PM3000A analyser** has 6 isolated input channels (3 voltage - 3 current) with 12 ranges per channel. Anti-aliasing, low-pass filters with bandwidth range DC-25kHz are applied by default at power-up of the analyser. All channels are sampled at a sampling rate of 220 samples/cycle, set by a microprocessor. The analogue to digital conversion for all channels is simultaneous (no phasing errors). The data is stored in the memory until 400 samples for each channel are collected, which means a sampling time approximately 30ms at 50Hz. The data is then checked for over- or under-range. If the range is correct the frequency of the input is calculated. If the sampling rate is not correct for the input frequency, it is adjusted and 400 new samples are taken. The interface processor computes all the results for every phase and stores them in memory. These background results are available to the RS232 interface.

The PM3000A analyser can be operated in different modes performing the following tasks :
- measurement of the effective values of the voltage, current, active and reactive power on each phase of a 3-phase system
- recording of transients on a 3-phase system, with duration from a few milliseconds to several seconds
- estimation of flicker, based on measurement of the voltage or the current fluctuations
- harmonic analysis, for fluctuating or fixed harmonic content

The **NI-DAQ card** is used for the measurement of the external parameters, i.e. temperature, pressure, wind speed and direction, and the macroscopic characteristics of the power output of the wind turbine. The need for using the NI-DAQ card is to relate the power quality parameters to the external conditions and the wind turbine perform-

ance. The sampling rate and the time interval can be selected by the user. The collected data is analysed on line and the statistical properties of the measured quantities, i.e. mean, standard deviation, maximum and minimum, are calculated on the basis of 1min time interval and stored. The raw data is also stored for further analysis.

The system synchronisation is based on the computer's timer. The data collected with the two measuring systems are saved in different files, which are fully correlated. The PM3000A analyser can be operated as a stand-alone system or in parallel with the NI-DAQ card.

5.2   DEWI

The measurements were carried out with transient recording measuring systems, which are built for grid interference measurements in industrial areas and particularly deployed in industry and utilities. These measuring systems have been specially extended for use in connection with power quality measurements for wind turbines.

The measuring system consists of:
- Transient recorder TRA 700, company w+w electronic AG, Basel
- analogue input ports
- resolution 12 bit
- max. sampling rate 200 kHz per port
- memory depth 1 Mwords per port
- low-pass filter
- triggering manual, extern, reference-range trigger, channel trigger, level trigger, window in-out trigger, slew-rate, time-out, pre-post-trigger
- 2 quartz-crystal-controlled time bases
- 32 digital input ports

Software TRA 700, company w+w electronic AG, Basel
- representation Y-t, X-Y, Dual Y-t, Sep Y-t, extend, compress, shift
- analysis signal measurement with two cursors
- scalar functions min max, RMS, frequency, period etc.
- vector functions +,-,*,/, differentiation, integration, FFT
- software interface

Control box Siemos, company Siemens AG, branch Erfurt
- 4 voltages, 4 current inputs
- special hall generator hardware modules for signal conditioning
- PLL-clock-pulse generator module to produce TRA 700 sample impulses in the 2nd raster for synchronisation on the system frequency
- flicker measuring instrument

Software packet Siemos, company Siemens AG, branch Erfurt
- openloop control of the transient recorder TRA 700
- determines factors of power quality
- determines power and power factors
- harmonic analysis
- flicker valuation
- depiction of time series
- statistical analysis

Current clamp transformer 61C1, company Norma Goerz Instruments
* 1000 A / 1 V
* accuracy: 0.2 %
* frequency range: 10 Hz – 30 kHz

Current clamp transformer D 35, company Chauvin Arnoux, Kehl/Rhein
* 1000/2000/3000 A to 5 A
* accuracy: 1 % (range 1000 A/5 A) - 0,5 % (range 2000 A/5 A and 3000 A /5 A)

5.3   NEL

NELs measurement system is based on a Voltech power analyser connected to a PC with an RS-232 bus. The PC is installed with dedicated software from Voltech:
* Visual power analyses software VPAS for Windows to set up analyser and read and display results.
* IEC555 testing of e.g. flicker (DOS).

5.4   Risø

Risøs power quality measurement equipment is based on Risøs data acquisition system software DAQ, which is used for performance measurements and load measurements as well. For the power quality measurements, DAQ runs on a Laptop PC with an ADC board PCM-DAS16 from Computer Boards using the PCM/CIA slot of the Laptop PC. The PCM-DAS16 board is configured for 8 differential analogue input channels.

For the measurements in Hagshaw Hill, 3 transducers were connected to the PCM-DAS16 board. The first channel was for active power, measured with Camille Bauer type transducers. The second channel was for reactive power, also measured with a Camille Bauer tranducer. The third channel was for wind speed, connected to the analogue output of the anemometer that CRES brought.

The 3 phase voltage input to the Camille Bauer transducers were connected directly from the busbar in the wind turbine, whereas the 3 phase currents were taken from the CTs of the wind turbines control system. These CTs had the ratio 1/800, and the Camille Bauers are rated 2 kW and 2 kvar, so the measurement ranges are ±1600 kW and ±1600 kvar. The sampling rate is set to 100 Hz, and the sampled data is blocked to 50 Hz for P and Q and to 1 Hz for wind speed. The cut-off frequency of the Camille Bauer transducers is 28 Hz.

For the measurements in Gudum, the same system has been used. Only in Gudum, the wind speed measurement was taken from the nacelle anemometer. But in addition to this setup, another setup measuring instantaneous values of voltage and current has been used in Gudum. With this setup, the busbar voltages and control system CT currents were connected to a Voltech PM3000A power analyser. The Voltech power analyser has analogue output channels, which were configured to output instantaneous values of voltages and currents. The analogue channels were connected to the PCM-DAS16 board and logged with 800 Hz for flicker and 2500 Hz for transients during switching.

5.5   Chalmers

The measurements are performed with two different sets of equipment. The statistical measurements are performed with a Siemens Oscillostore P 513 power analyser. The dynamic and transient measurements are performed with DAP (Data Acquisition Processor) based measurement system developed by System Technology. This system consists of hardware as well as software from DASyLab. The software is installed on a PC, connected to the hardware.

6   Verification of measurement procedures

To verify the measurement procedures, all partners have measured power quality characteristics simultaneously on the 600 kW Bonus wind turbine in Hagshaw Hill wind farm in Scotland 13 - 17 October.

The power quality characteristics that were measured were reactive power, power variability, flicker, transients and harmonics. Both Measnet and IEC definitions have been applied.

The Measnet and IEC standards prescribe ten min values for flicker and power variability for continuous operation of the wind turbine. Therefore, the ideal procedure would be to log ten minutes times series. Due to instrument failure, DEWI used a data logger in Hagshaw Hill, which was only able to log five minutes time series with the required sampling frequency of 800 Hz. The whole measurement campaign was therefore based on five minutes values rather than ten minutes values for continuous operation of the wind turbine.

Two types of measurements were performed: *synchronised* measurements and *running* measurements. These measurements were used for an overall comparison of the measurements of the partners. Subsequently, some of DEWIs measurements have been selected as *reference* measurements and used to compare the power quality evaluation software of the partners.

The synchronised measurements were performed at exactly (or within a few seconds) the same time. The purpose was to compare measurements of fx. 5 minutes flicker values from all partners with exactly the same sequence of events.

The running measurements are performed during the same period and at the same wind turbine, but the measurements are not synchronised. Therefore, these measurements are compared on a statistical basis. In addition to that, the running measurements have been compared as time series.

The following DEWIs measurements have been selected as reference measurements:

- Six 5 minutes runs with 800 Hz data have been selected to reflect continuous operation of the wind turbine in the whole power range including a log where the wind turbine generator is not connected to the grid.
- Two 40 seconds runs with 6.4 kHz data for continuous operation have been selected to compare harmonic analyses.
- One 40 seconds runs with sample frequency 6.4kHz of wind turbine cut-in

- One 20 seconds run with wind turbine cut-out sampled with 12.8kHz.

The synchronised measurements were logged during a short period where the mean wind speed was relatively low, and consequently the power range was also low. To be able to compare Risø and DEWI measurements in the whole power range, Risøs measurements have been synchronised with the six five minutes reference measurements.

6.1   Wind speed

The wind speed was measured on an 11m mast as described in section 4.1. The measurement of wind speeds is very difficult in complex terrain. This is illustrated in Figure 6, where the one minute mean values of power are plotted vs. one minute mean values of wind speed.
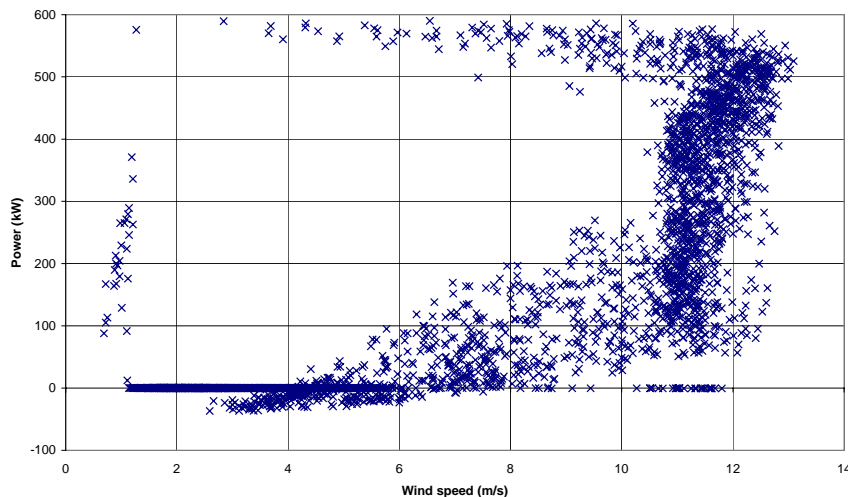

Figure 6. One minute averages of power vs. wind speed measured on the 11 m mast in Hagshaw Hill.

The Figure 6 illustrates that the correlation between the wind speed measurement and the power measurement is very poor. There are several reasons for the bad correlation:
- The mast is much lower than the hub height.
- Wake effects have not been avoided because the wind direction is not measured.
- The measurement of wind speeds in complex terrain is complicated.

As a result of the above, the wind speed measurements in have not been used as reference for the measurements in Hagshaw Hill. Instead, the mean values of the power have been used.

6.2   Reactive power

The synchronised measurements made for flicker comparisons have been used to compare the measured active and reactive power. This was only possible with Risøs and DEWIs measurements, because the Voltech power analysers used by CRES and NEL are not able to measure other parameters when they are measuring flicker. The results are shown in Table 1. The results indicate that Risø measures higher values for the power but lower absolute values for the reactive power.

Table 1. 5 minute averages of active power and reactive power measured synchronously by DEWI and Risø.

Synch. meas. #	Power (kW)		Reactive power (kvar)	
	DEWI	Risø	DEWI	Risø
1	39	41	-19	-16
2	52	55	-19	-17
3	44	47	-20	-17

The running measurements have been used to verify this, and to compare DEWIs and Risøs measurements to CRESs measurements. The three partners all measured statistics 16 October 1997 in the hour between 14:00 and 15:00. Only data from this period is included, because the voltage level has a significant influence on the reactive power consumption of the wind turbine. The result is shown in Figure 7.
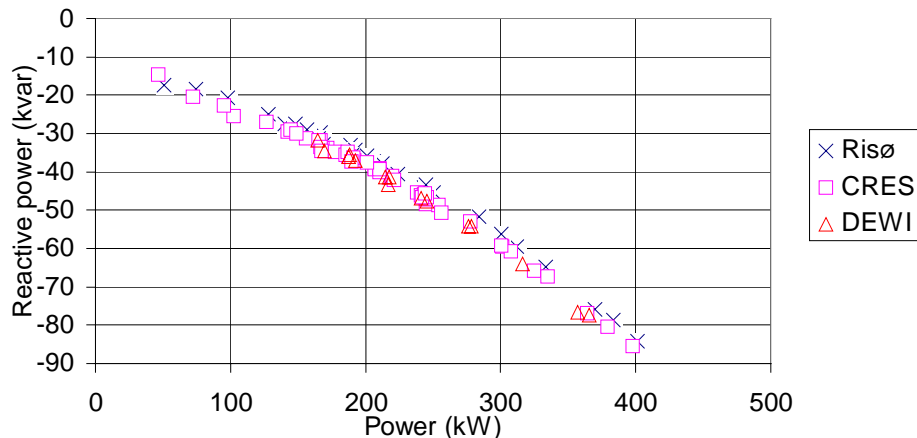

Figure 7. 1 min. mean values of reactive power vs. active power measured 16. October 1997 between 14:00 and 15:00

CRES actually measured reactive power without sign, i.e. as $Q = (S^2 - P^2)^{1/2}$, but the measurements have been signed with a minus to make the graphical comparison to DEWIs and Risøs measurements.

It is seen from Figure 7 that DEWIs and Risøs measurements deviate some from each others. CRESs measurements seem to be in between Risøs and DEWIs, but closest to DEWIs.

To include the whole power range from 0 kW to 600 kW, Risøs and DEWIs measurements during a longer period are compared in Figure 8. During that period, CRES was measuring on the feeder in the wind farm control room, so CRES measurements

are not available. It is evident from Figure 8 that the difference increases with increasing power level.
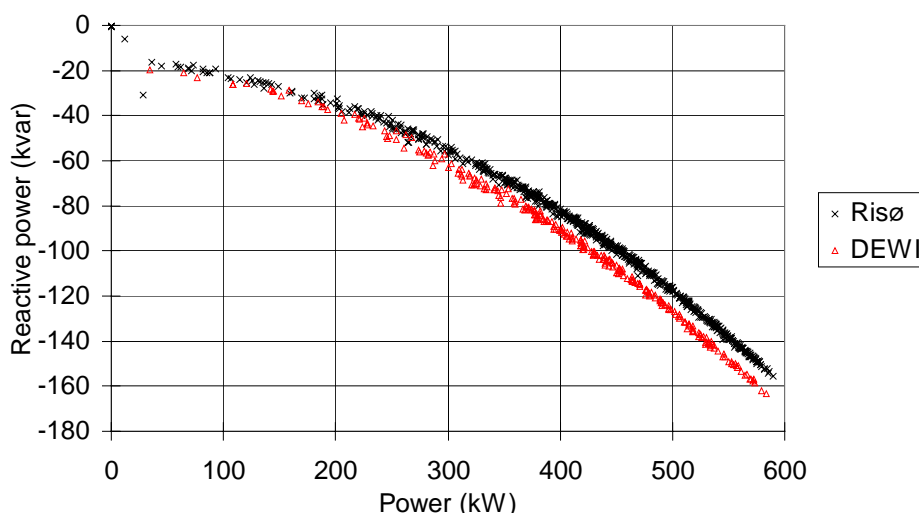

Figure 8. 1 min. mean values of reactive power vs. active power measured between 16 October 1997 15:00 and 17 October 4:00.

Figure 8 does not show if the difference in the *P,Q* curves at the higher power range are due to different reactive power or different active power. The synchronised reference measurements have been analysed to examine this. First, the mean values of the reference values measured by DEWI are compared to the mean values of the Risø synchronised measurements in Table 2.

Table 2. 5 minute averages of active power and reactive power of the 5 reference measurements from DEWI and the synchronised Risø measurements

Reference meas. #	Power		Reactive power	
	DEWI	Risø	DEWI	Risø
1	-16.19	-14.26	-14.59	-10.92
2	-1.70	0.26	-0.29	-0.64
3	270.38	273.39	-53.75	-50.84
4	220.38	223.43	-40.62	-37.80
5	559.79	567.84	-151.56	-144.89

.

Table 2 shows that DEWIs and Risøs 5 minutes mean values of reference measurement #5 are more different than DEWIs and Risøs mean values of the other measurements. Since reference measurement #5 is the highest power level, this could suggest that the slopes of the DEWI and Risø measurements are different. However, the number of mean values is too small to conclude that.

To get more values to compare, the 5 minutes time series of power and reactive power have been block averaged in 10 sec. blocks giving a total of 30 values for each time series. The 10 sec. average values of power are plotted in Figure 9 and 10 sec. average values of reactive power are plotted in Figure 10 as Risø measurements versus DEWI measurements.
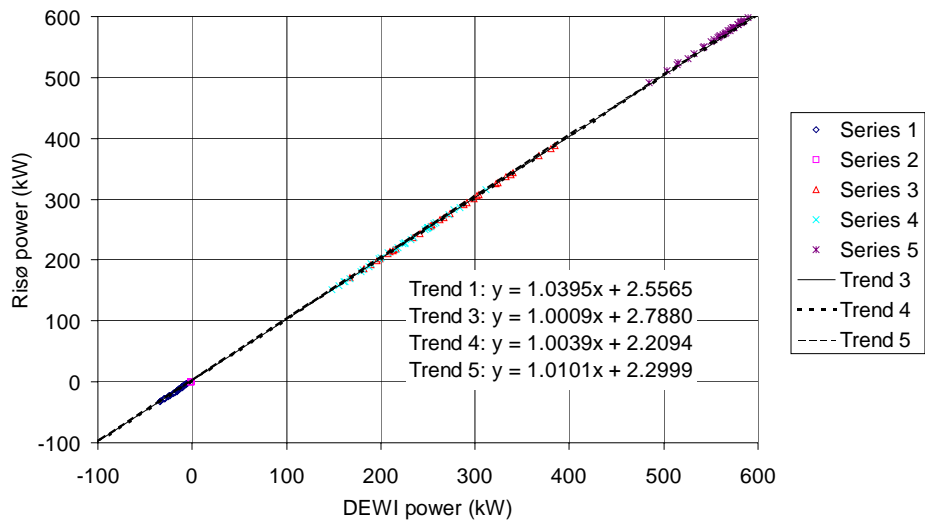
Figure 9. 10 sec. average values of power measured simultaneously by DEWI and Risø.
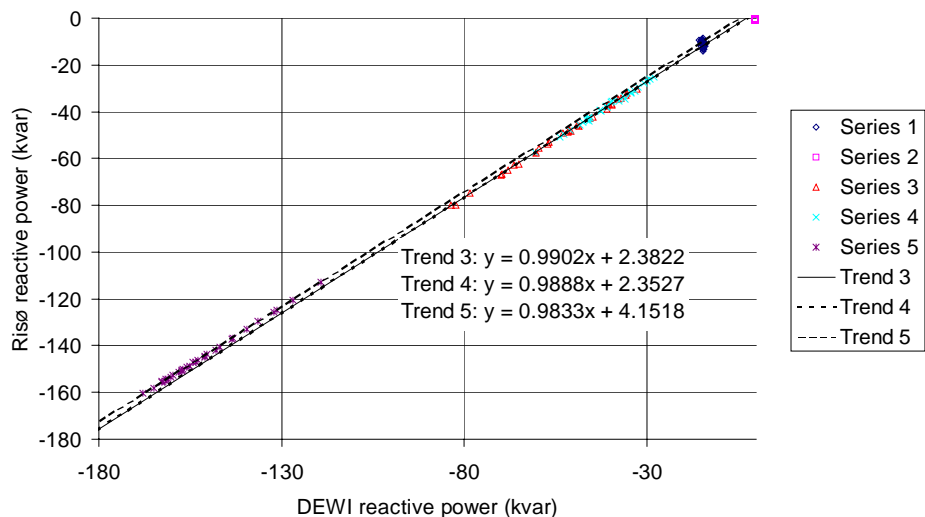

Figure 10. 10 sec. average values of reactive power measured simultaneously by DEWI and Risø.

Figure 9 shows that the synchronisation is good, since the scatter is a minimal. The trend lines of the power values have been calculated for of the individual time series except series 2 which is stand still, and the trend lines for series 3, 4 and 5 are plotted. The data of the trend lines show that the offset difference is less than ½ % and the slope difference is approximately 1 % in the high power range. The slope difference for trend line 1 is almost 4 %, but this is based on data in a power range which is only approximately 6 % of rated. The overall difference in the active power is less than 1½ % of reference power for all the shown data. This accuracy is within the required 2 % in the Measnet procedure.

The similar plot is shown for reactive power in Figure 10. The trend lines of the reactive power values have only been plotted for time series 3, 4 and 5, because the variations in reactive power is very small for time series 1. The three trend lines are very close to be parallel, meaning that the difference between the time series is mainly in the offset. The maximum offset is 4.15 kvar (trend 5) corresponding to 0.7 % of rated

power. The maximum slope difference is 1.7 %, which would give a total difference of 2.4 % of rated power if the trend line is extended to –600 kvar.

The reactive power range is relatively small compared to the rated power range. Therefore, differences in reactive power are graphically more visual than differences in active power. The difference is less than 2 % of rated active power in all cases.

The values of series 1 in Figure 10 show constant values for DEWI measurements whereas Risø measure different values. Figure 11 shows series 1 as PQ-curve. Figure 11 shows that the reactive power measured by Risø is correlated to the active power whereas DEWIs reactive power is independent on active power.
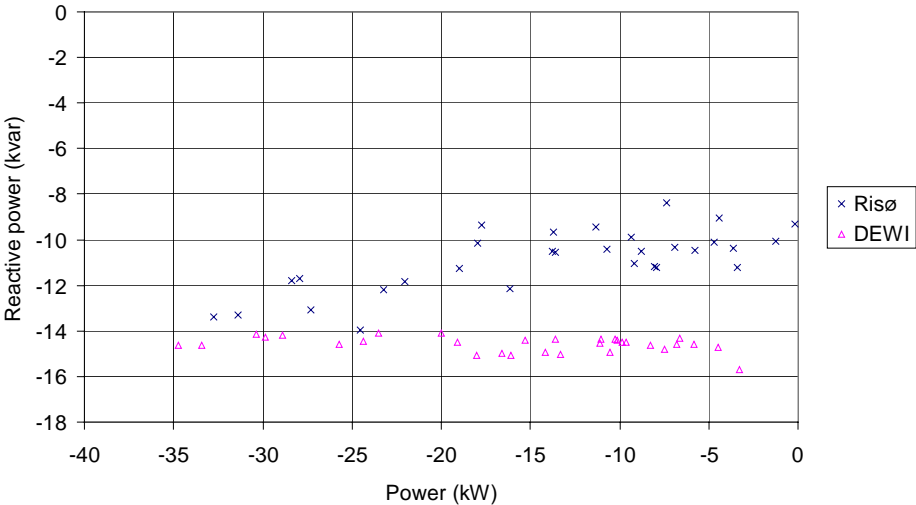
Figure 11. Reactive power vs. power for reference measurement #1.

6.3   Power variability

The measured power variability has also been compared. The one minute standard deviations are compared in Figure 12 and the 1 minute maximum values are compared in Figure 13. Only Risø and CRES have calculated the standard deviations of the measurements. DEWI, Risø and CRES have calculated maximum values. NEL did not have software to control running data logging. Therefore, NEL has no data for subsequent statistical analysis.

Figure 12 shows that the standard deviations are very close whereas the maximum values of CRES seem to be generally lower than Risøs and DEWIs maximum values. To verify that this is not only due to different measurement periods, time series of maximum values are also compared in Figure 14. The reason why CRES maximum values are generally lower is that the sampling rate is lower. Thus each of CRESs one minute maximum values are based on 21-24 samples.
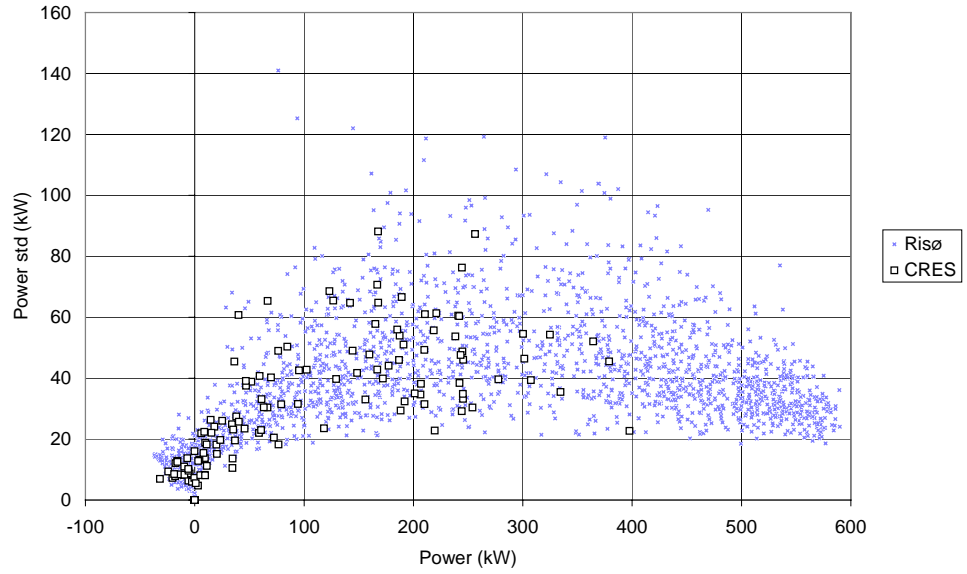
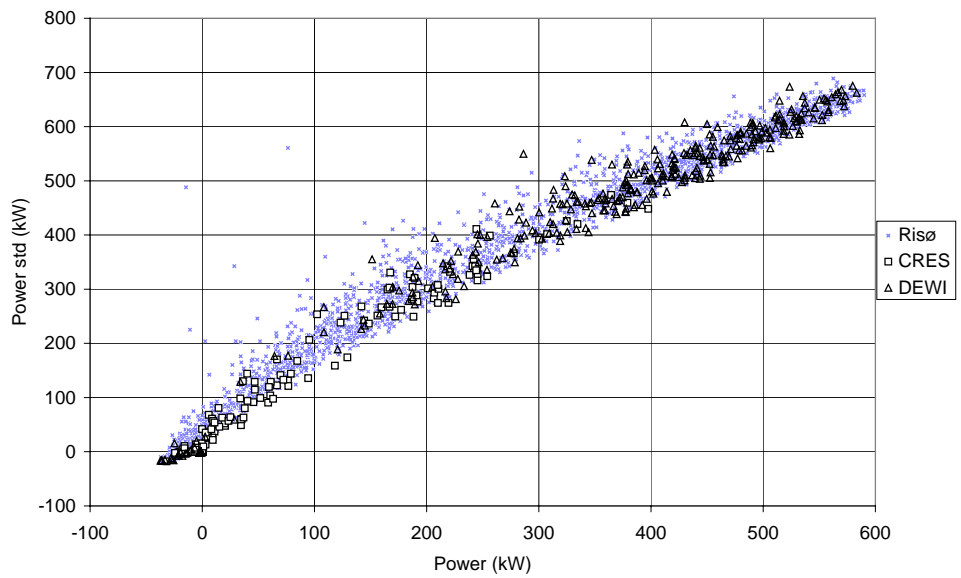*Figure 12. 1 minute power standard deviation vs. mean value*

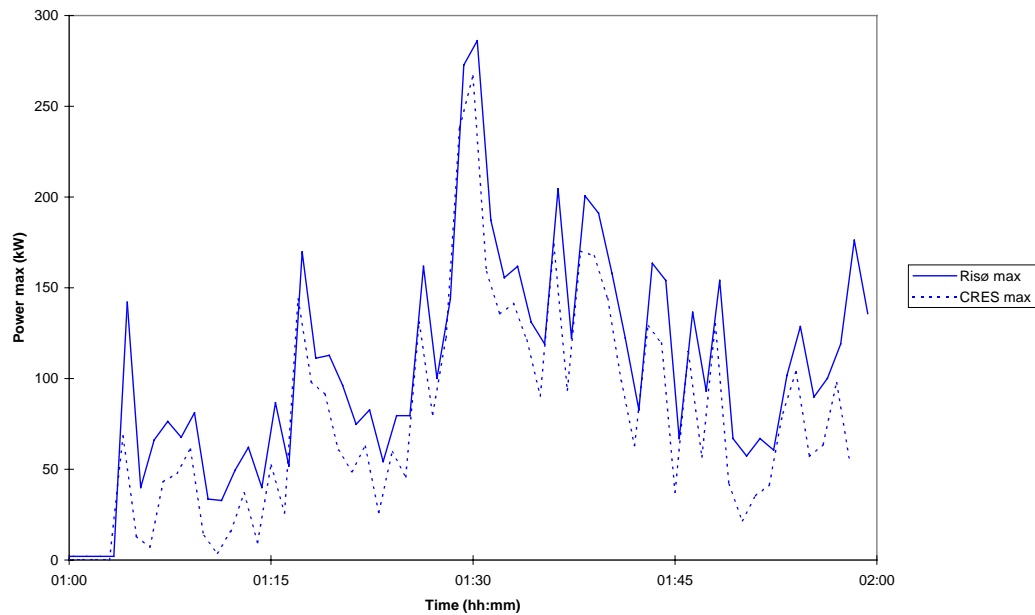

Figure 13. 1 minute power maximum vs. mean value

Figure 14. Time series of 1 minute power maximum

6.4 Flicker

Flicker is defined in IEC 61000-4-15 [5] to quantify the annoyance in the illumination from lamps. This annoyance depends on the voltage fluctuations at the consumers.

The voltage fluctuations at the consumers depend on fluctuating loads as well as fluctuating production in the power system. The power from wind turbines is fluctuating, and therefore the wind turbines contribute to the voltage fluctuations on the grid.

6.4.1 Measurement methods

IEC 61000-3-7 [6] states a method to plan the voltage flicker level in the MV and HV level of a power system, based on the emission level of the individual loads on the system. The emission level of a single fluctuating load is defined as the flicker level, which would be produced in the power system if no other fluctuating loads were present.

The ideal way to measure the flicker emission from a wind turbine would therefore be to connect it to a grid with no other fluctuating loads, and then measure the flicker on the voltage at the connection point to the grid. Such a test method would be extremely expensive, and also have limited applicability because the flicker level would depend on the size and angle of the grid impedance.

Alternatively, the flicker emission is measured indirectly, based on a simulated voltage on a fictitious grid. Such a measurement requires a method to simulate the volt-

age on the fictitious grid. The methods can be separated into two classes, one class based on voltage and current measurements (current flicker) and one class based on active and reactive power measurements (power flicker).

As mentioned in section 2, the Measnet procedure specifies the use of a current flicker method. Early versions of the IEC draft proposed a power flicker method, but the IEC procedure is now also based on a current flicker method. A description of the power flicker method is given in [7].

The current flicker method has not been described in the Measnet procedure. This is insufficient, because in principle the current flicker calculation can be implemented in a variety of ways. Therefore, a more specific description is given in the IEC document.

The basis for the description in the IEC document is that the measured instantaneous values of phases to neutral voltages and phase currents are used to simulate the instantaneous values of the voltages on a fictitious reference grids with no other fluctuating loads than the wind turbine. The phase diagram of the fictitious grid is shown in Figure 15.
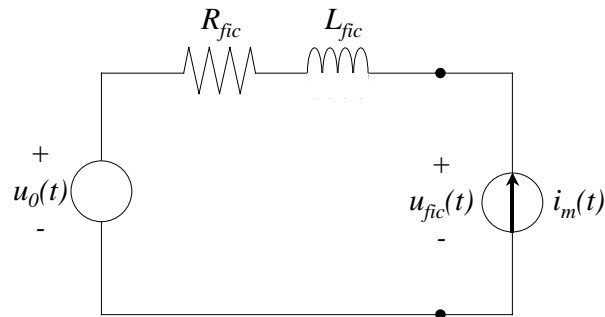

Figure 15. The fictitious voltage $u_{fic}(t)$ *is simulated on a fictitious reference grid with the ideal voltage* $u_0(t)$.

The fictitious grid is represented by an ideal phase to neutral voltage source $u_0(t)$ and a grid impedance gives as a resistance R_{fic} in series with an inductance L_{fic}. The wind turbine is represented by the current generator $i_m(t)$, which is the measured instantaneous value of the phase current. With this simple model, the fluctuating voltage $u_{fic}(t)$ in the power system is given as

$$u_{fic}(t) = u_0(t) + R_{fic} \cdot i_m(t) + L_{fic} \cdot \frac{di_m(t)}{dt}$$

$u_{fic}(t)$ is then used as input to a voltage flicker algorithm as described in IEC 868.

This simulation is straight forward except for the generation of the ideal voltage source $u_0(t)$. Two properties of the ideal voltage should be fulfilled:
- The ideal voltage should be without any fluctuations, i.e. the flicker on the voltage should be zero.
- The voltage on the fictitious grid impedance must have the correct phase relatively to $u_0(t)$. This is only obtained if $u_0(t)$ has the same phase as the measured voltage, or more specific, the same phase as the fundamental of the measured voltage. For some grid impedance angles, the voltage fluctuations are very sensi-

tive to the angle of ideal voltage, so the accuracy of the angle must be as high as possible.

From these properties it is seen that the source to the ideal voltage must be the measured voltage. But the fluctuations must be removed from the measured voltage. This can be done in a number of ways, depending also on the sampling technique, e.g.:

- If the voltages and currents are measured with phase lock equipment, then the number of samples per period is constant. With a constant number of samples per period, a Fourier transform can be applied to calculate the angle of the fundamental for a period. With this angle, the ideal voltage can be calculated as a sine wave with constant amplitude, i.e. correct angle and no fluctuation. DEWI uses this method.
- If the voltages and currents are sampled with a constant sampling frequency, then the above method cannot be applied, because the grid frequency can deviate from rated. In that case, the fundamental of the measured voltage can be found by filtering the measured voltage and determine the zero crossings of the filtered signal. This method is complicated because the filter itself introduces a phase displacement, which must be compensated. Risø uses this method.

The simulated flicker Pst value will depend on the short circuit power of the grid and the angle of the grid impedance angle. To reduce data, IEC 61400-21 defines a flicker coefficient $c_c(\Psi_k)$, which is calculated as a normalised quantity according to

$$c_c(\psi_k) = P_{st,fic} \cdot \frac{S_{k,fic}}{S_{ref}}$$

where $P_{st,fic}$ *is the Pst value calculated on a grid with a short circuit power* $S_{k,fic}$ *and a grid impedance angle* Ψ_k*. and* S_{ref} *is the reference power of the wind turbine. This definition gives a flicker coefficient,*
which is in principle independent on the short circuit power, as a higher short circuit power gives a lower Pst value. The flicker coefficient can then be applied to calculate the Pst value on any other grids with different short circuit powers.

6.4.2 Comparison of simultaneous measurements

Table 3 shows the flicker results of all the partners for the synchronised flicker measurements. CRES, DEWI, and NEL results are based on current and voltage measurements on phase 1 whereas Risø results are based on active and reactive power measurements on all 3 phases together.

Table 3. The results of the synchronised flicker measurements

Synch. meas. #	$S_{k,fic}/S_{ref}$	Ψ_k	CRES	DEWI	NEL	Risø
1	20	30	0.185	0.184	0.169	0.191
	20	30	0.179	-	0.191	-
2	20	50	0.121	0.129	0.116	0.138
	20	50	0.126	-	0.129	0.143
3	20	30		0.138		0.142
	20	50		0.094		0.099
	20	70		0.042		0.053
	20	85		0.025		0.041
4	20	70	0.074	0.060	0.074	-
	20	70	0.080	-	0.098	-

Generally, the table shows a good agreement between the flicker Pst values measured by the partners. Still some general remarks should be noted.

The first remark is that the Voltech power analyser, which is used by CRES and by NEL, has a minimum Pst value of 0.074. This is due to the binning of instantaneous flicker as explained in section 6.4.5. The minimum Pst value is reached in the synchronised measurement 4, where the grid angle is set to 70 deg.

The second remark to the results in Table 3 is that Risø generally calculates higher flicker values than the others, especially for higher grid impedance angles. This can be due to a combination of flickermeter calibration and noise on Risøs active and reactive power measurement.

To gain more significance, the running measurements of flicker P_{st} values are compared on statistical basis. Figure 16 - Figure 19 show the 5 minutes Pst values vs mean value of power with a grid angle of 30 deg, 50 deg, 70 deg, and 85 deg respectively.

CRES did not log power together with flicker. Therefore, CRESs 5 minutes Pst measurements are plotted versus Risøs 5 minute average values of power measurements. Due to uncertainty in the synchronisation between CRESs flicker measurements and Risøs power measurements, there can be up to 2 minutes difference in the synchronisation between CRES Pst and power.

The y-axis of the graphs in Figure 16 - Figure 19 have been selected in order to highlight the Pst values for *continuous* operation of the wind turbine. Higher flicker values are measured during cut-in of the wind turbine.

It seems from Figure 16 and Figure 17 that DEWIs flicker values are lower than the others. However, it should be noted that the values in these figures includes all measurements, and therefore they are not measured during the same periods.

To compare measurements during same periods, Figure 20 - Figure 23 show time series of Pst values with the 30 deg and 50 deg grid impedance angles. It is seen that the Risø values are systematically higher than both DEWI and CRES values when the same measurement period is selected, except when CRESs Voltech power analyser reaches it minimum due to classification (Figure 20).
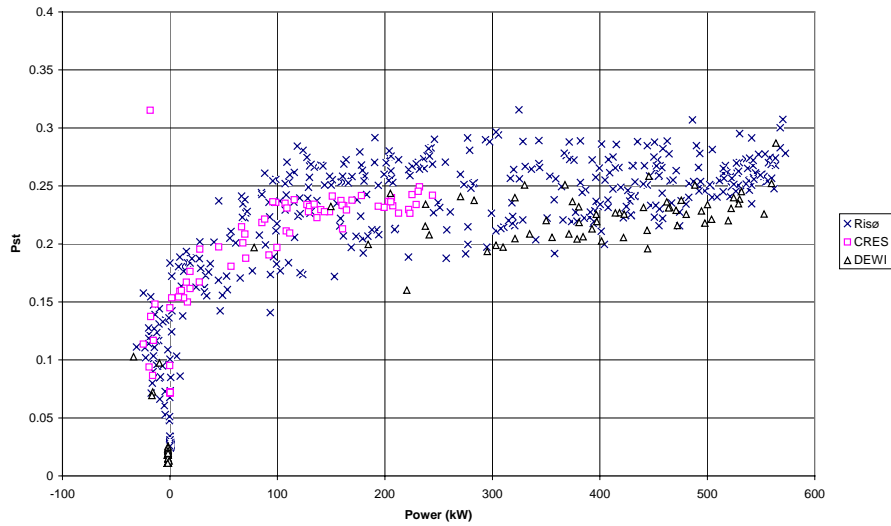
Figure 16. 5 minutes Pst values with grid angle 30 deg and short circuit ratio 20 vs. mean value of power.
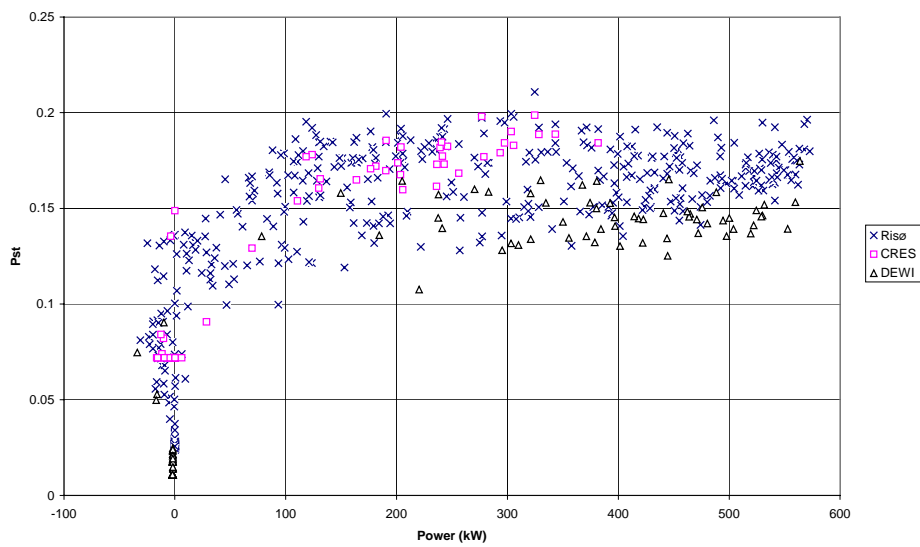

Figure 17. 5 minutes Pst values with grid angle 50 deg and short circuit ratio 20 vs. mean value of power.
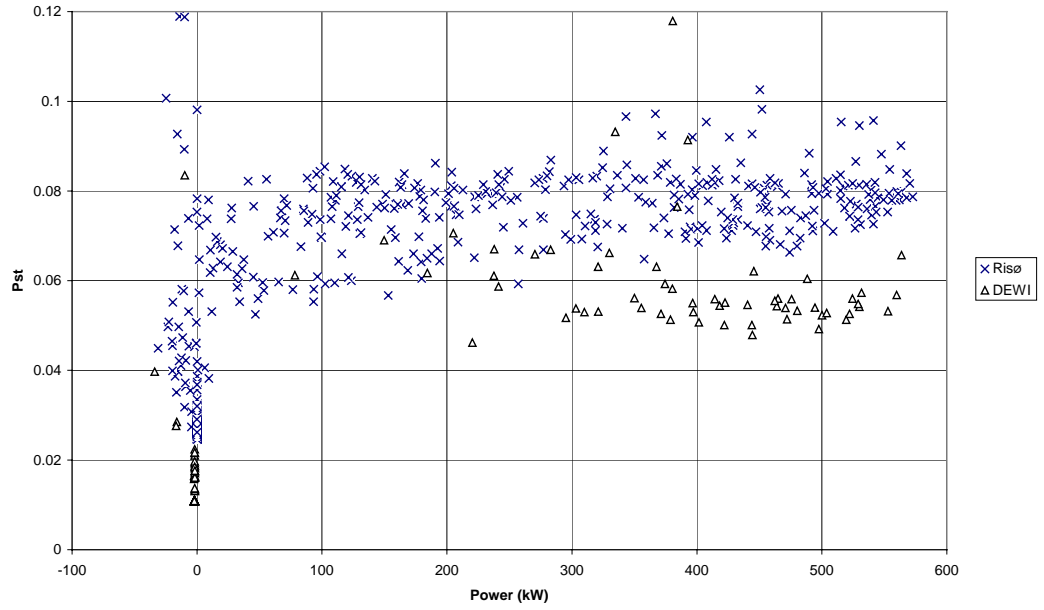
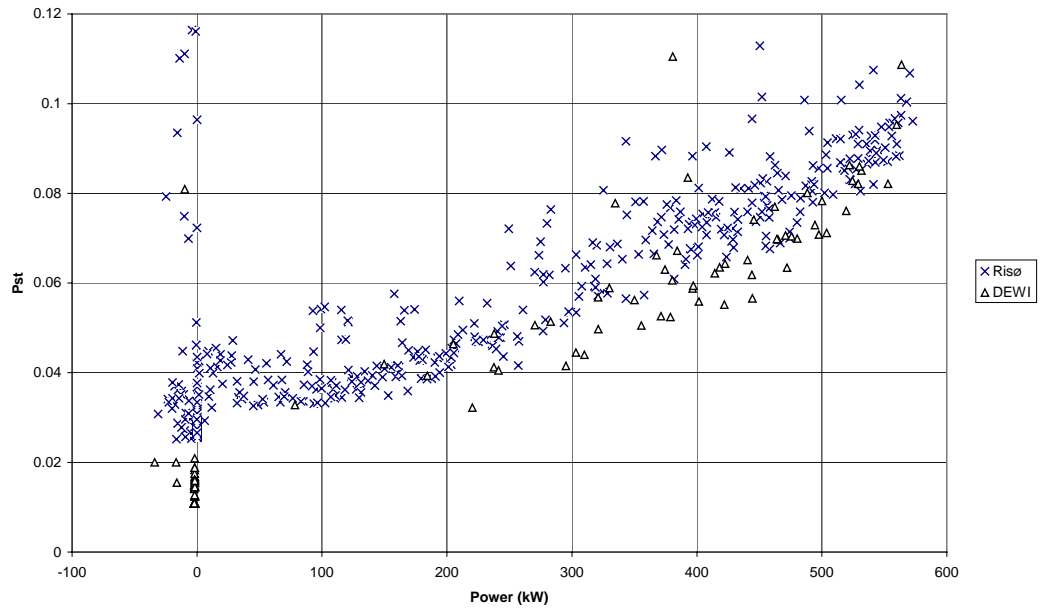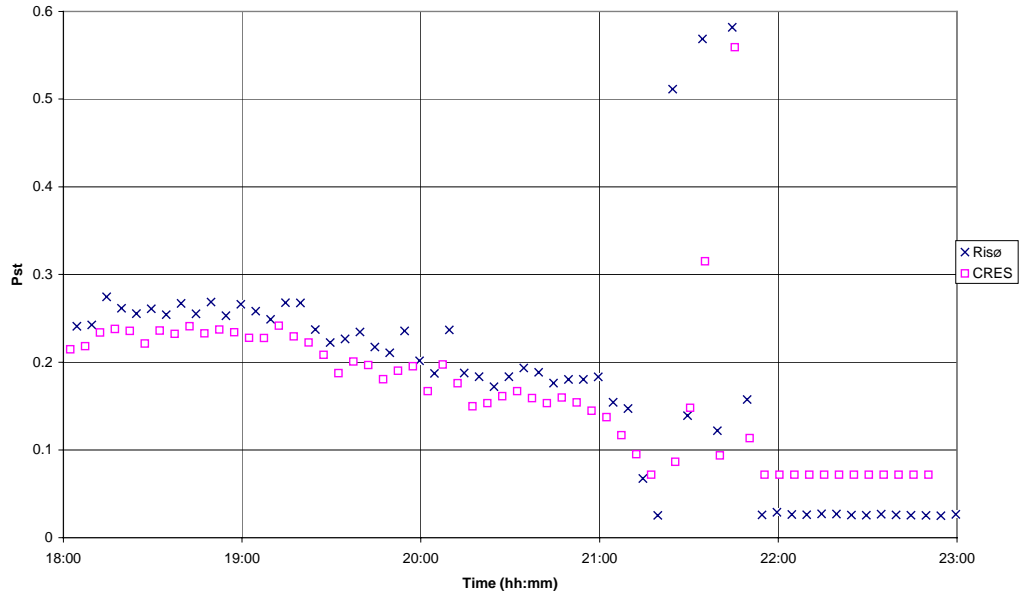*Figure 18. 5 minutes Pst values with grid angle 70 deg and short circuit ratio 20 vs. mean value of power.*

Figure 19. 5 minutes Pst values with grid angle 85 deg and short circuit ratio 20 vs. mean value of power.

Figure 20. Time series of 5 minutes Pst values with grid angle 30 deg and short circuit ratio 20. The measurements were taken 14 October 1997.
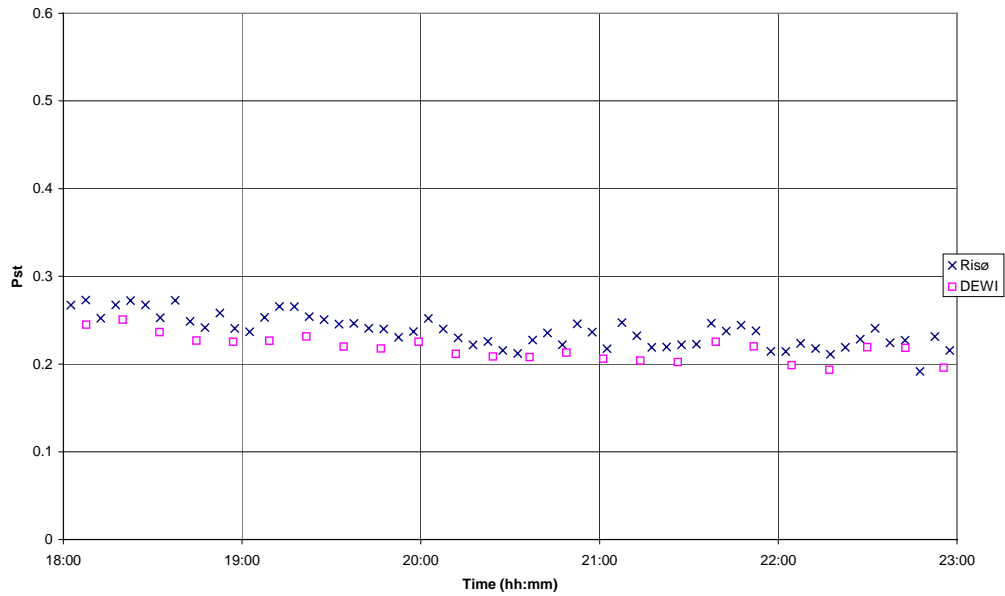
Figure 21. Time series of 5 minutes Pst values with grid angle 30 deg and short circuit ratio 20. The measurements were taken 16 October 1997.
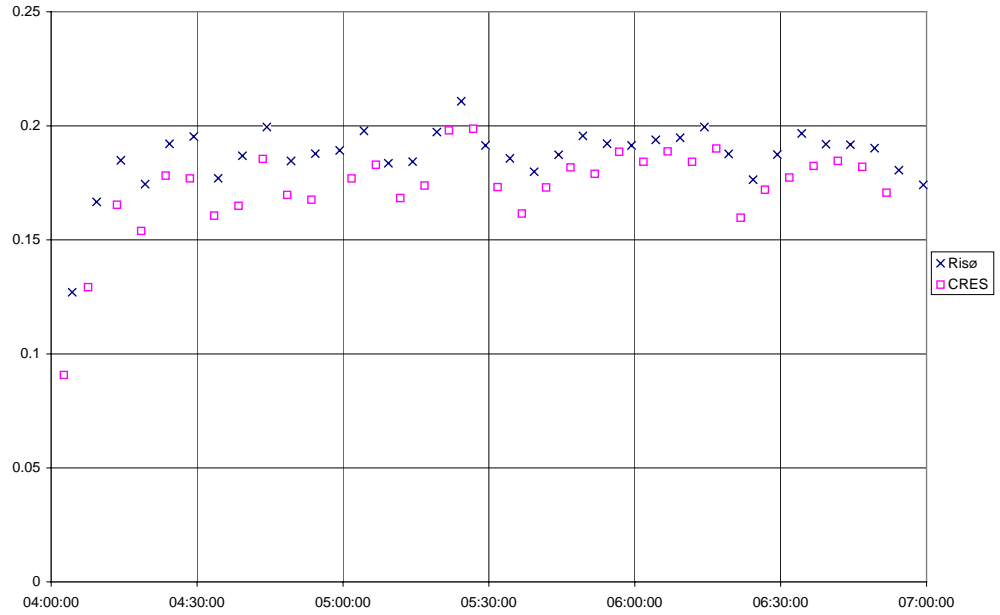
Figure 22. Time series of 5 minutes Pst values with grid angle 50 deg and short circuit ratio 20. The measurements were taken 16 October 1997.
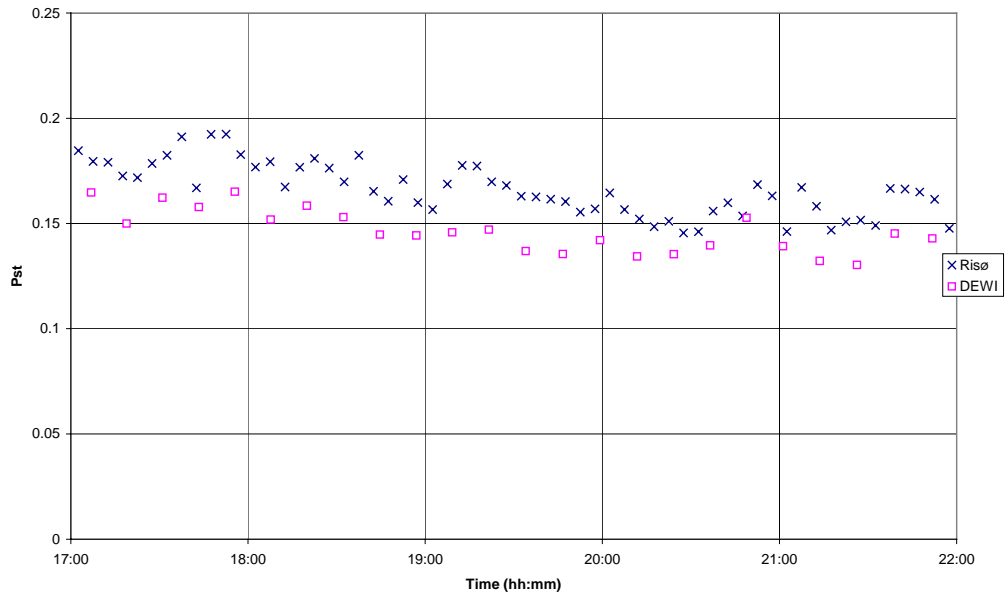
Figure 23. Time series of 5 minutes Pst values with grid angle 50 deg and short circuit ratio 20. The measurements were taken 16 October 1997.

6.4.3   Comparison of flicker calculation programs

The 6 reference measurements of instantaneous currents and voltages have been used to verify the flicker routines. The calculated 5 minute Pst values of each reference measurements are compared in Figure 24 - Figure 29.

First, DEWI, Risø and CRES have calculated the Pst values for all 3 phases applying DEWIs measurements of voltage and current. Then Risø has calculated Pst values applying DEWIs P and Q measurements as input. Finally, Risø has calculated Pst values applying Risøs own P and Q measurements as input. Risøs P and Q measurements are synchronised within 100 ms with DEWIs P and Q measurements for the 6 reference measurements.

The results agree very well. The most significant deviation is with Risøs flicker calculation based on Risøs PQ measurements. The main reason for this deviation is noise in Risøs PQ measurements due to a drifting common mode of the differential measurement signal from the P and Q power converters. Grounding the signal through an appropriately high resistance has reduced this noise in the succeeding measurements in Gudum.

The differences in the Pst values are highlighted with the stand still measurements in Figure 29. In that case, the Pst values should be close to zero. Therefore, Figure 29 gives a good impression of the noise. The noise includes both measurement noise and flicker calculation noise.

From the stand still case it is evident that the relatively strong noise on Risøs flicker calculations with Risøs PQ measurements is due to noise on the P and Q measurements. This is seen comparing these flicker calculations to Risøs similar flicker calculation with DEWIs PQ measurements. DEWIs PQ measurements have approximately the same bandwidth as Risøs, but the Pst values are lower with DEWIs PQ measurements.
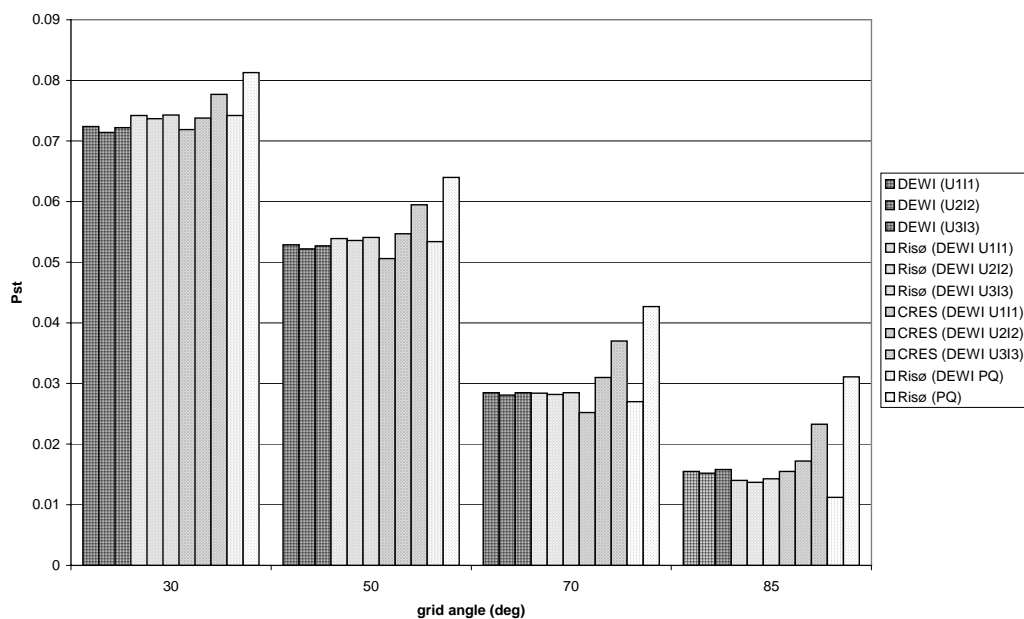

Figure 24. 5 min. flicker Pst values calculated with short circuit ratio S_k/S_n=20 for time series measured at cut-in wind speed (P_{mean}=-16 kW)
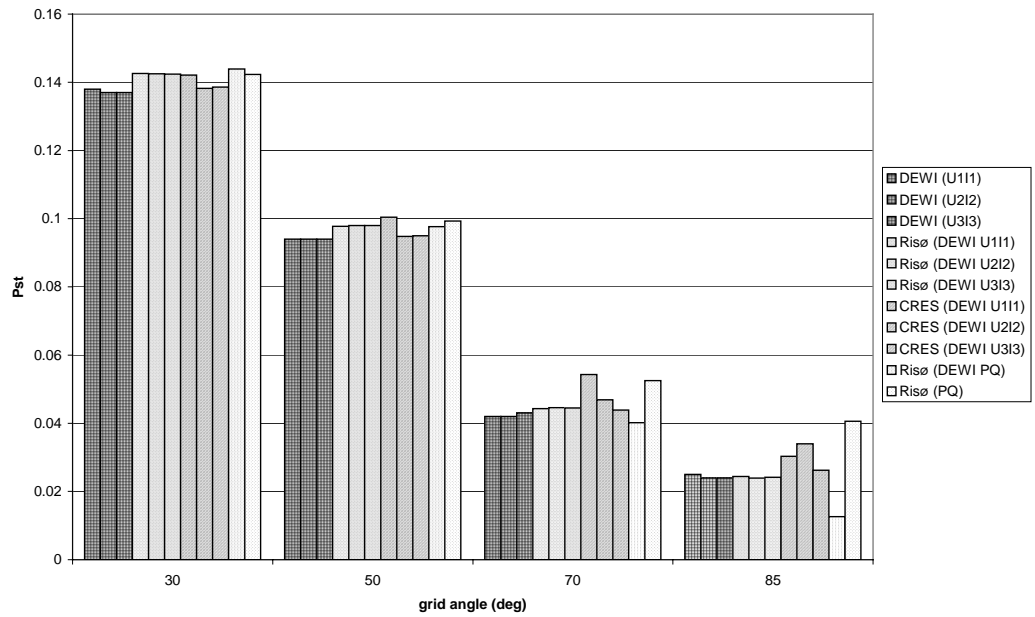
Figure 25. 5 min. flicker Pst values calculated with short circuit ratio $S_k/S_n=20$ for time series measured at cut-in wind speed ($P_{mean}=44$ kW)
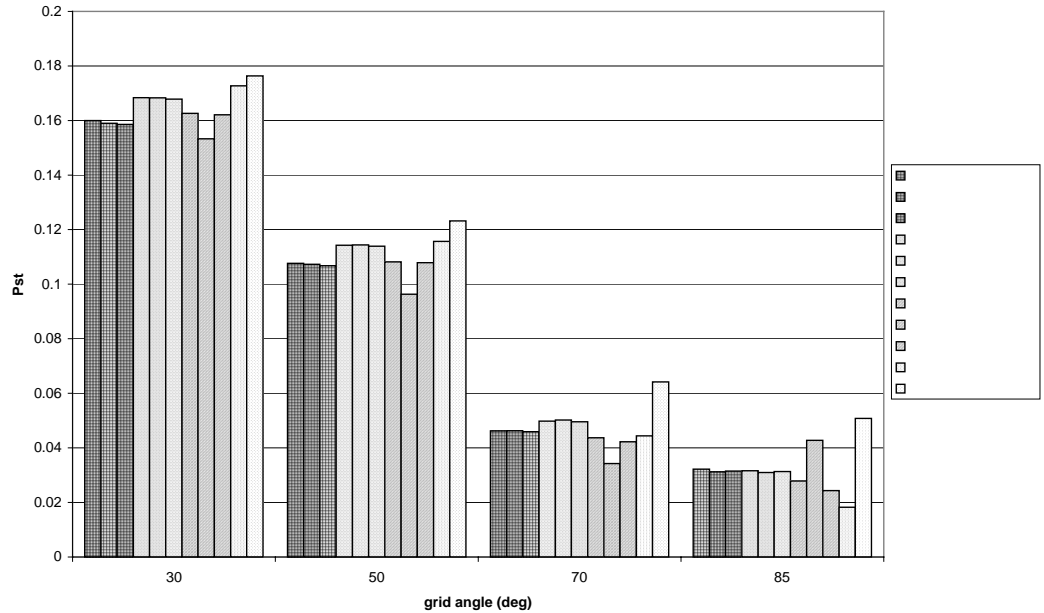

Figure 26. 5 min. flicker Pst values calculated with short circuit ratio $S_k/S_n=20$ for time series measured with wind turbine producing half of the rated power ($P_{mean}=220$ kW)
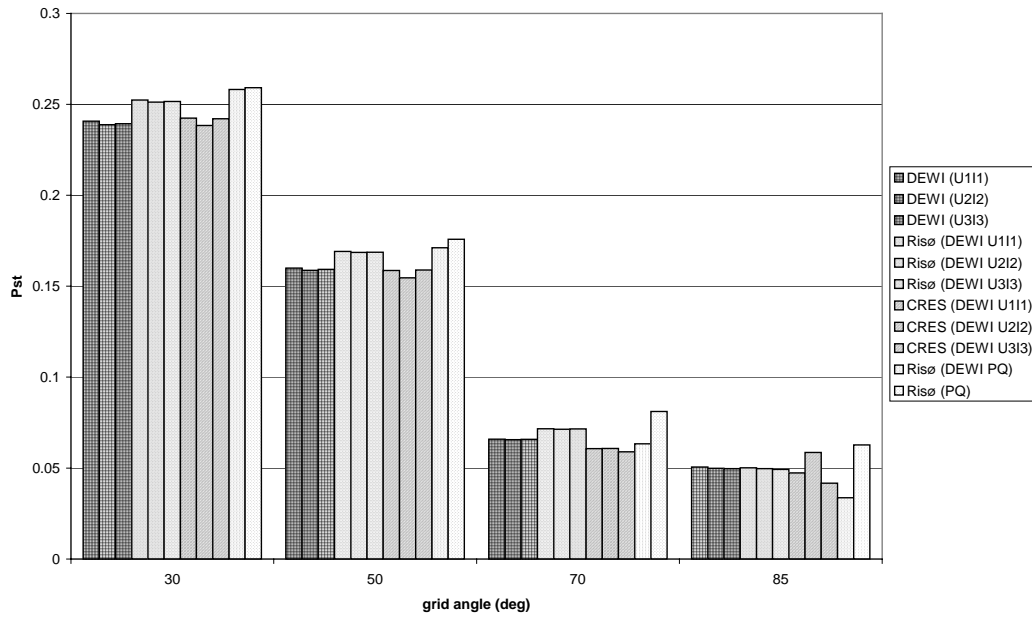
Figure 27. 5 min. flicker Pst values calculated with short circuit ratio $S_k/S_n=20$ for time series measured with wind turbine producing half of the rated power ($P_{mean}=270$ kW)
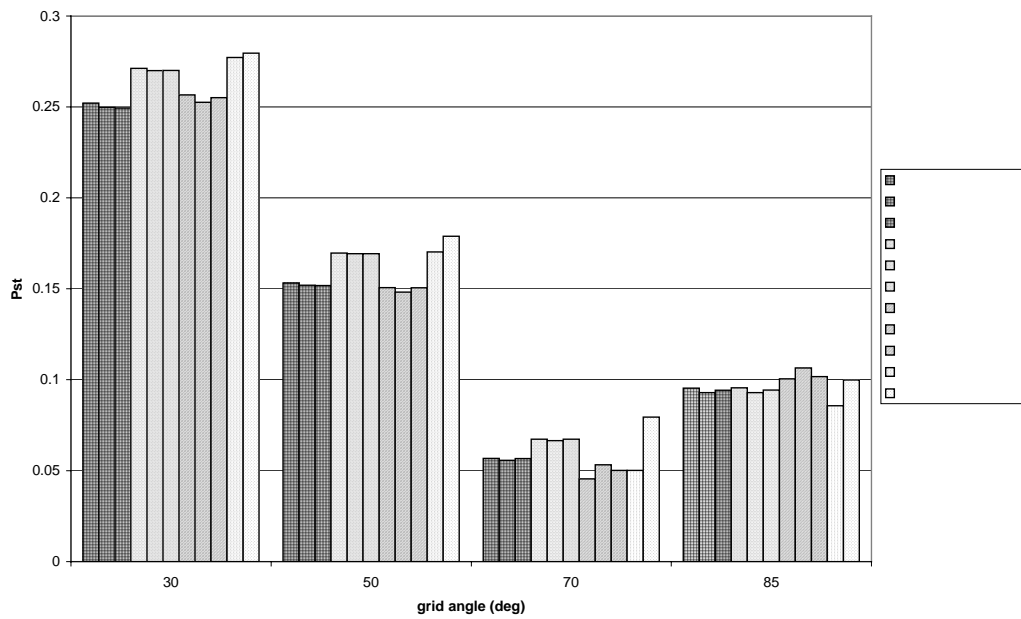

Figure 28. 5 min. flicker Pst values calculated with short circuit ratio $S_k/S_n=20$ for time series measured with wind turbine producing rated power ($P_{mean}=560$ kW)
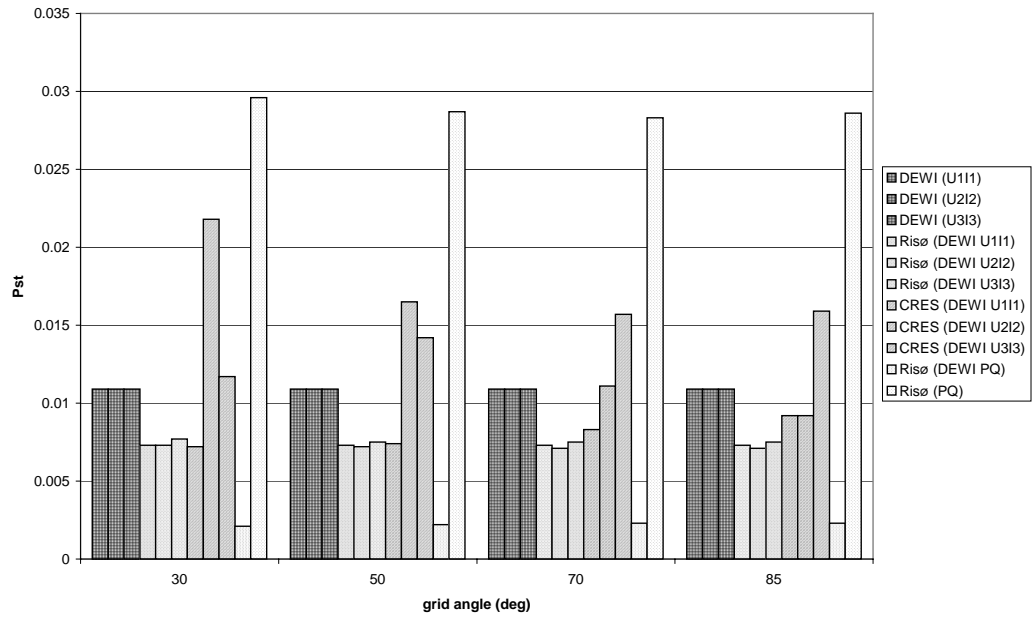
Figure 29. 5 min. flicker Pst values calculated with short circuit ratio $S_k/S_n=20$ for time series measured with stand still of the wind turbine ($P_{mean}=0$)

6.4.4 Influence of sampling frequency and cut-off frequency

The sampling frequency for the current and voltage measurements has an influence on the costs of the measurements. A data acquisition system has a limited sampling rate, and the storage requirement also depends on the sampling rate. Therefore, it has been analysed how high a sampling frequency is required to maintain the accuracy in the measurements.

The sampling frequency should be minimum $2 \cdot f_c$, where f_c is the bandwidth of the signal. To ensure that the bandwidth is limited, the measurement signal can be filtered with a cut-off frequency f_c before it is sampled.

When the bandwidth of the measurement signals for currents and voltages is limited, the harmonics are filtered. In principle, this has an influence on the flicker value of the measurements, because the signals are modified.

Figure 30 shows how the Pst values for different grid impedance angles depend on the cut-off frequency of a digital 6th order Butterworth filter. The first 6.4kHz reference measurement with continuous operation has been applied. The filter has been applied to both voltage and current to ensure an even phase displacement of both signals.

For the dashed line, the filtered voltage and current signals with the original sampling frequency 6.4kHz have been processed directly by Risøs flicker calculation program. For the solid line, the filtered signals have been reduced to the sampling frequency $2 \cdot f_c$ before the flicker calculation. To keep Figure 30 as simple as possible, only phase 1 results are shown. The other phases have also been calculated, but they are very similar.
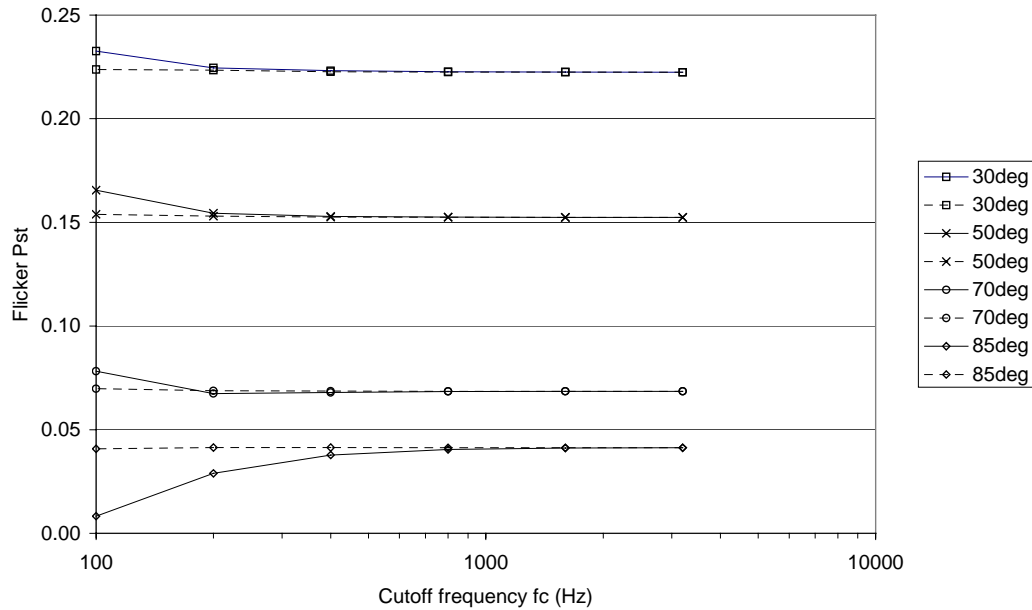
Figure 30. Flicker Pst values for the 6.4kHz DEWI measurement of continuous operation filtered with the cut-off frequency f_c*. The dashed lines keep the original sampling frequency 6.4kHz, and the solid lines are re-sampled to the sampling frequency* $2 \cdot f_c$*.*

It is seen from Figure 30 that the main reason for deviation in Pst values for low cut-off frequencies is not the filtering but the reduction of the sampling frequency.

For continuous operations of a wind turbine with directly connected induction generators, i.e. constant speed wind turbines, the harmonic emission is very small, and consequently, most of the signal is expected to be within the bandwidth of the fundamental. Therefore, it was expected that the pure filtering would modify the flicker calculation very little, which is confirmed by the dashed line.

The solid lines in Figure 30 show that the reduction of the sampling frequency plays a much more significant role on the flicker results. The sampling frequency is critical for several aspects of the flicker routines.

The first critical aspect is the generation of the ideal phase to neutral voltage $u_0(t)$ described in section 6.4.1, with the same phase as the measured voltage, but a constant amplitude. This aspect is important because even a minor phase displacement of the ideal voltage will have a significant influence on the flicker values for high grid impedance angles. It is also seen in Figure 30 that the influence on Pst is most significant for 85deg.

The second critical aspect is the deviation of the current, which is done to simulate the voltage fluctuations due to the inductive impedance of the grid. It is numerically more critical to calculate the slope of the current when only a few samples are available for each period. This aspect also mainly influences the Pst values for high grid impedance angles.

A third aspect can be the digital filtering in the flicker routine. A 35Hz Butterworth filter is specified in the IEC868 flicker routine, so when the sampling frequency moves down, this filter can become critical.

6.4.5 Influence of short circuit ratio of fictitious grid

A flickermeter according to IEC 61000-4-15 has a minimum Pst value due to the binning of the instantaneous flicker level in classes. IEC 61000-4-15 requires a minimum number of 64 classes. The Voltech power analyser use 1024 classes, and Risøs and DEWIs flicker routines use even more detailed classification.

The description of the flickermeter in IEC868 suits the purpose to predict if the voltage flicker level exceed the limit Pst ≈ 1, but is not good to calculate the lower Pst values of the flicker emission from a single load or wind turbine. As an example, the bin size for the instantaneous flicker in the Voltech is aproximately 0.01, but calculating P_{st} according to IEC 61000-4-15 as

$$P_{st} = \sqrt{0.0314P_{0.1} + 0.0525P_1 + 0.0657P_3 + 0.28P_{10} + 0.08P_{50}}$$

where P_i is the ith percentile of instantaneous flicker, the minimum value becomes P_{st} ≈ 0.07 (setting all P_i=0.01). The maximum Pst value of the Voltech is approximately P_{st} ≈ 2.3 (setting all P_i=1024·0.01). So even with 1024 bins, the resolution of Pst values is very bad for small P_{st} values, which is due to the square root in the Pst calculation.

Consequently, a weak reference grid (i.e. low short circuit power) shall be selected for the reference calculations. If a too strong grid is selected then the calculated flicker value will be the minimum value of the instrument. Using this Pst value to estimate Pst on weaker grids will only give a scaled minimum value.

On the other hand, the reference grid must not be selected so weak that the maximum instantaneous flicker level of the instrument is reached.

Thus it is given implicit by the specifications in IEC 868 that the flickermeter is designed to predict if Pst=1 is exceeded or not. But IEC 868 is self-contradictory in this point, because the accepted accuracy is stated to be 5 % (probably 5 % of P_{st} =1) which can never be obtained for low flicker values when only 64 instantaneous flicker bin classes are applied.

Using PC software to calculate the Pst values, the binning can be very detailed. Still, the selection of the short circuit power has an influence on the result. This is illustrated in Figure 31 below, where DEWI has calculated the flicker coefficient with different short circuit ratios. The wind turbine is stall controlled with constant rotor speed.
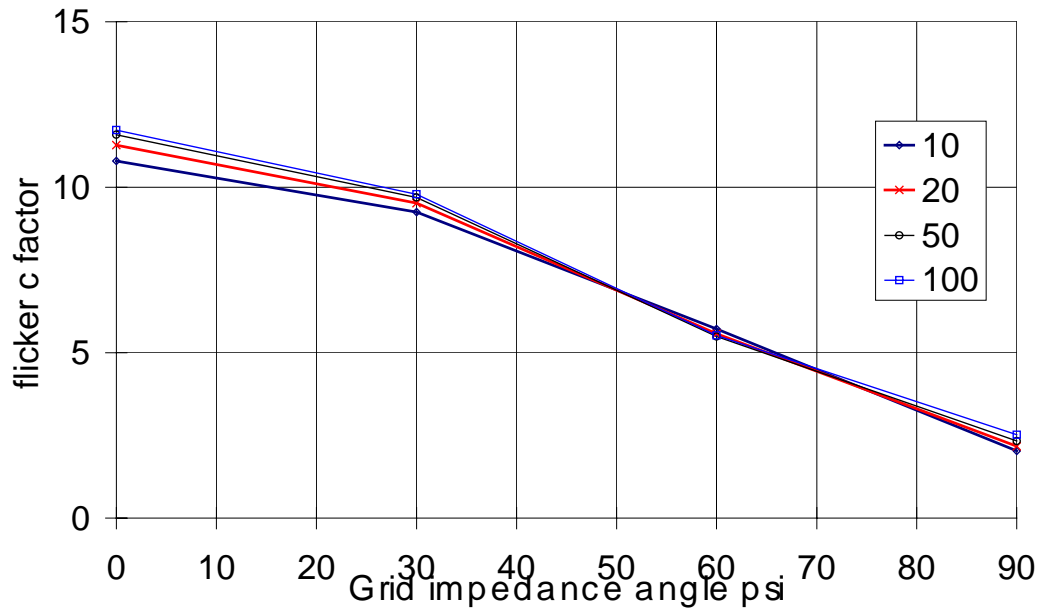
Figure 31. Flicker coefficients dependence on the short circuit ratio for different grid impedance angles.

Figure 31 shows that when the short circuit ratio of the fictitious grid is too low, then the flicker coefficient also deviates from the stable level, which it has for higher short circuit ratios. This is because the voltage fluctuations increase for decreasing short circuit power, and when the fluctuations get too high, the unlinearities of the flicker calculations gets more influence on the result.

Figure 31 does not illustrate, that if the short circuit ratio becomes too large, then the binning will influence the result instead as explained above. But this is illustrated e.g. in Figure 20.

6.5 Transients during switching

6.5.1 Definitions for IEC 61400-21

In the draft Measnet procedure, a current spike factor $k_{i\,max}$ is defined as

$$k_{i\,max} = I_{max} / I_G$$

where I_{max} is the maximum 20 ms RMS value of the measured current, and I_G is the nominal current of the wind turbine. I_G is determined form the nominal apparent power S_G of the wind turbine and nominal voltage U_{nG}.

From the point of view of power quality, the influence on the voltage is more interesting than the size of the maximum current. If the wind turbine is connected to a grid with the short circuit power S_k, then the current spike factor can be applied to calculate a "worst case" of the maximum relative variation Δu of the voltage according to

$$\Delta u = \frac{I_{max} \cdot |Z_k|}{U_{nG}/\sqrt{3}} = \frac{k_{i\,max} \cdot I_G \cdot |Z_k|}{U_{nG}/\sqrt{3}} = k_{i\,max} \cdot \frac{\sqrt{3} \cdot U_{nG} \cdot I_G}{U_{nG}^2/|Z_k|} = k_{i\,max} \cdot \frac{S_G}{S_k}$$

The actual maximum relative variation of the voltage, which will occur on the grid, will depend on the angle of the grid impedance angle. Therefore, Measnet defines a grid dependent switching factor $k_{i\psi}$ according to

$$\Delta u = k_{i\psi} \cdot \frac{S_G}{S_k}$$

Using a similar method, the draft IEC 61400-21 defines a voltage change factor $k_U(\psi_k)$ as

$$k_U(\psi_k) = \frac{U_{fic,max} - U_{fic,min}}{U_n / \sqrt{3}} \cdot \frac{S_{k,fic}}{S_{ref}}$$

where $U_{fic,max}$ and $U_{fic,min}$ are the maximum and minimum values respectively of the simulated phase to neutral voltage $u_{fic}(t)$ simulated on the fictitious grid as described in section 6.4.1.

IEC 1000-3-3 defines an analytical method to assess flicker, based on a voltage change and a form factor. The form factor F=1 corresponds to a stepwise voltage change. This method is used to define the flicker step factor $k_f(\psi_k)$ in the draft IEC 61400-21. The flicker step factor is defined so that it can be used to calculate a voltage change as above, and this voltage change can then be used to calculate the flicker severity according to the analytical method in IEC 1000-3-3.

According to the above, the voltage change in percentage, d_{max} can be calculated as

$$d_{max} = k_f(\psi_k) \cdot \frac{S_{ref}}{S_{k,fic}} \cdot 100$$

using the draft IEC 61400-21 symbols. Applying the IEC 1000-3-3 analytical method, the flicker severity $P_{st,fic}$ of a single switching operation can be calculated as

$$P_{st,fic} = \left(t_f / T_p \right)^{1/3.2} = \left(\left(2.3 \cdot d_{max}^{3.2} \right) / T_p \right)^{1/3.2} = \left(2.3 / T_p \right)^{1/3.2} \cdot d_{max} = \left(2.3 / T_p \right)^{1/3.2} \cdot k_f(\psi_k) \cdot \frac{S_{ref}}{S_{k,fic}} \cdot 100$$

Using this result, the draft IEC61400-21 defines the flicker step factor $k_f(\psi_k)$ is defined as

$$k_f(\psi_k) = \frac{S_{k,fic}}{100 \cdot S_{ref}} \cdot \left(\frac{T_P}{2.3} \right)^{1/3.2} \cdot P_{st,fic}$$

T_P is the length of the simulated voltage time series in seconds. In the draft IEC 61400-21, it has been assumed that T_P=60s, but here we will apply the formula to shorter measurements.

6.5.2 Comparison of simultaneous measurements

Two sets of synchronous measurements of transient operation of the wind turbine were taken. One measurement with cut-out, and another with cut-in of the wind turbine to the grid. DEWI logged three phase instantaneous values of voltages and currents, CRES logged three phase RMS values of voltages and currents, and Risø logged active and reactive power. NEL was attempting to log RMS values with the Voltech like CRES, but NEL did not manage to trigger the data logging with the cut-in and cut-out operation of the wind turbine.

DEWIs measurements have been applied to calculate 20ms RMS values of the voltages and currents. Figure 32 shows the RMS values of the cut-out measurements and Figure 33 shows the RMS values of the cut-in measurements. In both cases, only phase 1 is shown, because there is very little difference between the RMS values of the phases.
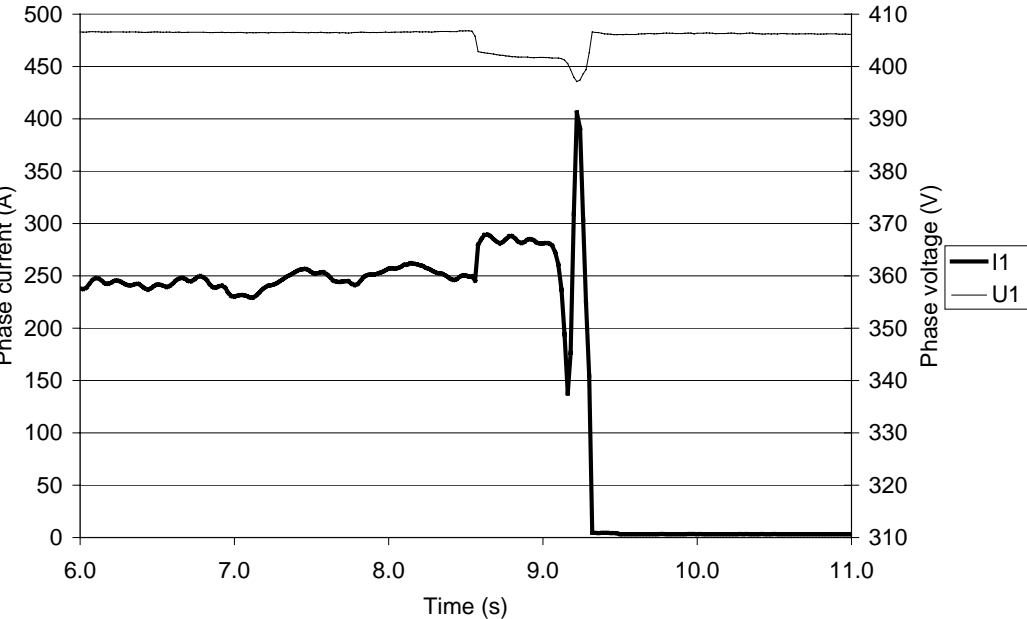
Figure 32. RMS values of current and voltage of phase 1 for cut-out operation of wind turbine.
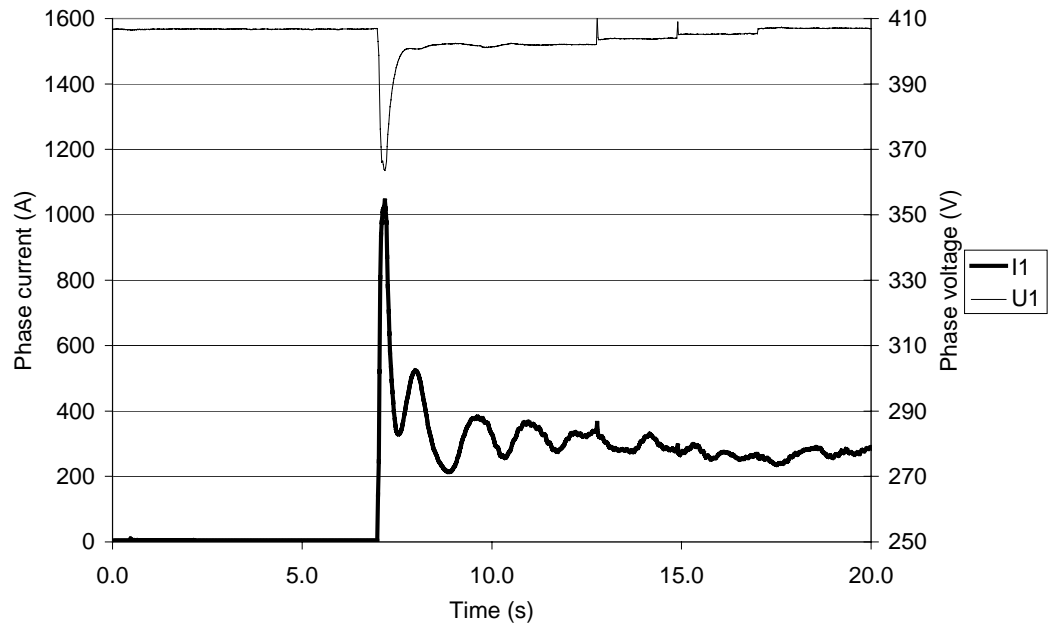
Figure 33. RMS values of current and voltage of phase 1 for cut-in operation of wind turbine.

The measured current spike factors of the synchronised measurements are shown in Table 4 for each partner. DEWI and CRES measured the phase current directly, whereas Risø estimated the current by the measured active and reactive power, and assuming the voltage had its rated value. Therefore, CRES and DEWI has a result for each of the three phases, whereas Risø only has one result for the active and reactive power.

The nominal current I_G is determined by the rated apparent power S_G and the rated voltage U_{nG} according to

$$I_G = S_G / \left(\sqrt{3} U_{nG} \right)$$

The rated apparent power has been approximated to the rated active power $S_G \approx 600$ kW and the rated voltage is $U_{nG}=690$V. Thus, the nominal current $I_G=502$A has been applied. The approximation has been done to have results on site, before the reactive power was documented. Extrapolating the curve in Figure 8, the reactive power consumption at rated power is estimated to $Q_G=-175$kvar, and consequently the actual rated apparent power $S_G=625$kVA. This is 4% more than the approximated apparent power. Consequently, the current spike factors in Table 4 are overestimated with 4%.

Table 4. Measured current spike factors k_p *for synchronised measurements of transients (cut-out and cut-in.*

Type	m/s	CRES1	CRES2	CRES3	DEWI1	DEWI2	DEWI3	Risø
cut-out	9.3	0.821	0.817	0.818	0.809	0.792	0.791	0.799
cut-in	11.9	2.072	2071	2.101	2.078	2.068	2.085	1.875

The agreement between DEWIs and CRESs measurements is excellent. Risøs calculations are not done according to the standards, because they are based on power measurements. As expected, the Risø current spike factor for cut-in is significantly less than the DEWI and CRES values. The main reason is that the voltage drops to approximately 9% below rated when the current is maximum as seen in Figure 33. Consequently, Risø underestimates the current spike with approximately 9 %, using power measurements and assuming rated voltage to estimate the current. The filtering of Risøs power transducers is not expected to reduces the spikes significantly, because the bandwidth of the power transducers is very high (approximately 28 Hz).

6.5.3 Comparison of calculation routines

DEWIs measurements of instantaneous voltages and currents during cut-in and cut-out have been used as reference measurements to verify the calculation routines for voltage change factors and flicker step factors.

The results are shown in Figure 34 - Figure 37. Generally, the agreement is very good, but CRESs flicker step factors are generally higher than Risøs and DEWIs.
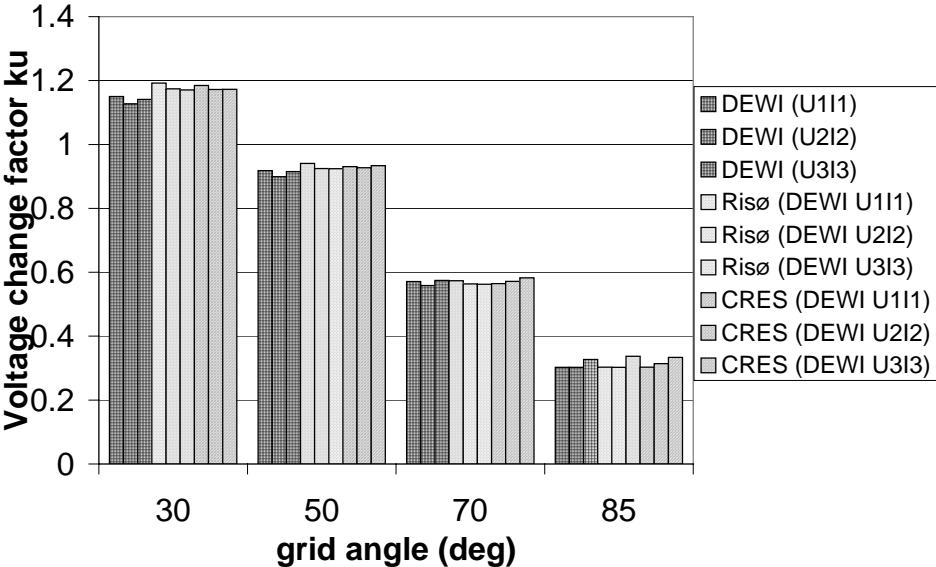
Figure 34. Comparison of calculated voltage change factors k_U *during cut-out.*
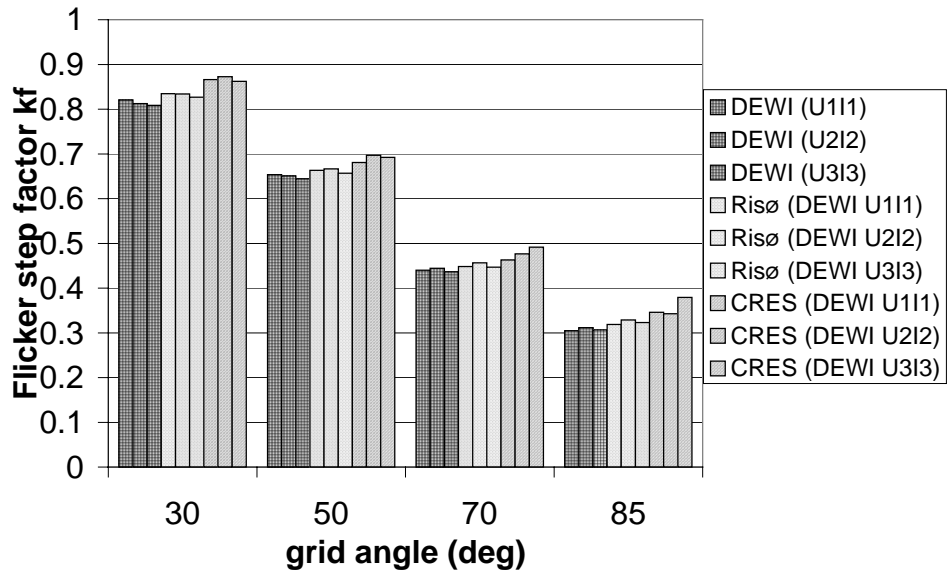
Figure 35. Comparison of calculated flicker step factors k_f *during cut-out.*
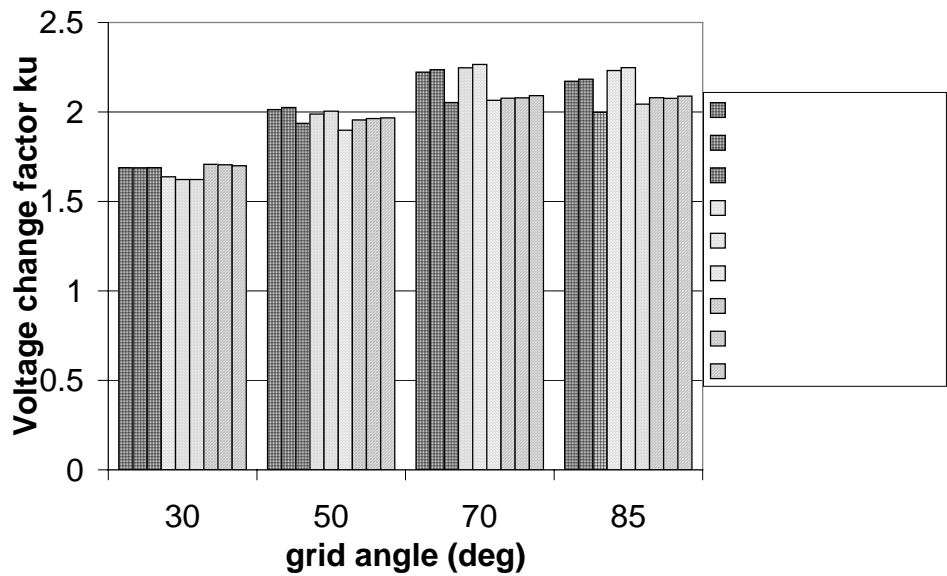
Figure 36. Comparison of calculated voltage change factors k_U *during cut-in.*
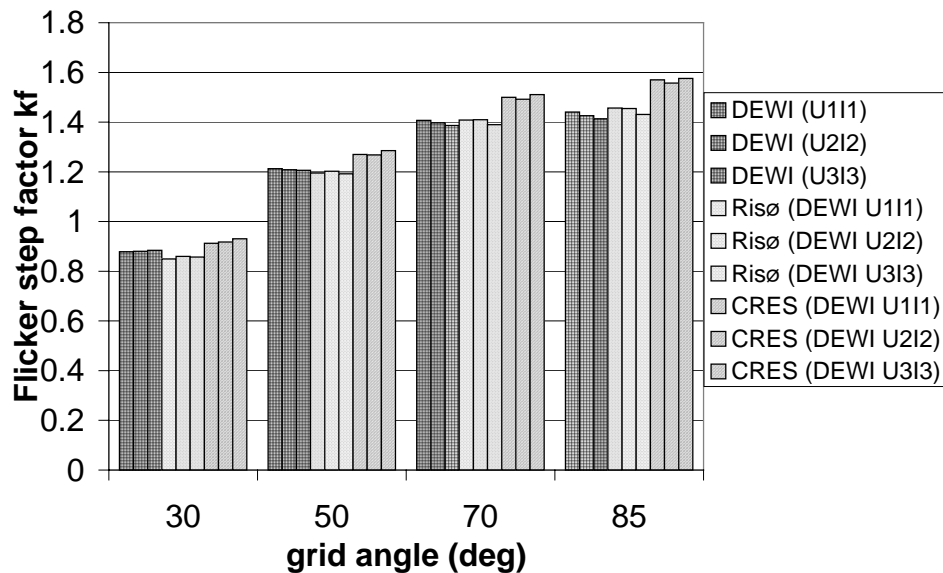
Figure 37. Comparison of calculated flicker step factors k_f *during cut-in.*

6.5.4 Influence of sampling frequency and cut-off frequency

Figure 30 showed how the Pst values for different grid impedance angles depends on the filter cut-off frequency and sampling frequency for continuous operation. It was shown that the cut-off frequency of the filter had very little influence on the flicker severity, but the reduction of the sampling frequency had a significant influence.

For cut-in operations, the soft starter of the Bonus wind turbine generates fluctuating harmonics on the currents. Besides, the switchings of capacitors also cause fluctuating harmonics. It is therefore useful to make a similar test for a cut-in operation.

The 6.4kHz cut-in reference measurement shown in Figure 33 has been applied to investigate the influence of filtering and reduction of sampling frequency for cut-in. The result is shown in Figure 38.
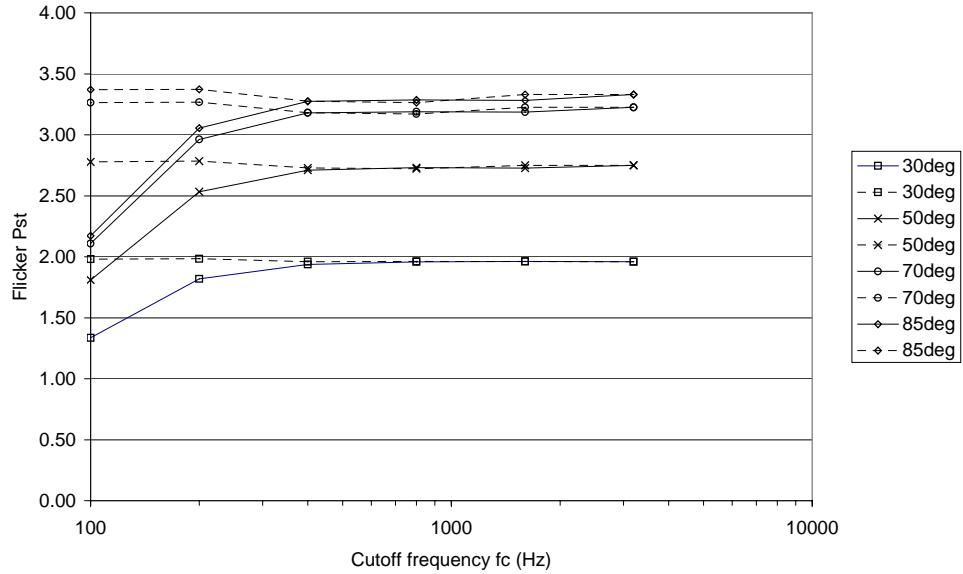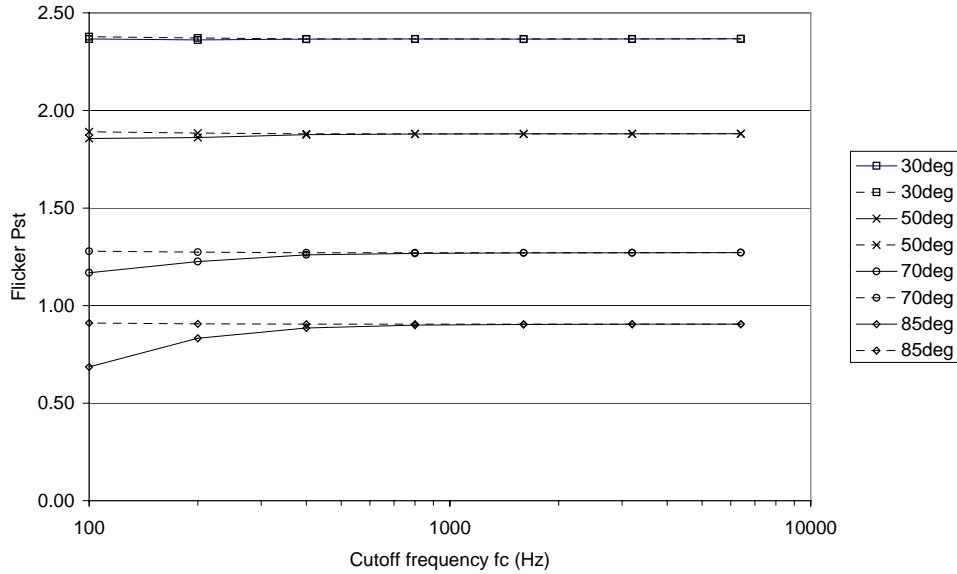
Figure 38. Flicker Pst values for the 6.4kHz DEWI measurement of cut-in operation filtered with the cut-off frequency f$_c$*. The dashed lines keep the original sampling frequency 6.4kHz, and the solid lines the data is reduced to the sampling frequency 2·*f$_c$*.*

It is seen from the dashed lines in Figure 38 that the filtering itself has very little influence on the flicker calculations, like for continuous operation, even though the soft starter generates significant fluctuating harmonics.

The reason for this small influence is that the flickermeter generates the RMS value of the simulated fictitious voltage, and then uses the fluctuations in the RMS value to calculate flicker severity. But the harmonics have very little influence on the total RMS value, because the total RMS value is the square sum of the RMS values of each order, so even a 20 % harmonic of a given order will only add aproximately 2% to the RMS value ($\sqrt{1^2 + 0.2^2} = 1.02$).

It is seen from the solid lines in Figure 38 that the reduction of the sampling frequency plays an even more significant role for this cut-in operation than for the continuous operation in Figure 30. It is also seen that the influence is strongest for high grid impedance angles.

For the sake of completeness, the 6.4kHz cut-out reference measurement shown in Figure 32 has been applied to investigate the influence of filtering and reduction of sampling frequency for cut-out. The result is shown in Figure 39.

Figure 39. Flicker Pst values for the 6.4kHz DEWI measurement of cut-out operation filtered with the cut-off frequency f_c. *The dashed lines keep the original sampling frequency 6.4kHz, and the solid lines the data is reduced to the sampling frequency* $2 \cdot f_c$.

6.6   Harmonics

6.6.1   Comparison of simultaneous measurements

DEWI and CRES measured harmonics simultaneously in Hagshaw Hill. CRES measured 30 minutes with the Voltech and DEWI measured in two 40 second periods, in the beginning and in the end of CRESs measurement period.

The mean values of the measured harmonic currents are shown in Figure 40, and the mean values of the measured harmonic voltages are shown in Figure 41. The harmonic levels are very low as expected. The current harmonics are low because the wind turbine has a directly connected induction generator, and the voltage harmonics are low because the grid is dominated by the induction generators of the wind turbines.

Taking the low harmonic level into account, the agreement between DEWIs and CRESs measurements is good. The specifications of the Voltech is an accuracy of 0.1% of the fundamental. The deviations from DEWIs measurements are less than these 0.1% for all fundamentals.
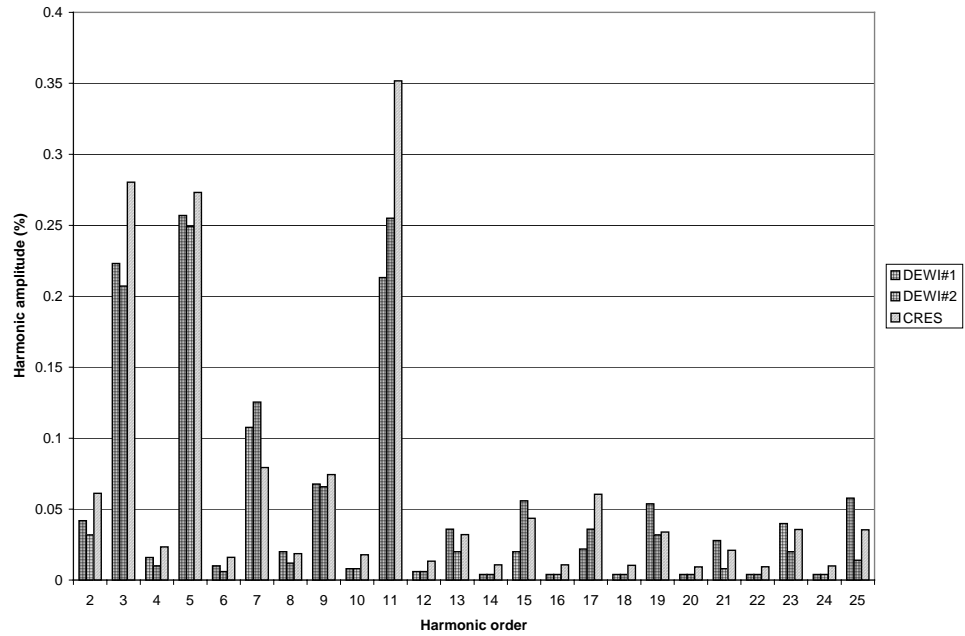
Figure 40. Comparison of simultaneous harmonic current measurements of DEWI and CRES.
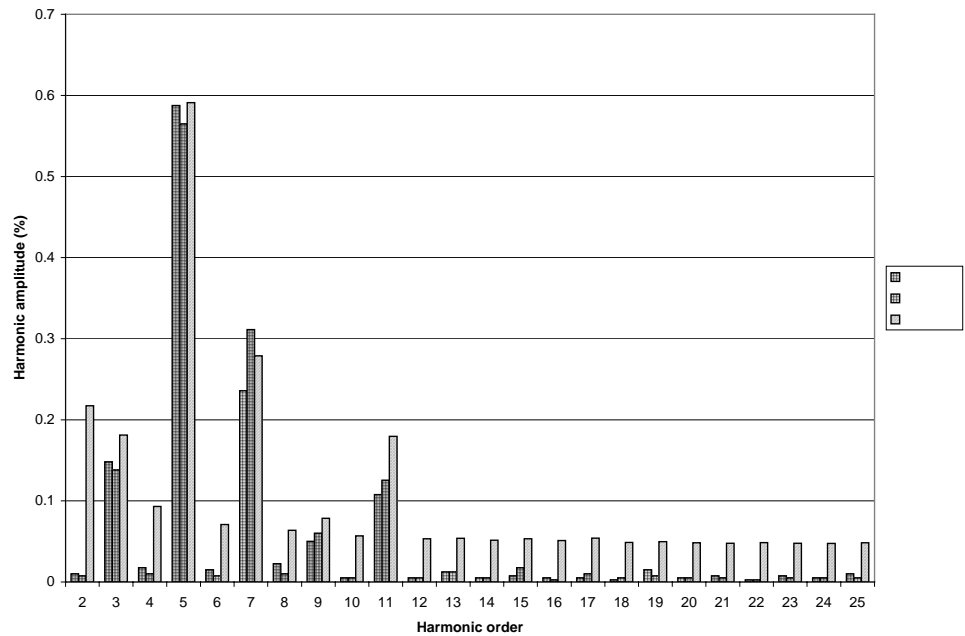
Figure 41. Comparison of simultaneous harmonic voltage measurements of DEWI and CRES.

6.6.2 Comparison of calculation routines

DEWIs 6.4 kHz reference measurements of instantaneous currents and voltages have been used to verify the harmonic calculation routines. DEWI, Risø and CRES have

used the measurements to calculate relative RMS values of each current and voltage harmonic, relative to rated current and voltage respectively.

Figure 42 - Figure 45 below shows the comparison of the calculations. Both mean values and maximum values of current and voltage harmonics are compared. Only up to 25 harmonics are shown because the remainder values are very small. It is seen that the agreement is excellent.
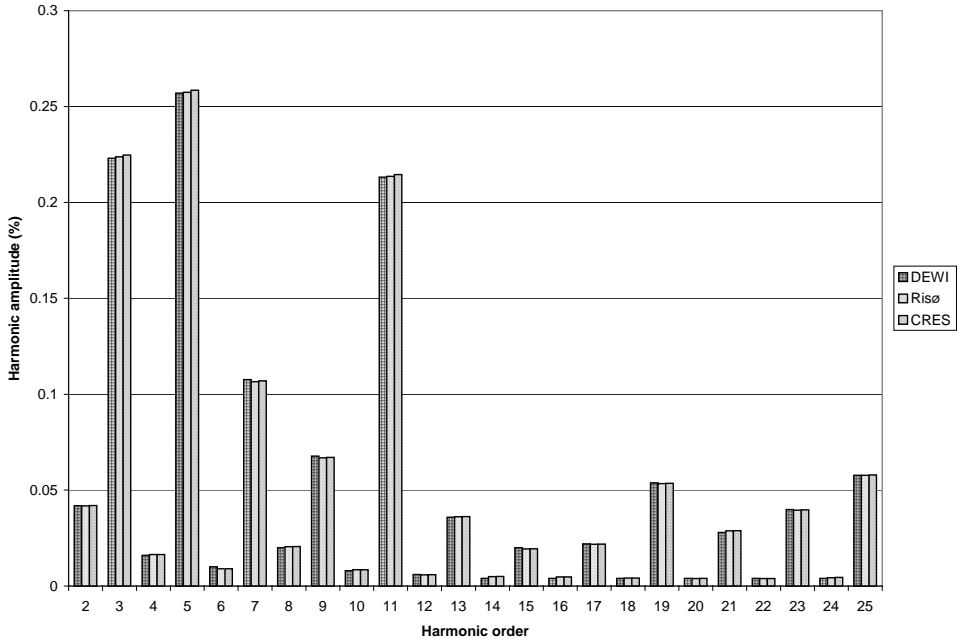
Figure 42. Mean values of harmonic currents in percentage of rated current, calculated on the 40 sec reference time series measured by DEWI.
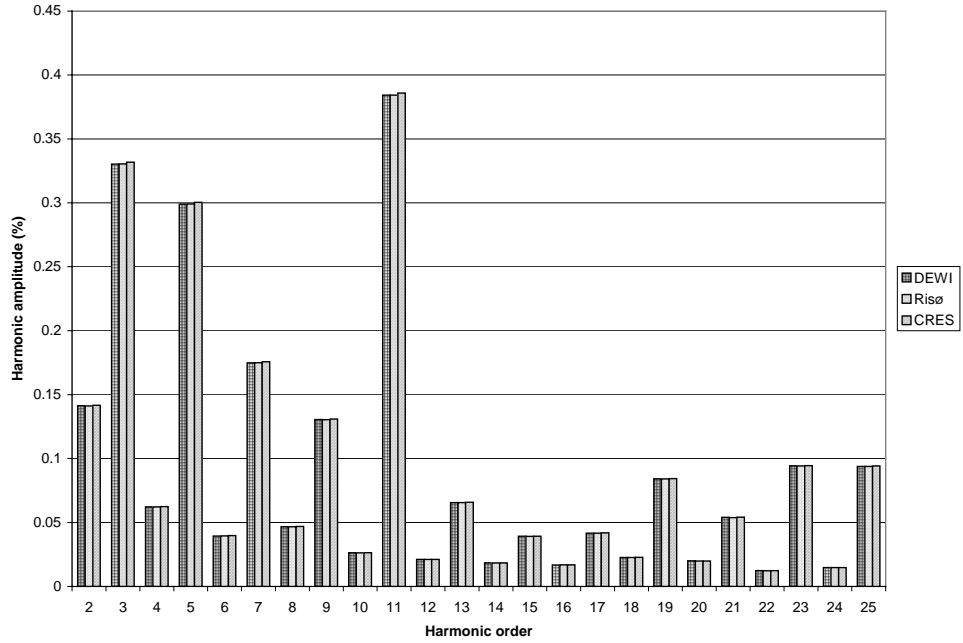
Figure 43. Maximum values of harmonic currents in percentage of rated current, calculated on the 40 sec reference time series measured by DEWI.
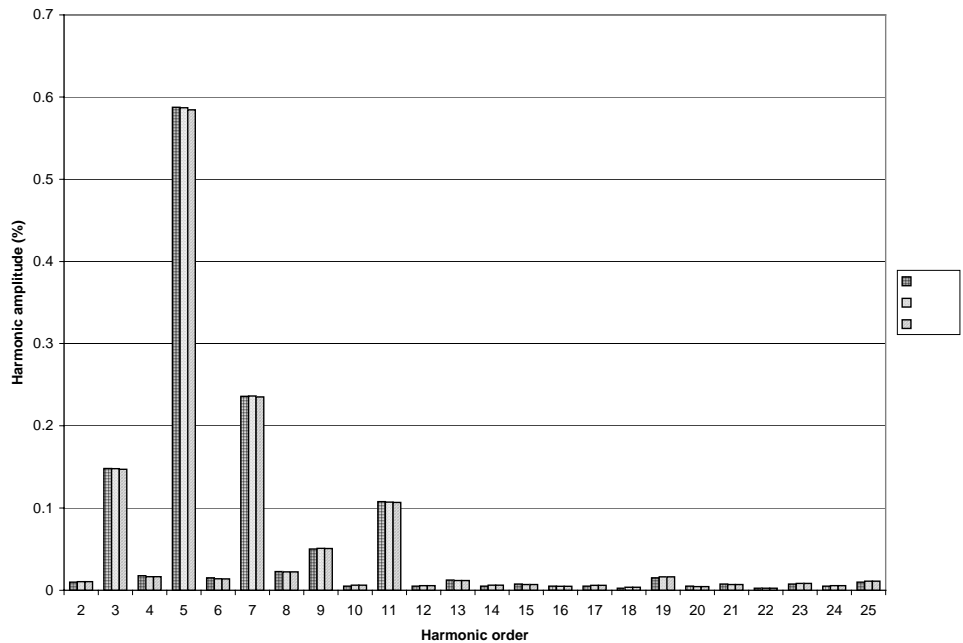
Figure 44. Mean values of harmonic voltages in percentage of rated voltage, calculated on the 40 sec reference time series measured by DEWI.
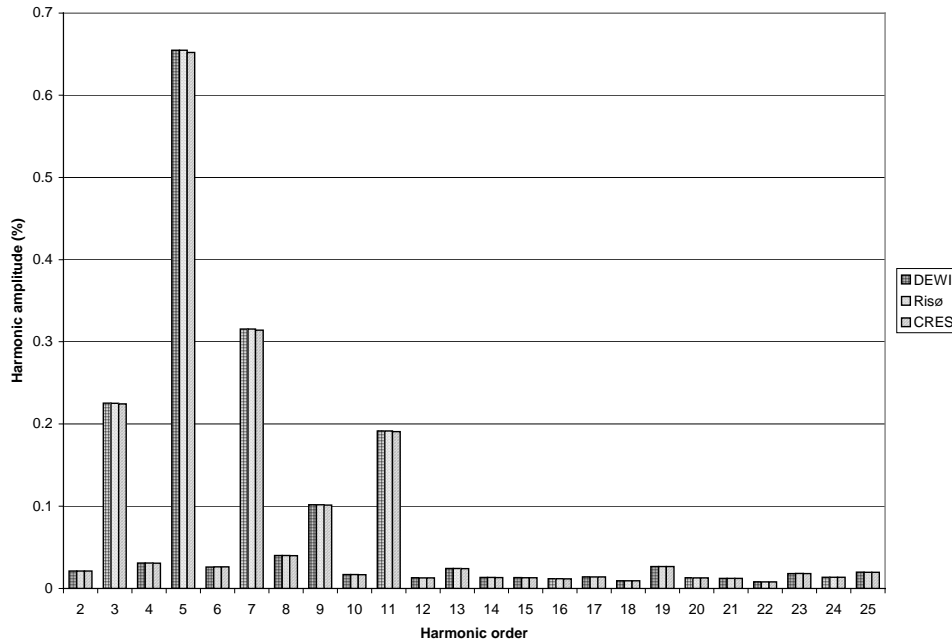
Figure 45. Maximum values of harmonic voltages in percentage of rated voltage, calculated on the 40 sec reference time series measured by DEWI.

7 Constant speed wind turbines

This section is mainly based on the comparison of power quality measurements on two constant speed wind turbines of the same type. The type of the wind turbines is a stall regulated 600 kW Bonus with an induction generator directly connected to the grid. The generator has only one set of windings, corresponding to a single speed.

One of the wind turbines is sited in complex terrain in Hagshaw Hill in Scotland, and the other is sited on the more flat terrain in Gudum in Denmark. The selection of these two sites mainly supports the investigation of the influence of the terrain on the power quality from a qualitative point of you, i.e. answer to the question if the power quality is significantly influenced by the terrain or not.

7.1 Reactive power

The Bonus wind turbines are equipped with capacitor banks to compensate for the reactive power consumption of the induction generator. The capacitor banks are divided into three banks, which are connected subsequently shortly after connection of the wind turbine to the grid. Consequently, all three capacitor banks are always connected during continuous operation.

Figure 46 shows 10 min mean values of the reactive power vs active power measured by Risø with the same power transducers in Hagshaw Hill and Gudum. It is seen that the curves deviate some, which can have a number of explanations, but most likely is a combination.
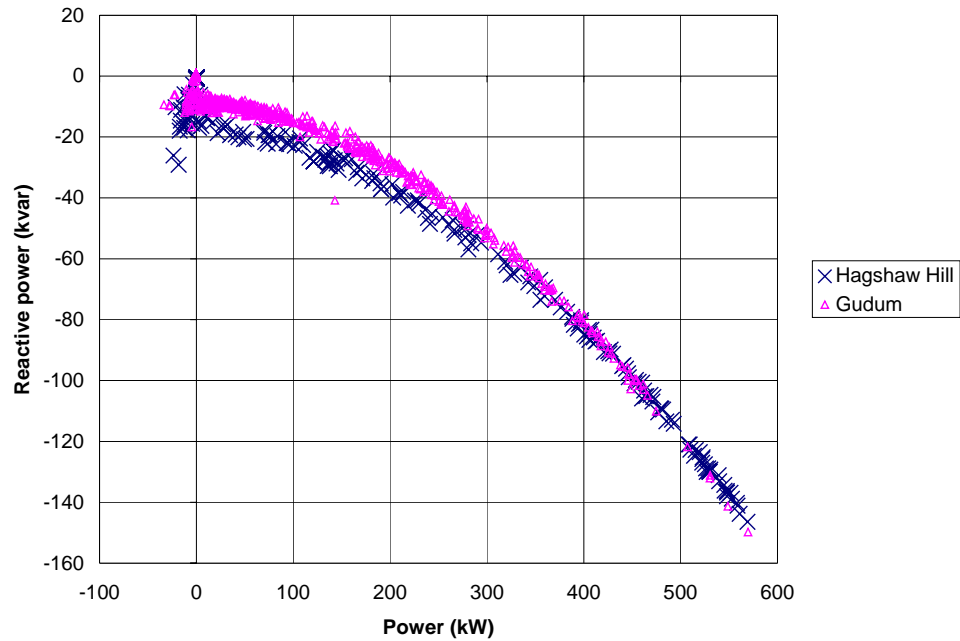
Figure 46. The reactive power consumption of the Bonus 600 kW wind turbine in Hagshaw Hill (Scotland) and Gudum (Denmark)

The idle consumption of reactive power (e.g. the consumption of reactive power when the active power is small) is determined by the magnetising reactance of the induction generator and by the capacitor banks. Increasing voltage will increase the consumed reactive power of the induction generator and increase the produced reactive power of the capacitor banks. Both these components are connected in parallel, so the reactive power will increase with the square of the voltage. When they have approximately same size, they will equalise the changes due to voltage changes. Therefore, the voltage level has a secondary influence on the reactive power consumption of the wind turbine at idle operation.

The two generators are the same type, but deviations in the air gaps size will influence the magnetising reactance. However, the most likely explanation to the difference in reactive power consumption at idle operation is deviations in the capacitor banks. If this is the case, then the capacitor banks in the Hagshaw Hill wind turbine are approximately 10 kvar less than the capacitor banks in Gudum.

When the power increases, the reactive power consumption in Gudum increases faster than in Hagshaw Hill. One reason for this is the different voltage levels on the two sites. Figure 47 shows the voltage levels versus wind turbine power production in Hagshaw Hill and in Gudum. The Hagshaw Hill data is the 5 minutes mean values of DEWIs measurements, and the Gudum data is 10 minutes mean values of Risø measurements.
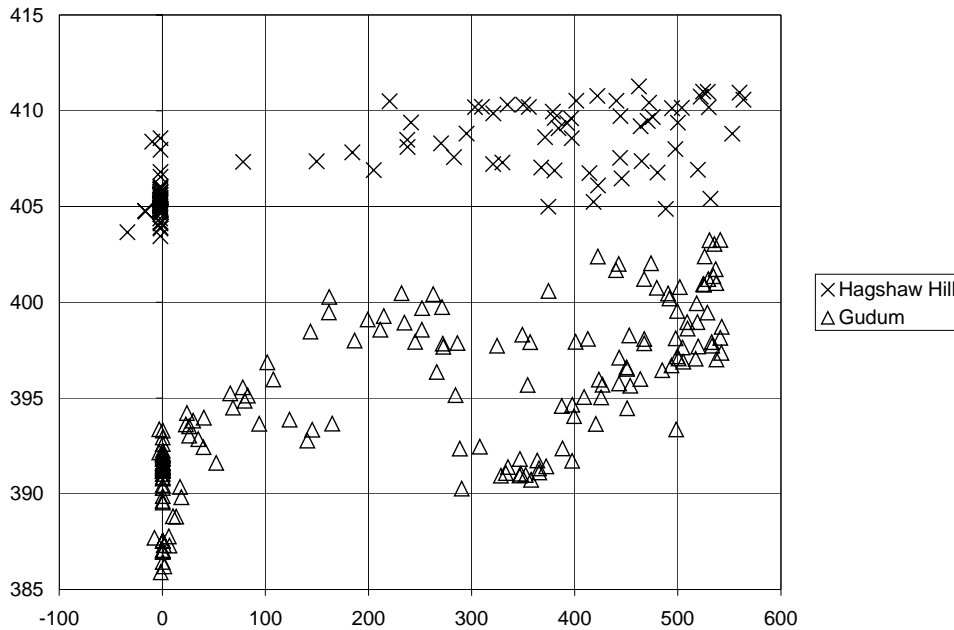
Figure 47. Voltage levels versus wind turbine power production measured in Hagshaw Hill and Gudum

The voltage level is significantly higher in Hagshaw Hill than in Gudum. When the wind turbine power is high, the current is also high, and therefore the leak reactance in the induction generator has increasing influence on the reactive power. When the voltage is higher in Hagshaw Hill than in Gudum, less current is required in the induction generator to transmit the power in Hagshaw Hill. Therefore, the reactive power consumption increases less with increasing power in Hagshaw Hill, compared to Gudum.

7.2   Power variability

The one minute standard deviations versus mean values of the power in Hagshaw Hill and Gudum have been compared in Figure 48. It is seen that for lower power mean values, corresponding to lower wind speeds, the standard deviation is significantly higher in Hagshaw Hill than in Gudum. For power mean values above 400 kW, the standard deviations are more alike in Hagshaw Hill and in Gudum.
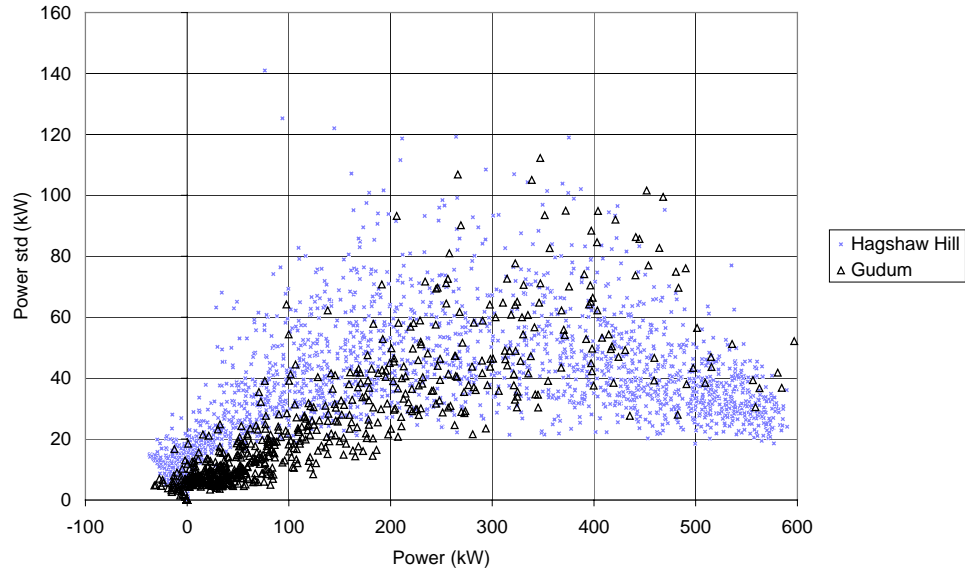
Figure 48. One minute standard deviation vs. mean value of power in Hagshaw Hill (complex terrain) and Gudum (flat terrain).

Risø measurements of wind turbine loads in other sites with complex terrain have shown similar results. The turbulence intensity can be very high at low wind speeds, but drop to a very low level at high wind speeds in complex terrain.

Figure 49 shows the corresponding one minute maximum values of the power. Again, it is seen how the high turbulence in Hagshaw Hill at lower power levels gives higher maximum values. But the overall maximum, which occurs at high mean values, depend very little on the sites in this case. It even seems that the maximum in Gudum becomes higher than in Hagshaw Hill, but this can be due to wake effects. The effect of wakes from other wind turbines has not been included in the present analysis, because the wind direction has not been measured.
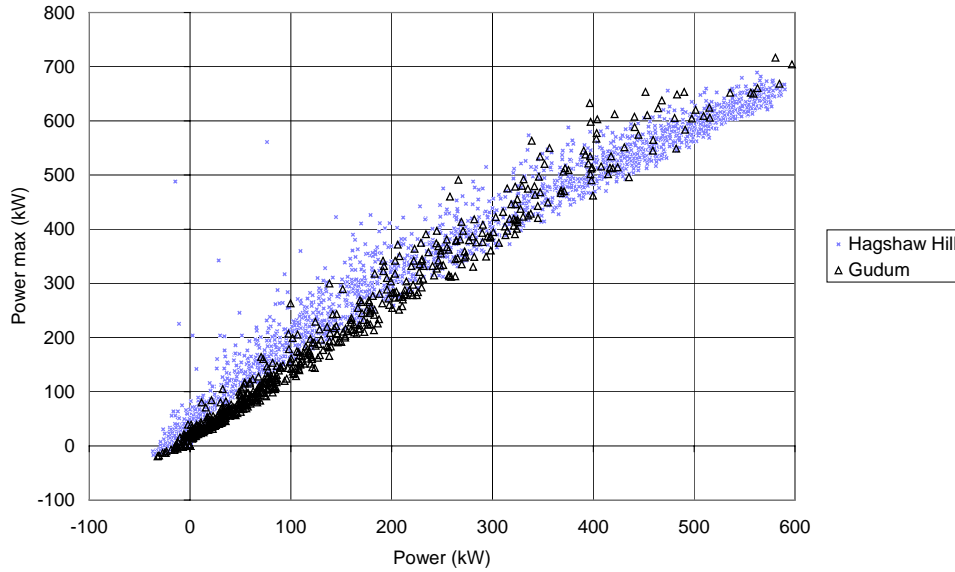
Figure 49. One minute maximum vs. mean value of power in Hagshaw Hill (complex terrain) and Gudum (flat terrain).

7.3 Flicker

7.3.1 Terrain effects

Risøs power measurements have been used to calculate the flicker severity in both Hagshaw Hill and Gudum. 10 minute time series have been applied. Figure 50 - Figure 53 shows the results for different grid impedance angles.

Generally, the Pst values are higher in Hagshaw Hill than in Gudum. This is as expected because the variability in the power is highest in Hagshaw Hill. It is also seen that the flicker values increase faster with power in Gudum than in Hagshaw Hill, like the standard deviations. At 100 kW, the Pst values are approximately 100 % higher in Hagshaw Hill than in Gudum, but at 500 kW, the difference is not much more than 20 %. The 99% percentile of the Pst values will mainly be influenced by the Pst values at high power, so the 99 % percentiles will not be very much higher in Hagshaw Hill than in Gudum.
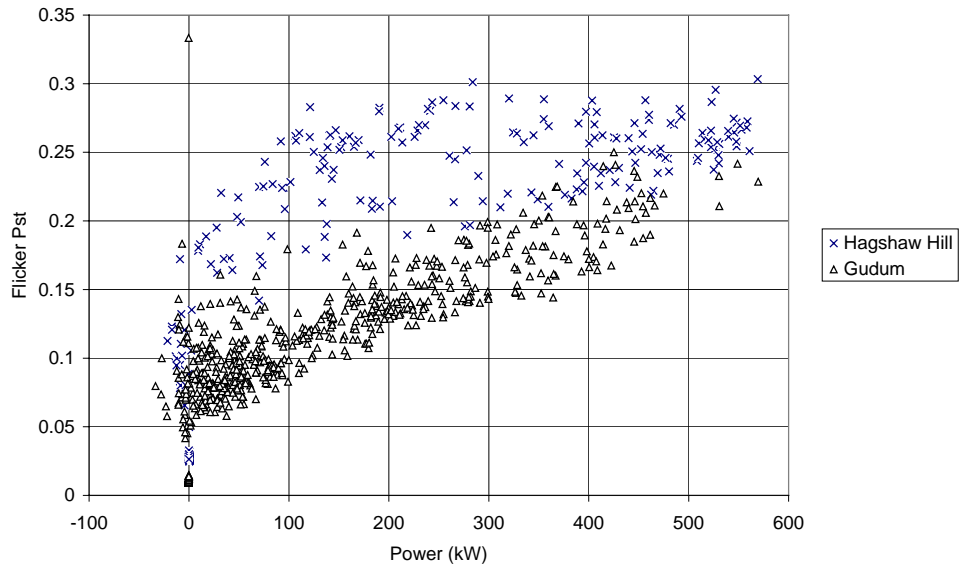
Figure 50 Flicker Pst values vs. active power of Bonus 600 kW wind turbines in Hagshaw Hill (complex terrain) and Gudum (flat terrain).for grid angle 30 deg.
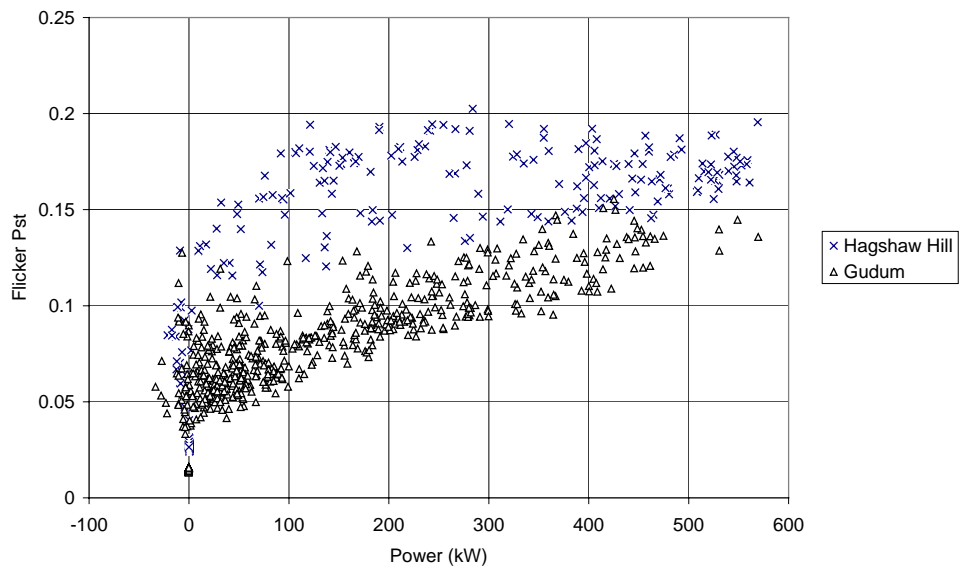

Figure 51. Flicker Pst values vs. active power of Bonus 600 kW wind turbines in Hagshaw Hill (complex terrain) and Gudum (flat terrain).for grid angle 50 deg.
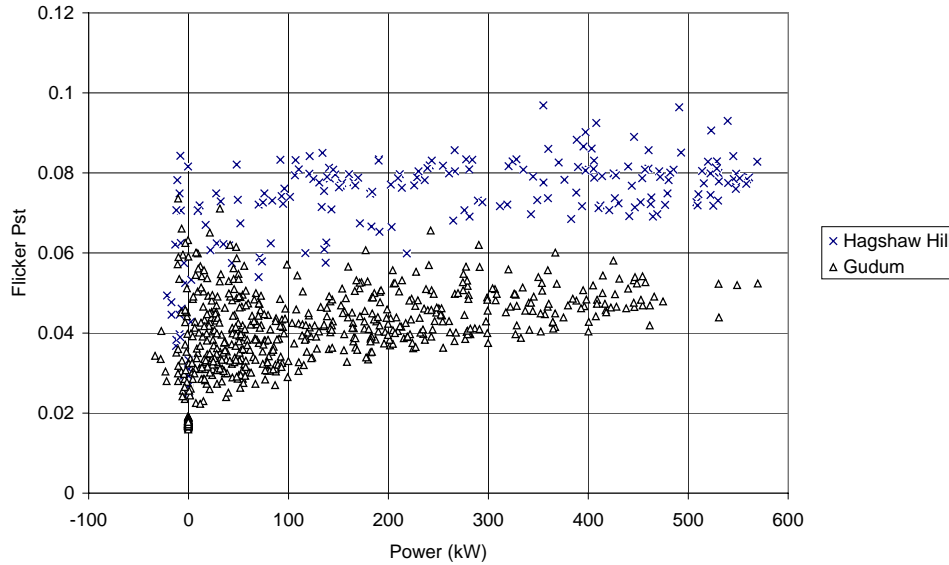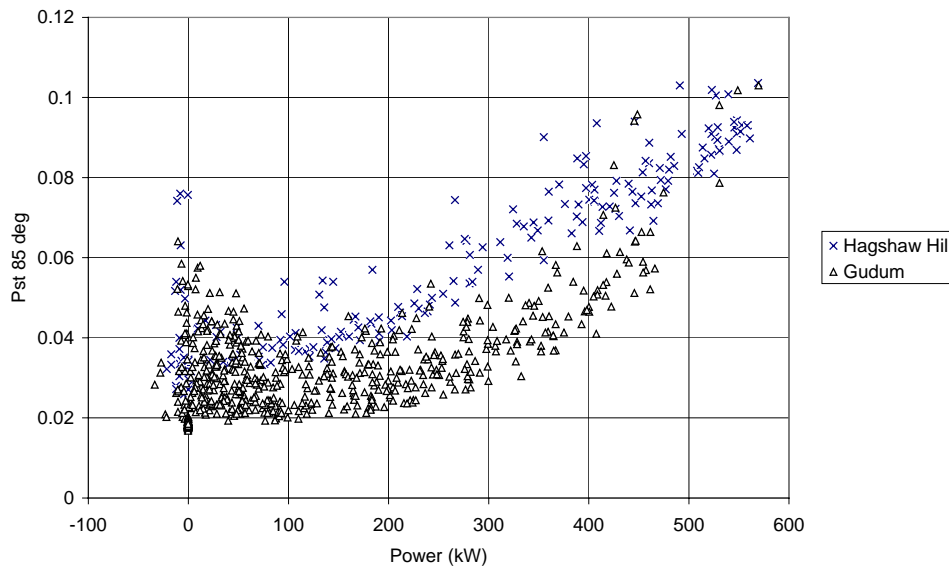
Figure 52. Flicker Pst values vs. active power of Bonus 600 kW wind turbines in Hagshaw Hill (complex terrain) and Gudum (flat terrain).for grid angle 70 deg.

Figure 53. Flicker Pst values vs. active power of Bonus 600 kW wind turbines in Hagshaw Hill (complex terrain) and Gudum (flat terrain).for grid angle 85 deg.

7.3.2   Flicker from wind farms

The calculations in this section on flicker from a wind farm is based on pure power measurements on two 450 kW stall controlled wind turbines in Vindeby in Denmark. The power transducer has a cut-off frequency of 8 Hz., and the reactive power is calculated from the active power based on the PQ characteristics of the generator. To justify this method, it has been tested on measurements on a 600 kW Wind World wind turbine below.

There are two different ways to measure the power; either by using power transducers or by calculating the power from measured time series of the three phase voltages and three phase currents. The short term flicker emission P_{st} from a fixed-speed Wind World 600 kW at different cut-off frequencies has been calculated using three different methods to measure the power:

1. Active and reactive power measured by means of a power transducer. In Figure 55 they are called Pm and Qm. The sampling frequency was originally 5 kHz, the power has been filtered at different cut-off frequencies before the calculation of short term flicker emission P_{st}.
2. Active and reactive power calculated from the three phase voltages and the three phase currents. In Figure 55 they are called Pb and Qb. The sampling frequency of the voltages and currents was originally 5 kHz, the power has been filtered at different cut-off frequencies before the calculation of short term flicker emission P_{st}.
3. From the measured active power the reactive power has been calculated using the reactive power consumption for continuos operation of the wind turbine, see Figure 54. In Figure 55 they are called Pm and Qcalc.
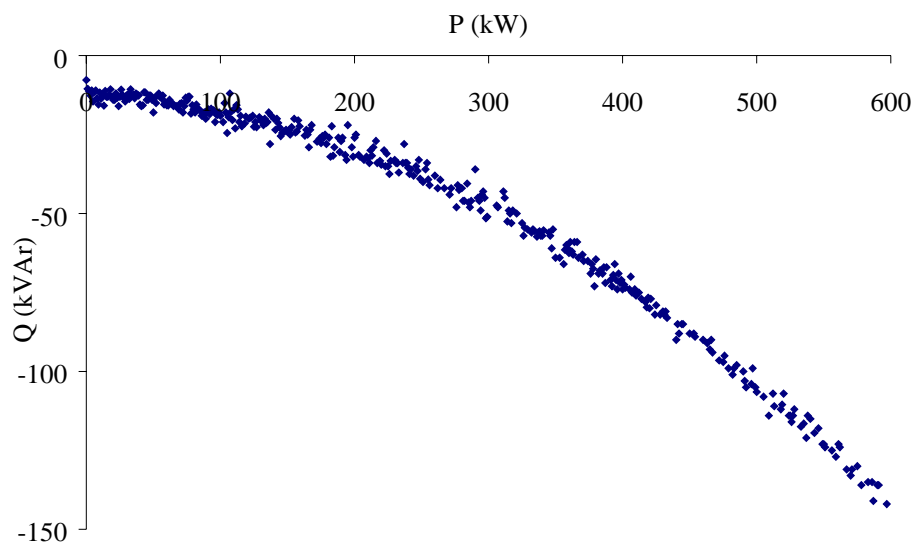

Figure 54. Measured reactive power as a function of active power from fixed-speed Wind World 600 kW wind turbine.

Figure 55 shows the short term flicker emission P_{st} from a fixed-speed Wind World 600 kW at different cut-off frequencies. As can be seen, there is almost no difference in P_{st} between the measured and calculated power, Pm/Qm and Pb/Qb respectively. When it comes to the calculated reactive power, Pb/Qcalc, there is a small difference compared to the measured values, Pm/Qm. The deviation is, although, less than then maximum tolerance of ±5% prescribed for the IEC 61000-4-15 flickermeter standard.
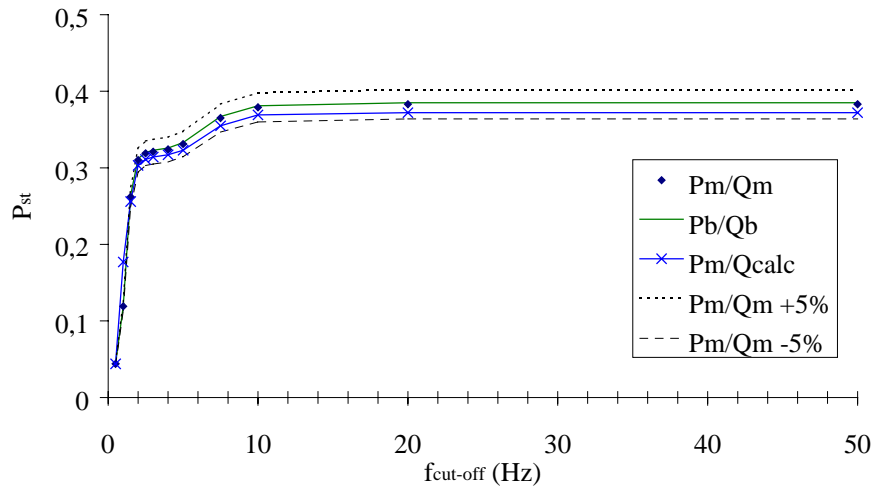
Figure 55. Short term flicker emission P_{st} from a fixed-speed stall-regulated Wind World 600 kW wind turbine calculated at different cut-off frequencies of the measured and calculated active and reactive power.

According to the draft IEC 61400-21, the following equation apply for determine the flicker contribution from more wind turbines connected to a common point:

$$P_{st\,\Sigma} = \sqrt{\sum_{i=1}^{N_{wt}} P_{st,i}^2}$$

where $P_{st,i}$ is the flicker emission from the individual single wind turbine.

Figure 56 shows the calculated short term flicker emission from 30 different measured time series of two constant-speed Bonus 450 kW wind turbines at the Vindeby wind farm.

First, the reactive power consumptions Q_1 and Q_2 of the two wind turbines are calculated applying the *PQ* curves of the wind turbines. Then $P_{st(P1+P2)}$ is calculated as the Pst value generated by the power P_1+P_2 and the reactive power Q_1+Q_2. Then P_{st1} and P_{st2} are calculated as the Pst values generated by the individual wind turbines. Finally, $P_{st\Sigma}$ is calculated as the square sum of P_{st1} and P_{st2}, and compared to $P_{st(P1+P2)}$.
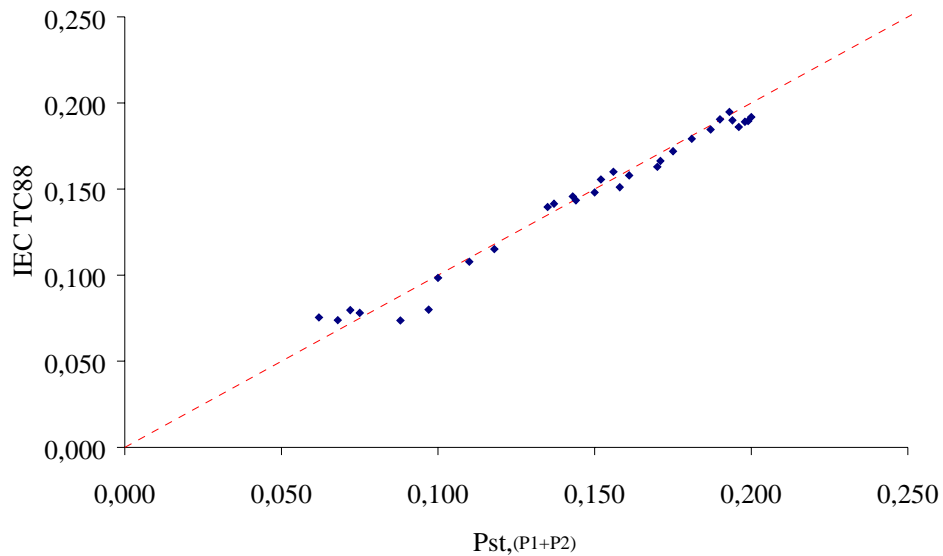
Figure 56. Calculated short term flicker emission from 30 different measured time series of two constant speed Bonus 450 kW wind turbines (dots). The cut-off frequency of the measurements is 8 Hz.

7.4 Transients during switching

The active and reactive power measured by Risø in Hagshaw Hill and Gudum also include runs with cut-ins at cut-in wind speed due to increasing wind speed. The flicker Pst values have also been calculated for these runs, applying the power flicker method. The results are shown in Figure 57 and Figure 58 for grid impedance angle 30 deg and 85 deg respectively. The Pst values for cut-ins are shown together with Pst values for continuous operation, but they can be identified as the group of relatively high Pst values for power values about 0kW.

It is seen from Figure 57 and Figure 58 that the Pst values for cut-ins are significantly higher in Hagshaw Hill than in Gudum. This difference can be due to the higher voltage level in Hagshaw Hill, verified in section 7.1. A higher voltage level will require a higher initial current to magnetise the induction generator, and consequently a higher initioa reactive power consumption.

The voltage has not been measured during the shown cut-in operations. But the reactive power measurements confirm the voltage dependence. In Figure 59, the Pst values in Hagshaw Hill and Gudum are shown versus the minimum reactive power, i.e. the maximum consumed initial reactive power to magnetise the induction generator. Figure 59 shows that the Pst values depend significantly on the minimum reactive power, and that the maximum consumed reactive power is systematically lower in Gudum where the voltage level is lower.
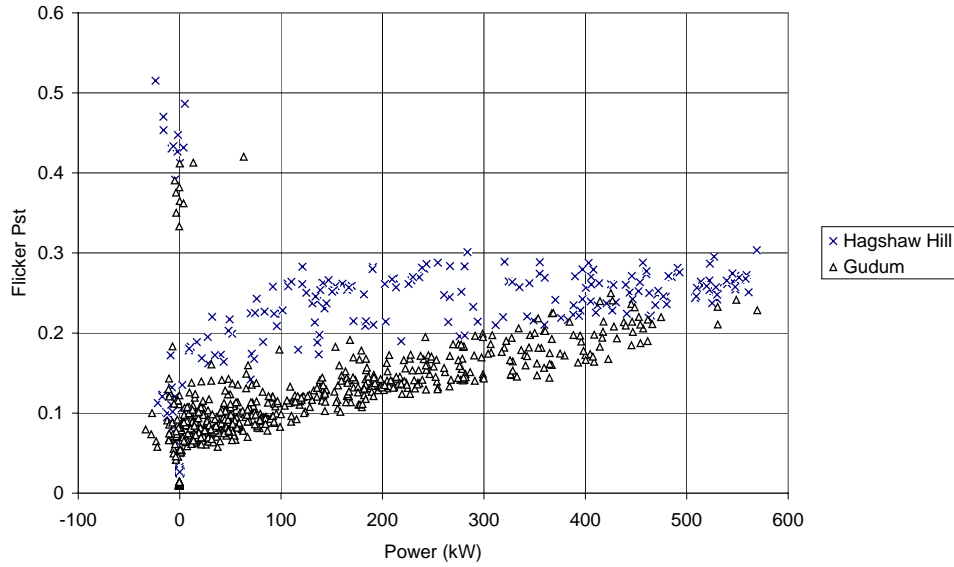
Figure 57. Flicker Pst values vs. active power of Bonus 600 kW wind turbines in Hagshaw Hill and Gudum for grid angle 30 deg, including cut-in operations at cut-in wind speed.
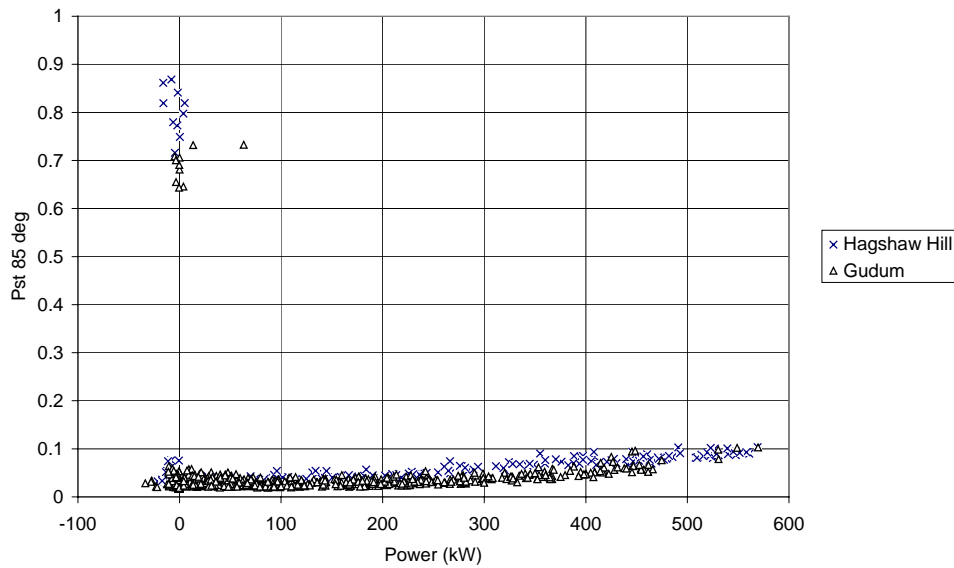

Figure 58. Flicker Pst values vs. active power of Bonus 600 kW wind turbines in Hagshaw Hill and Gudum for grid angle 85 deg, including cut-in operations at cut-in wind speed.
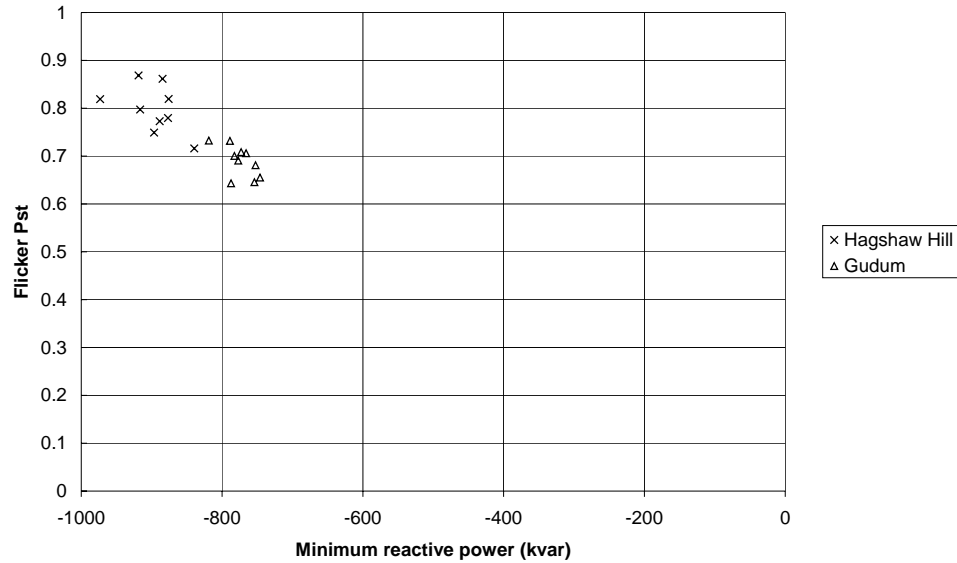
Figure 59. Flicker Pst values for cut-ins at cut-in wind speed, shown vs. minimum (i.e. maximum consumed) reactive power of Bonus 600 kW wind turbines in Hagshaw Hill and Gudum. The grid angle is 85 deg.

If voltage flicker method had been applied, then the difference would probably not have been quite as pronounced. This is because both current and voltage is increasing when the voltage level is high, and both voltage and current contribute to the reactive power, while the current flicker method calculates the flicker based on rated voltage level.

8 Variable speed wind turbines

The measurements in Emden are divided into two different types:
1. Flicker measurements performed at a sampling frequency of 800 Hz. From the measured voltages and currents, active power and phase angle have been calculated. The sampling frequency of the calculated values is 50 Hz and the length of each measurement is 10 minutes.
2. Harmonics measurements performed at a sampling frequency of 12 800 Hz. The length of each measurement is 20 seconds and consists of one phase voltage and one phase current at each location previously mentioned.

8.1 Reactive power

The forced-commutated inverter used in Enercon makes it possible to choose power factor. The power factor may, according to the manufacturer, be chosen freely from 0.96 leading to 0.96 lagging.

Figure 60 shows the measured reactive power as a function of the active power from two different sites. The averaging time in the measurements are in both cases 1 minute. A constant power factor should in this figure give a straight line. As can be seen, the inverter used by Enercon is not able to keep

the power factor constant. The reason to this malfunction may be that the power factor is controlled by measurements performed at the inverter while the power quality measurements are performed at the transformer. Between the inverter and the transformer there are filters connected. At the site in Skåne, the ordinary filters used are complemented with high pass filters. There are, however, different power factors chosen at the two sites. At Gotland the power factor is approximately 0,98 and at Skåne 0,99.
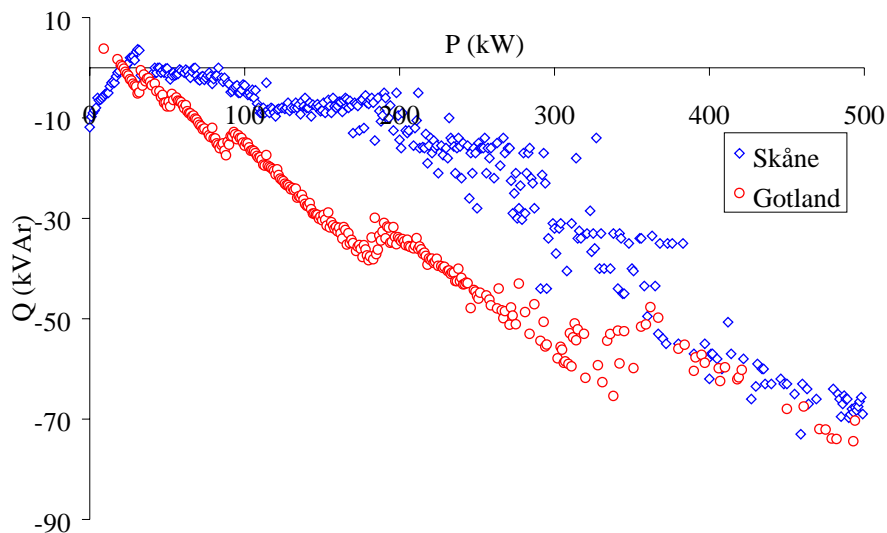

Figure 60. Reactive power as a function of active power from two different sites, Gotland and Skåne.

It is also seen in Figure 60 that the PQ-curves are discontinuous. This discontinuity can not be explained by the filter, but rather by a discretisation in the control system.

8.2 Flicker

8.2.1 Summation of Flicker

Figure 2.7 shows the short term flicker emission from two variable-speed Enercon 500 kW wind turbines at the Emden wind farm calculated with the power flicker method applying power signal filters with different cut-off frequencies. The P_{st} is calculated in two different ways:

1. Directly by using the sum of the time series of power from the wind turbines.
2. By using the summation of $P_{st,i}$ from individual wind turbines according to the draft IEC 61400-21.
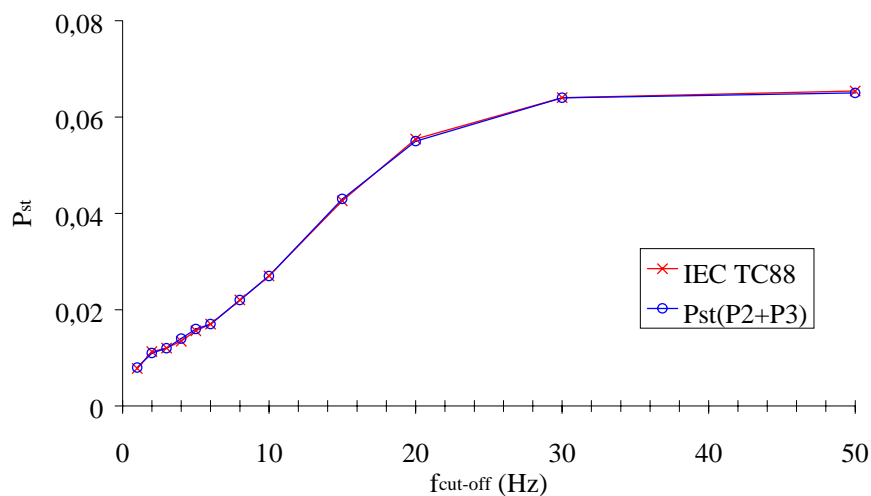
Figure 61. Short term flicker emission from two variable-speed Enercon 500 kW wind turbines calculated at different cut-off frequencies.

There is, as can be seen in the figure, a perfect agreement between the two curves.

Figure 62 shows the calculated short term flicker emission from ten different measured time series of two variable-speed Enercon 500 kW wind turbines. The cut-off frequency of the measurements is 50 Hz. As can be seen in the figure, the short term flicker emission varies due to variations in the wind, i.e. turbulence. The mismatch of the two different ways of calculating the flicker (i.e. deviation from the dotted line) is although small.
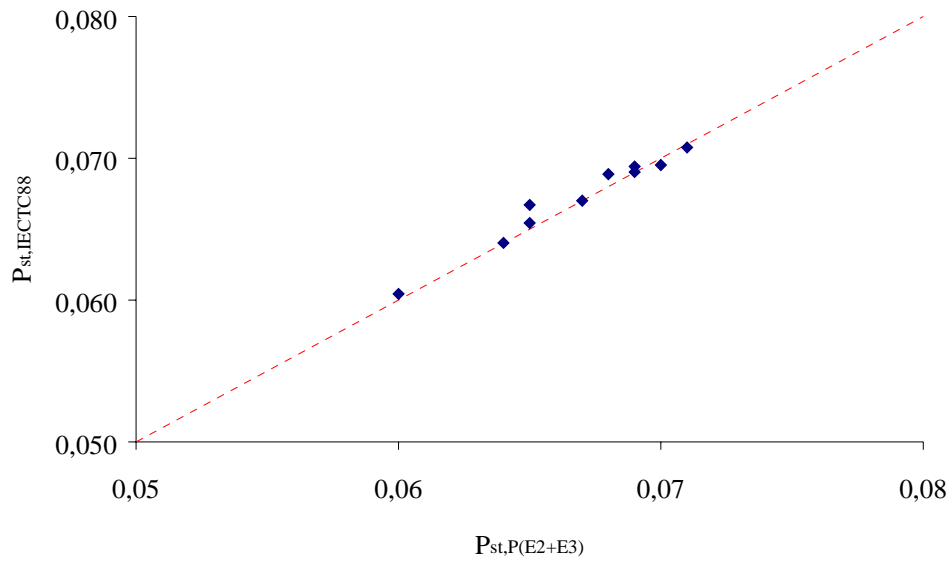
Figure 62. Calculated short term flicker emission from ten different measured time series of two variable-speed Enercon 500 kW wind turbines (dots). The cut-off frequency of the measurements is 50 Hz.

8.3 Transients during switching

8.3.1 Start

Figure 4.1 shows the active and reactive power during start of the Enercon E-40 located in Gotland at high wind speed conditions. At the time, t=30 s., the generator is connected to the grid via the converter. The active power rises slowly from a standstill to rated power. The whole process takes approximately 50 s. During the time the active power rises, the reactive power is controlled in order to keep the power factor constant.
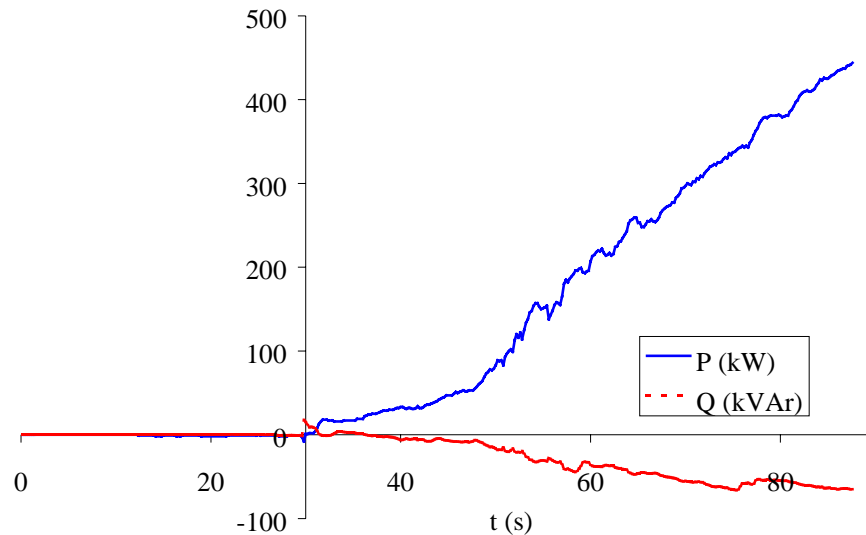
Figure 63. Active and reactive power during start of an Enercon E-40 located in Gotland in high wind conditions. The upper (positive) curve is the active power and the lower (negative) curve is the reactive power.

Figure 64 shows the current during start. As the converter is being connected, a small peak current occurs. The current peak can be seen in the figure at time t=29 s. The current peak is small, only 10% of the rated current, compared to the 200% as sometimes occur at constant speed wind turbines.
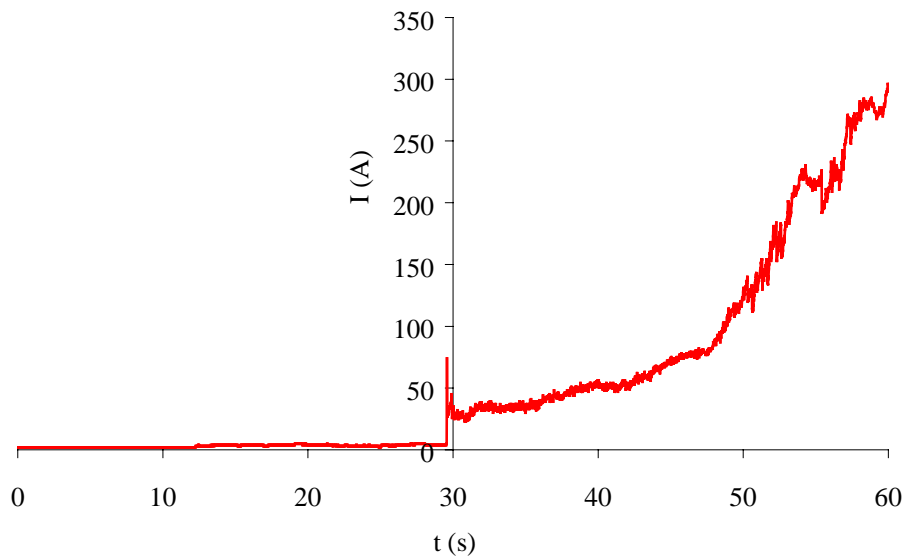
Figure 64. Current during start.

The start during high wind conditions were measured on the Enercon E-40 located at Gotland. An other start during lower wind conditions is shown in Figure 4.3. The measurements are taken from an Enercon E-40 located at Skåne in Sweden.

When the wind turbines were installed, some interference with the telephone lines were observed. In order to eliminate this interference, the Enercon wind turbines were equipped with extra filters. The installed filters are of a high-pass type including capacitors. In Figure 4.3 the connection of the filters can be seen at time, t=3 s. When the filters are connected to the grid, the capacitors in the filters start to produce reactive power. The reactive power from the turbine is then being controlled at time, t=30 s., when the inverter starts to operate.
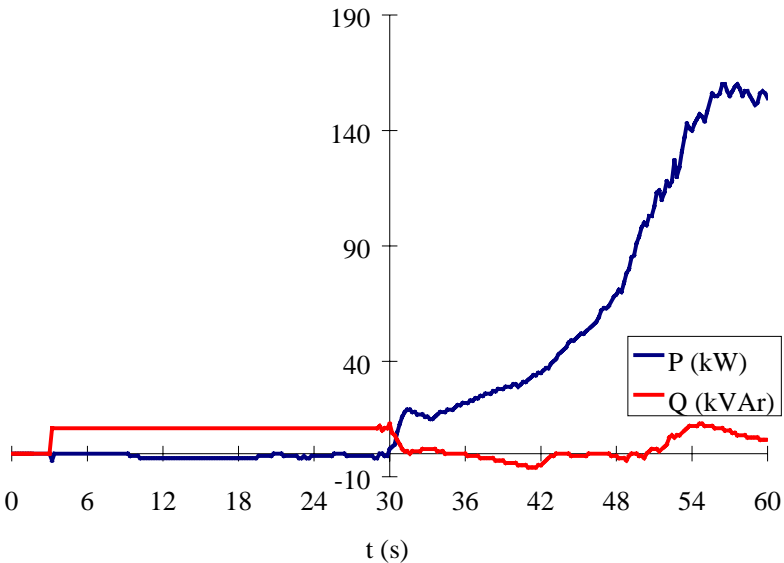

Figure 65. Active and reactive power during start of the Enercon E-40 located in Skåne. The upper (positive) curve is the active power and the lower (negative) curve is the reactive power.

8.3.2 Stop

Figure 66 shows the stop of an Enercon E-40 in high wind conditions. As can be seen, the wind turbine is operating at rated power. At time, t=16 s. the power from the wind turbine begins to be reduced. Four seconds later the power is reduced from rated power down to zero.
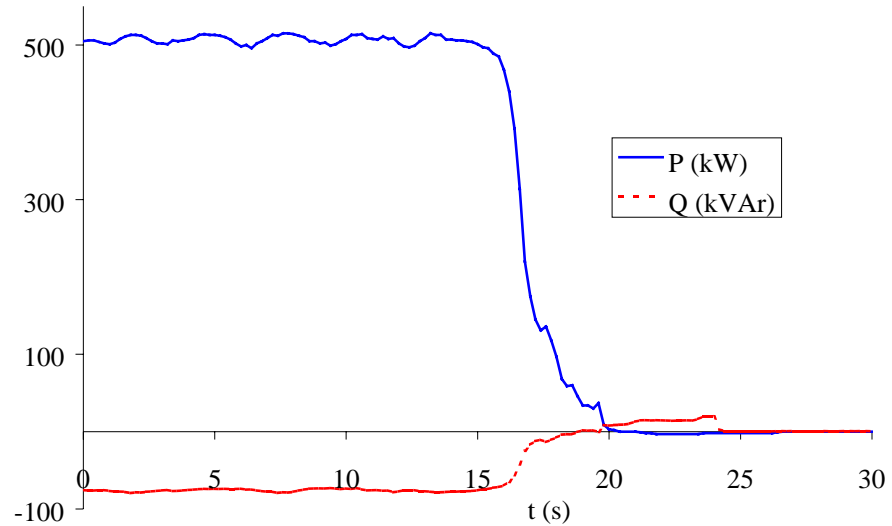

Figure 66. Active and reactive power during stop of an Enercon E-40 in high wind conditions. The upper (positive) curve is the active power and the lower (negative) curve is the reactive power.
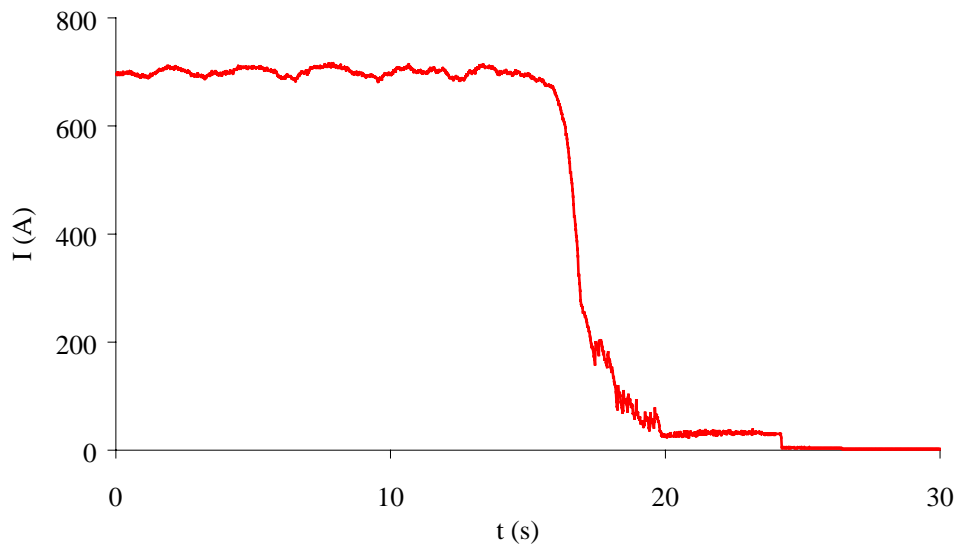
Figure 67 shows the current during stop.

Figure 67. Current during stop of an Enercon E-40 in high wind conditions.

8.4 Harmonics and interharmonics

Harmonics and interharmonics are defined in IEC 61000-4-7 [4]. The studies in this chapter are based on the revision version [8], which is quite similar to [4].

The signal which is to be analysed is sampled, A/D-converted and stored. These samples form a window of time ("window width") on which discrete Fourier transform is performed. The window width shall, according to the CD of the revision of IEC 61000-4-7, be 10 lineperiods in a 50 Hz system. This window width will give a distance between two consecutive interharmonic components of 5 Hz. Figure 68 shows the interharmonic components in the measured current from an Enercon E-40 at Gotland. The current is analysed in accordance with IEC 1000-4-7.
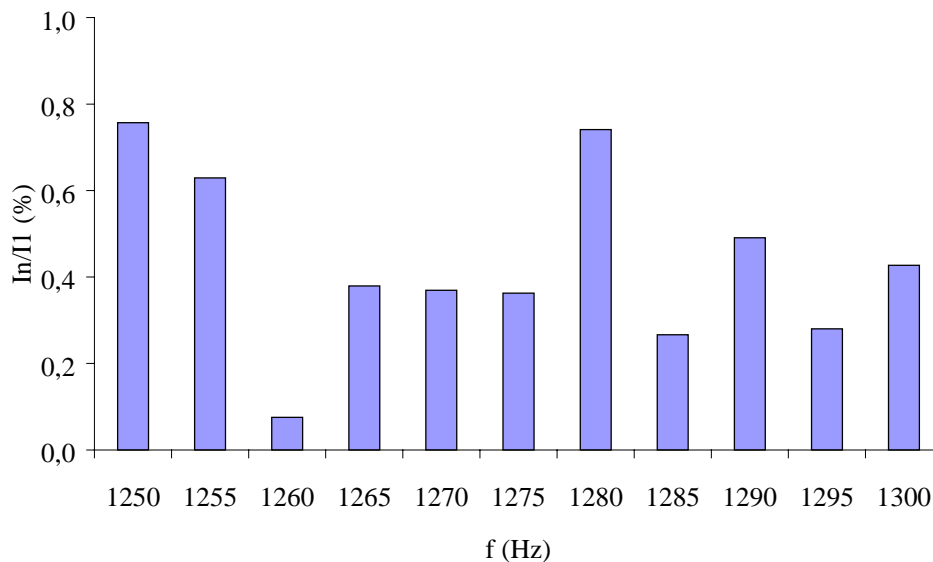
Figure 68. Current interharmonics content between 1250-1300 Hz from a variable speed Enercon 500 kW wind turbine.

The definition of harmonics is, according to the CD of the revision of IEC 1000-4-7, components at frequencies which are multiples of the supply frequency, i.e. 100 Hz, 150 Hz, 200 Hz etc.

Interharmonics are in a similar way defined as components of frequencies located between the harmonics of the supply frequency. The RMS value of all interharmonics components between two consecutive harmonic frequencies forms a interharmonic group. The interharmonic group frequency is the centre frequency of the harmonic frequency between which the group is situated. That is, a group between the harmonic orders n and n+1 is designated with n+0.5, i.e. the group between n=5 and n=6 is designated n=5.5.

Figure 69 shows the harmonics and interharmonic groups of order 20 to 25 of the measured current from an Enercon E-40 at Gotland.
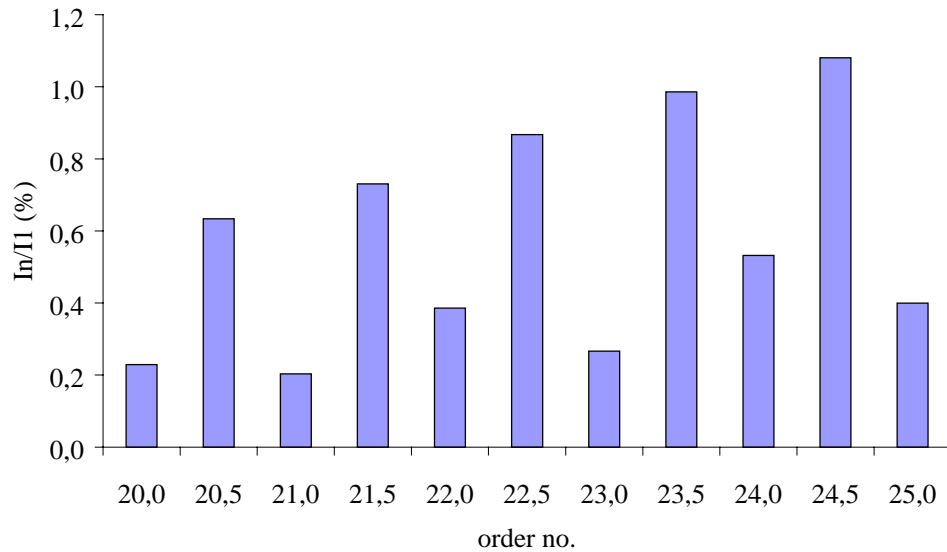
Figure 69. Current harmonics and interharmonic group from an variable speed Enercon 500 kW wind turbine.

8.4.1 Impact of window size

The window width shall according to the CD of the revision of IEC 61000-4-7 be 10 lineperiods in a 50 Hz system. A 10 lineperiod window width gives, as illustrated in Figure 3.1, a distance between two consecutive interharmonic components of 5 Hz.

If a window width of 16 lineperiods are used instead, the distance between two consecutive interharmonic components will be 3.125 Hz. Figure 70 shows the interharmonic components using a window width of 16 lineperiods. The current used in the figure is the same current as in Figure 68.
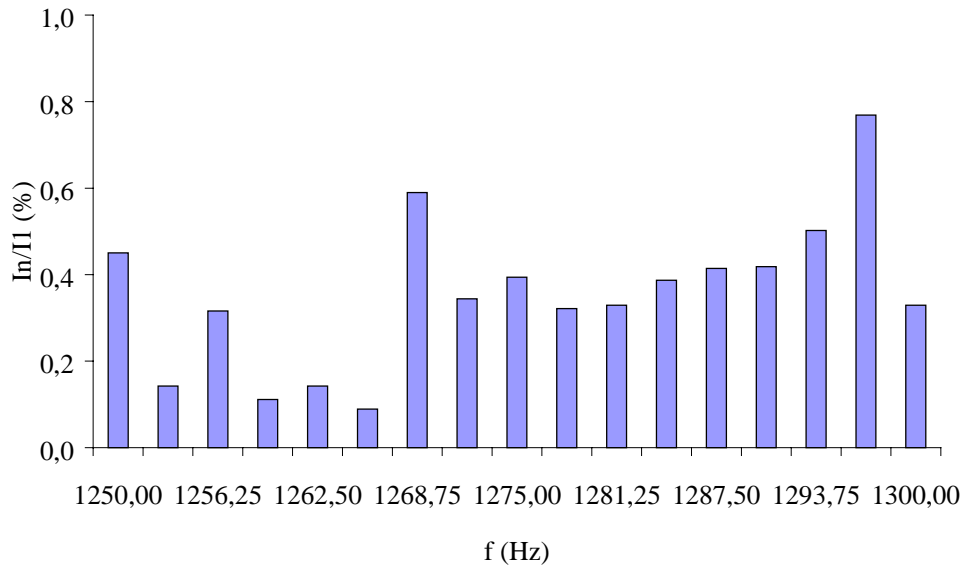
Figure 70. Interharmonics content in current using a window width of 16 lineperiods.

The use of a larger window decreases the distance between two consecutive interharmonic components. As a consequence, each interharmonic component will have a smaller content. Figure 71 shows the harmonics content in the same current using a window width of 10 and 16 lineperiods. As can be seen, the harmonic content will be larger in the smaller window. Note: an exact comparison can not be made since one window is 16 lineperiods and the other just 10 lineperiods.
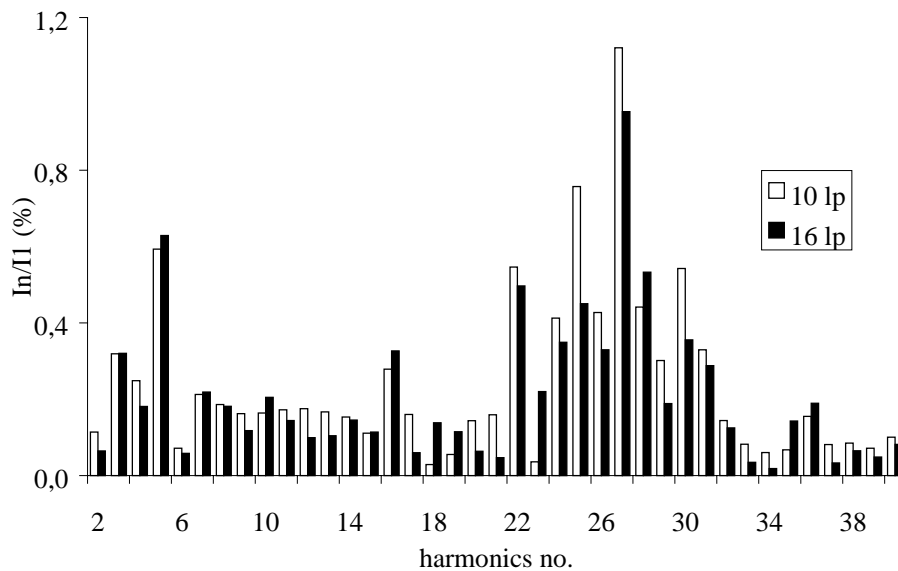

Figure 71. Harmonics content in current using a window width of 10 and 16 lineperiods.

Since the 10 lineperiod window only consists of 9 interharmonics between each harmonic, the interharmonic groups will only get 9/10 of the energy compared to 15/16 in a corresponding 16 lineperiod window. This will result in a smaller interharmonics group content for the 10 lineperiod window. Figure 72 shows the content in the interharmonics groups using a window width of 10 and 16 lineperiods.
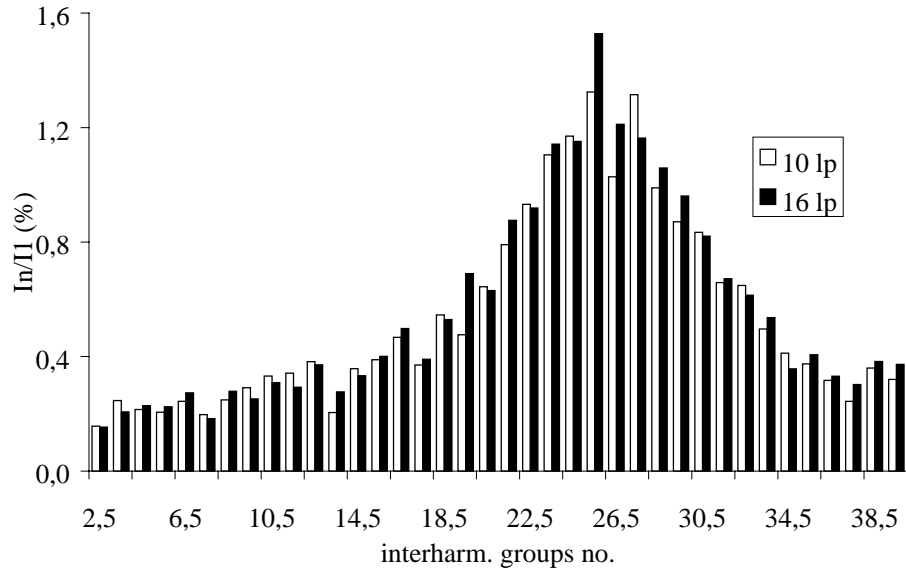

Figure 72. Interharmonic groups using a window width of 10 and 16 lineperiods.

8.4.2   Harmonics

At the Emden wind farm, DEWI have measured the current and voltages at the low and the high voltage sides of the transformer on one Enercon wind turbine. The current on the low voltage side has been measured using a clamp-on current transformer. On the high voltage side, the existing current transformers for the energy-meter has been used. In Figure 73, the harmonics content of the measured currents at the low and the high voltage side are shown.
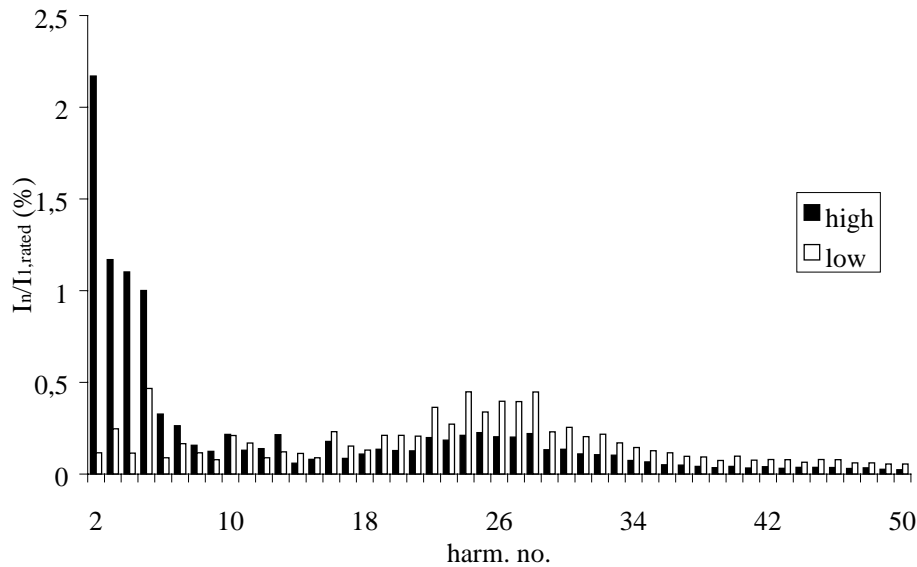
Figure 73. Current harmonics content on the low and the high voltage side of transformer from an variable speed Enercon 500 kW wind turbine.

There is a discrepancy between the current harmonics content on the low voltage and the high voltage side of the transformer. As can bee seen in the figure, the lower order harmonics (<10th order) measured on the high voltage side are much higher than the corresponding harmonics measured on the low voltage side. Most likely, this discrepancy emanates from a DC-saturation of the current transformer at the high voltage side which gives rise to additional harmonics.

When it comes to the higher order harmonics, the situation is the opposite. The harmonics content of the high voltage side are lower compared with the harmonics content on the low voltage side. This can be due to a limited bandwidth in the current transformer used at the high voltage side and due to the filtering of the transformer. It should be mentioned that the bandwidth of the clamp-on current transformer used at the low voltage side, 5 kHz, is sufficient.

The Enercon wind turbine is equipped with a 12-pulse inverter using IGBT valves. This implies that the first harmonics should appear around the switching frequency of the IGBT. The switching frequency of IGBTs can be rather high (5-10 kHz). One advantages with a high switching frequency is a low harmonics content, but the drawback is increased losses in the inverter. Hence, the switching frequency must be optimised regarding to losses and quality of power. The switching frequency must not be fixed, the controller could either employ a PWM pattern or it could be of the simple on-off-type having a small histories band which creates a lower limit for the time interval between two subsequent switching operations.

Figure 74 shows the harmonics content on the low voltage side of Enercon E-40. The measurements originates from two different sites, Emden in Germany and Gotland in Sweden. As can be seen in the figure, the harmonics content in the current from the two sites are almost identical. The largest discrepancy is on the 2:nd order harmonic, where the content at Gotland is 0,65% while it only is 0,2% at Emden. The large 2:nd order harmonic at Gotland does most likely depend on lack of phase-lock on the measurement equipment used at Gotland.

The switching frequency of the IGBTs is, as mentioned earlier, not fixed and it seems to be around 1 to 1,5 kHz, i.e. harmonics of order 20 – 30. In the figure a whole range of harmonics between 20 and 30 can be noticed. The harmonics content in Figure 3.11 is calculated as a mean value over several seconds.
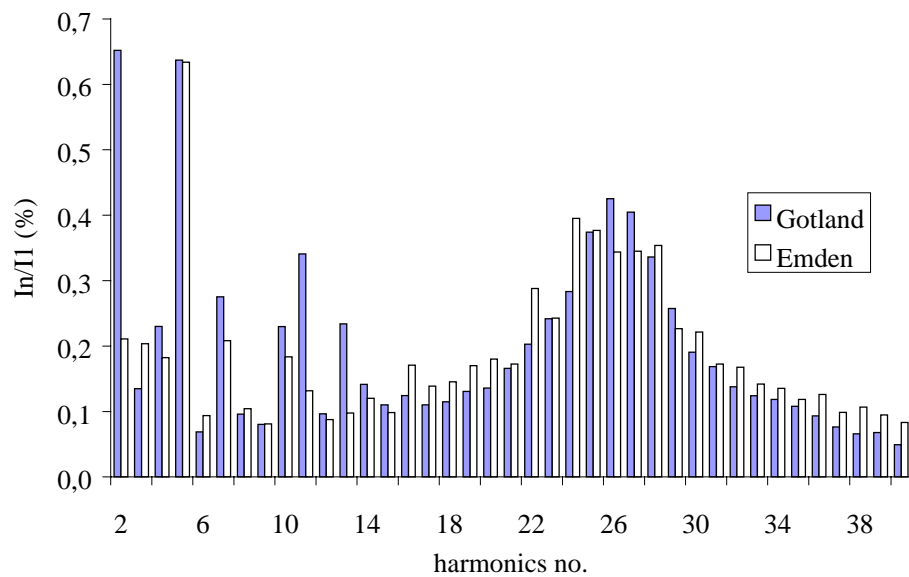

Figure 74. Current harmonics content on low side of transformer from two different variable speed Enercon 500 kW wind turbine. One site is Emden in Germany and the other site is Gotland in Sweden.

If the harmonics content is calculated as an instant value, just one harmonic round the switching frequency should appear. Figure 75 shows the harmonics content for 3 different sets of 10 lineperiods of the measured current. As can be seen in Figure 75, the harmonics content around the switching frequency varies all the time and are different for the three sets of 10 line periods.
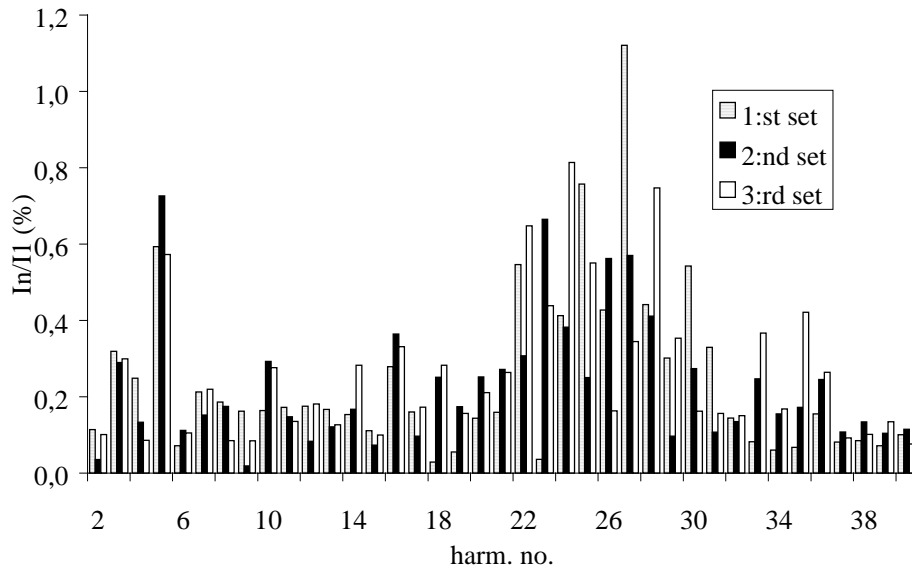
Figure 75. Harmonics content in current on the low voltage side of the trans-former.

The current also contains lower harmonics, for example 3rd, 5th and 7th order. These harmonics may originate from two different sources:

1. The low order harmonics may emanate from the inverter. A simple control of an inverter is simply to generate a current with the same shape as the voltage. If the voltage contain lower order harmonics, the current will also contain lower order harmonics.
2. In the Enercon, there are also other control equipment's and inverters used. For example, each blade has an electrical pitch mechanism by means of an electrical machine and a drive. Simple types of electrical drives (6-pulse and thyristors) generates harmonics of order 5th, 7th, 11th, 13th, etc. and single phase switched equipment generates harmonics of 3rd order.

Figure 76 shows the 5th and 7th order current harmonics as a function of the 5th and 7th order voltage harmonics from two different sites, Gotland and Skåne. At both sites, the same measurement equipment has been used, Siemens Oscillostore P 513. As can be seen in the figure, the 7th order current harmonics from the inverters are almost linear in relation to the 7th order voltage harmonic. Also the 5th current harmonics are increasing with an increasing 5th order voltage current, although not linear.
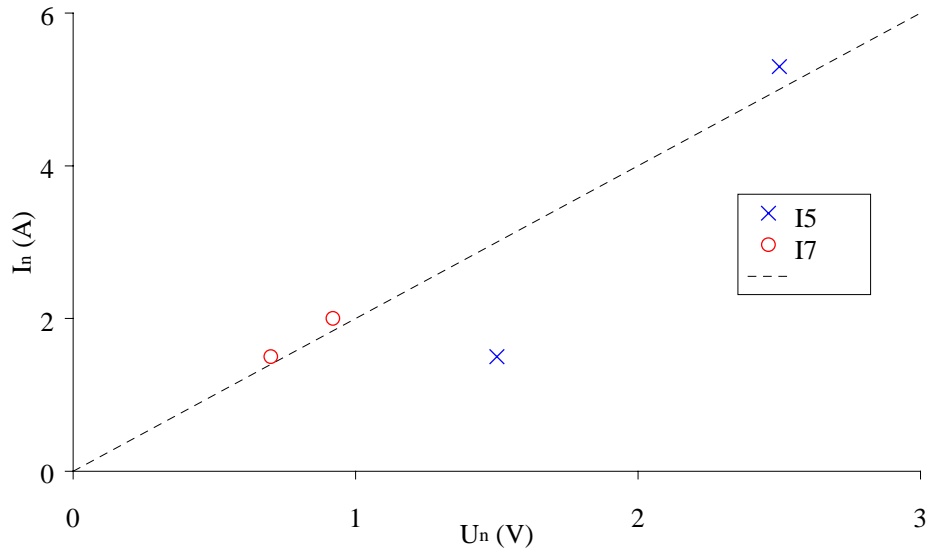
Figure 76. 5ᵗʰ and 7ᵗʰ order current harmonics as a function of 5ᵗʰ and 7ᵗʰ order voltage harmonics from two different sites, Gotland and Skåne. The dotted line just show linearity.

8.4.3 Summation of harmonics

Total harmonics content from more wind turbines is depending on what specific type of harmonics the wind turbines generates. According to IEC 61000-3-6 [9], the resulting harmonic current of order *n* is

$$I_{n,tot} = \sqrt[a]{\sum_i I_{n,i}^a}$$

were the following set of the factor *a* may be used:

Table 5. Summation exponents for harmonics.

a	harmonic order
1	h<5
1,4	5≤h≤10
2	h>10

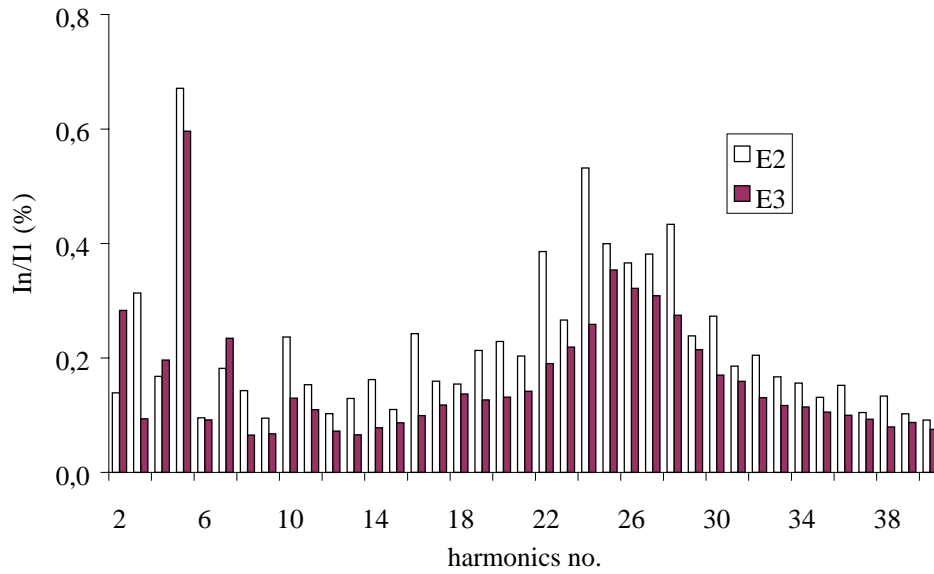Figure 77 shows the harmonics content from two Enercon E-40.

Figure 77. Harmonics content in current on low voltage side of transformer from two different Enercon E-40.

Figure 78 shows the harmonics content from the sum of the two Enercons and the calculated content. The harmonics content from the sum of the two Enercons is derived from the sum of the measured time series of the current. The calculated harmonics content has been performed by applying equation 4 on the harmonics content for each Enercon presented in Figure 77.
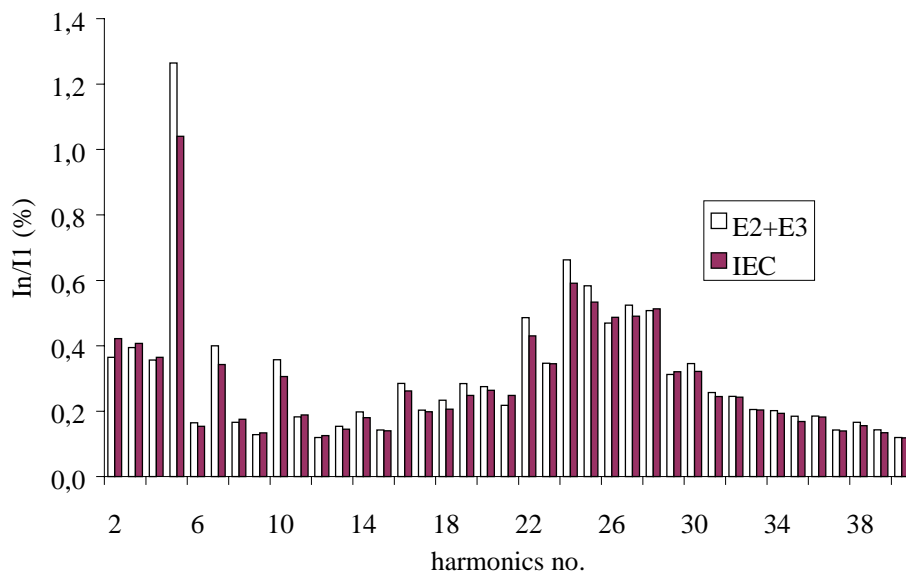

Figure 78. Calculated harmonics content from two different Enercon E-40 by means of the time series of current and by means of equation 4.

8.4.4 Interharmonics

Enercon wind turbines do not only produce harmonics, they also produce interharmonics, i.e. harmonics which are not a multiple of 50 Hz. Since the switching frequency of the inverter is not constant but varies, the harmonics will also vary. Consequently, since the switching frequency is arbitrary the harmonics are also arbitrary. Some times they are a multiple of 50 Hz and some times they are not. Figure 79 shows the total harmonics spectrum from one Enercon. As can be seen in the figure, at lower frequencies there are only pure harmonics but at higher frequencies there are a whole range of harmonics and interharmonics. This whole range of harmonics and interharmonics represents variations in the switching frequency of the Enercon inverter.
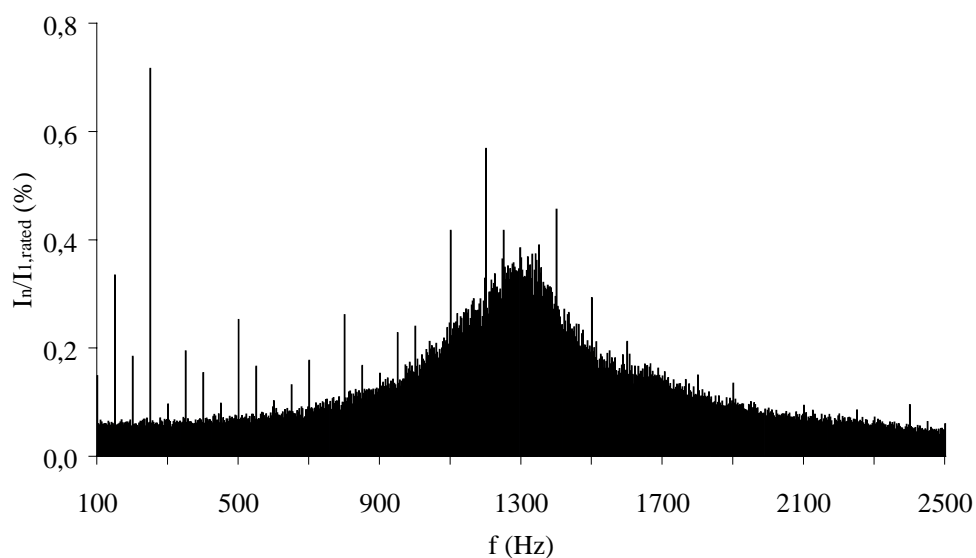

Figure 79. Harmonics and interharmonics content in current on low voltage side of transformer.

8.4.5 Summations of Interharmonic Groups

Summation of interharmonic groups from more wind turbines can be performed in the same way as harmonics. Figure 3.16 shows interharmonic groups in the current from two turbines.
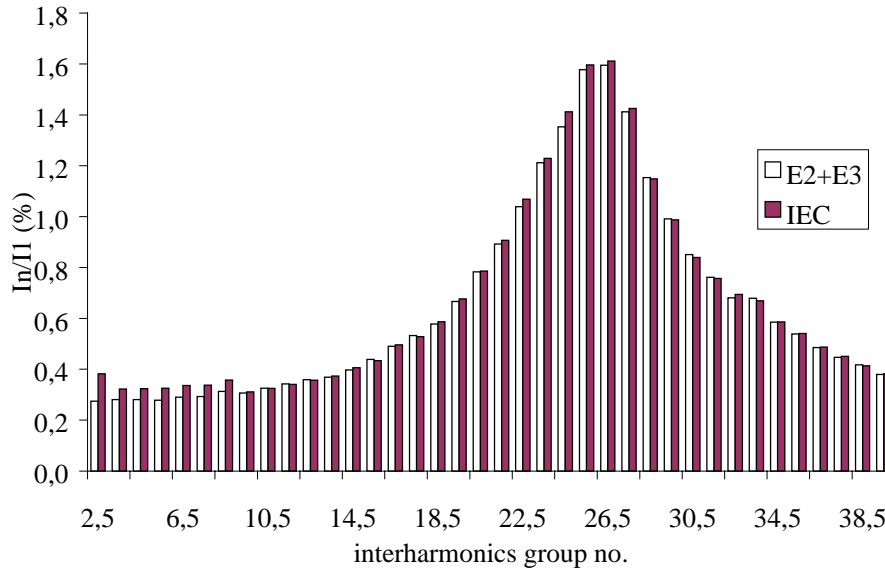
Figure 80. Interharmonics content in current from two wind turbines.

9   Conclusions

The results from comparisons of simultaneous measurements in Hagshaw Hill show good agreement between the measurements of Risø, DEWI, NEL and CRES. Moreover, the comparison of calculation results based on a set of DEWI measurements showed very good agreement between the analysis software of Risø, DEWI and CRES.

Generally, the influence of a wind turbine on the voltage quality of the grid depends not only on the wind turbine but also on the grid where the wind turbine is connected. Both Measnet and IEC define methods to measure power quality characteristics, which aim at being independent on the grid. These methods are based on power and current measurements. The measured power quality characteristics can then be applied to calculate the influence on the voltage quality on an explicit grid, given by the short circuit power and the impedance angle of the grid.

The report has illustrated that the grid properties still have an influence on the specified current and power based power quality characteristics. But this influence is of secondary order compared to the influence of short circuit power and grid impedance angle. E.g. it is shown that the voltage level influences the reactive power consumption of a constant speed wind turbine, and this again influences the flicker step factors for cut-in of the wind turbine to the grid.

Another factor, which influences the measurements, is the terrain. The comparison between measurements on a complex terrain in Scotland and a relatively flat terrain in Denmark showed significant difference between the measurements of power variability and flicker at low and medium wind speed. For high wind speeds, the variability and flicker values are less sensitive to the terrain. The design values are typical values at high wind speeds, which means that the design values will also be less sensitive to the terrain.

All these effects could be taken into account by advanced methods, but such methods would depend strongly on the technology. The strength of the existing methods is their simplicity combined with a high degree of independence of technology. But even the specified methods do have limits concerning the technology. For instance, the specified method to measure flicker emission is not relevant for a wind turbine with a voltage controlled power converter. Such a wind turbine will generate fluctuating currents to equalise the voltage fluctuations on the grid.

References

1. Draft IEC 61400-21. Ed.1: Wind turbine generator systems – Part 21: Measurement and assessment of power quality characteristics of grid connected wind turbines. Committee Draft for Vote (CDV) International Electrotechnical Commission, IEC 2000-11-15.
2. Measnet Measurement Procedure. Power Quality of Wind Turbines. Draft 27.11.96.
3. Measnet Power Quality Measurement Procedure - Version 2. November 2000.
4. IEC 61000-4-7. Electromagnetic compatibility (EMC) – Part 4: Testing and measurement techniques – Section 7: General guide on harmonics and interharmonics measurements and instrumentation, for power supply systems and equipment connected thereto. International Electrotechnical Commission, IEC 2000-12-15.
5. IEC 61000-4-15. Electromagnetic compatibility (EMC). Part 4. Testing and measurement techniques. Section 15. Flickermeter - Functional and design specifications. International Electrotechnical Commission 1997.
6. IEC 61000-3-7. Electromagnetic compatibility (EMC) – Part 3: Limits – Section 7: Assessment of emission limits for fluctuating loads on MV and HV power systems – Basic EMC publication (Technical Report). International Electrotechnical Commission 1996.
7. P.Sørensen. Methods for calculation of the Flicker Contributions from Wind Turbines. Risø-I-939(EN). Risø National Laboratory, Denmark, December 1995.
8. Revision of IEC 61000-4-7. Electromagnetic compatibility (EMC) – Part 4: Testing and measurement techniques – Section 7: General guide on harmonics and interharmonics measurements and instrumentation, for power supply systems and equipment connected thereto. International Electrotechnical Commission Committee draft 1997-12-15.
9. IEC 61000-3-6. Electromagnetic compatibility (EMC) – Part : Limits – Section 6: Assessment of emission limits for distorting loads in MV and HV power systems. Basic EMC publication (Technical Report) International Electrotechnical Commission 1996.

Abstract (max. 2000 characters)

The present report describes the work done in the power quality subtask of the European Wind Turbine Testing Procedure Developments project funded by the EU SMT program. The objective of the power quality subtask has been to make recommendations and provide background for new standards for measurement and testing of wind turbine power quality. The focus in the work has been to support the ongoing standardisation work in IEC with a new standard IEC61400-21 for measurement and assessment of power quality characteristics of grid connected wind turbines. The work has also been based on the power quality measuremnet procedure in the Measnet cooperation of European test stations for wind turbines. The first working item of the project has been to verify the state of the art of the measurement procedures by analyses and comparisons of the measurements and data processing software of the participating partners. The next item has been to investigate the influence of terrain, grid properties and wind farm summation on the power quality of wind turbines, considering both wind turbines with fixed rotor speed(s) and wind turbines with variable speed drives.